

Plectin-vimentin interaction: intermediate filament network formation, dynamics, and nitrosylation-induced collapse

Dissertation zur Erlangung des akademischen Grades
Doktor der Naturwissenschaften an der
Fakultät für Chemie der Universität Wien

Ausgeführt unter der Betreuung von Prof. Dr. Gerhard Wiche am
Department für Molekulare Zellbiologie
Dr. Bohrgasse 9, A-1030 Wien

Eingereicht von Mag. Radovan Spurny

Wien, im Oktober 2008

CONTENTS

1. ACKNOWLEDGEMENTS	6
2. ABBREVIATIONS	7
3. SUMMARY	9
4. ZUSAMMENFASSUNG	11
5. INTRODUCTION	13
5.1. The cytoskeleton	13
5.2. Actin microfilaments and microtubules	14
5.3. Intermediate filaments	14
5.3.1. Classification	15
5.3.2. Domain structure and function	15
5.3.3. IF assembly	16
5.4. Cytolinker proteins	17
5.4.1. The cytolinker protein plectin	20
Molecular structure	21
Molecular interactions	22
Functions beyond cytolinking	23
Plectin deficiency	24
5.5. S-Nitrosylation and oxidation	25
5.5.1. Oxidative stress and vascular NO release	26
5.5.2. Regulation of eNOS activation	27
6. MAJOR GOALS	29
7. MATERIALS AND METHODS	31
7.1. Homology modeling	31
7.2. cDNA constructs, plasmids, and site directed mutagenesis	31
7.3. Proteins	32
7.3.1. Expression of recombinant proteins in <i>E. coli</i>	32
7.3.2. Purification of recombinant plectin repeat domains	32
7.3.3. Purification of recombinant full length vimentin	33
7.3.4. Determination of protein concentration	33
7.3.5. Crystallization of plectin repeat domains	34
7.3.6. SDS-PAGE and immunoblotting	34
7.3.7. Oxidative cross-linking	34
7.3.8. Europium overlay binding assay	35
7.3.9. S-nitrosylation biotin-switch assay	36
7.3.10. Phosphorylation of proteins by Cdk1	37
7.3.11. IFs assembly in vitro	37
7.3.12. Electron microscopy	37

7.4. Mammalian cell culture	37
7.4.1. Cell culture	37
7.4.2. Preparation of cell lysates	38
7.4.3. NO donor mediated nitrosylation of endothelial cells	38
7.4.4. Spectrofluorimetric determination of NO released from endothelial cells	39
7.4.5. Synchronization by double thymidine block	39
7.4.6. Immunofluorescence microscopy	40
7.4.7. Cell transfection	40
7.4.8. Live-cell imaging	40
7.5. Antibodies	42
8. RESULTS	44
8.1. PURIFICATION AND CRYSTALLIZATION OF PROTEINS	44
8.1.1. Expression and purification	44
R5 wt	45
R5 Cys-free	46
R4-5	48
R5-6 and R5-6tail	48
Recombinant vimentin	48
8.1.2. Crystallization	53
R5 Cys-free	53
R4-5	54
8.2. NITROSYLATION OF PLECTIN: EFFECTS ON VIMENTIN-BINDING AND INVOLVEMENT IN IF COLLAPSE	55
8.2.1. Structure prediction for plectin repeats and implications for cysteine residue exposure	55
3D structure of plectin's repeat 5 domain and localization of cysteines	55
3D structure of plectin's repeat 1 domain and of plectin mutant E2798K	57
8.2.2. Disulfide cross-linking within and between plectin repeats, and between plectin and vimentin	59
Intramolecular disulfide bridges within the repeat 5 domain	59
Intermolecular disulfide bridges between repeat domains 4 and 5	60
Disulfide cross-linking between plectin's repeat 5 domain and vimentin	62
8.2.3. Effects of plectin's cysteine residues, of repeat domains neighboring the IF-binding site, and of the tail region on plectin-vimentin affinity	63
Increased vimentin-binding affinity of plectin's repeat domain 5 in its reduced form	63
Effects of plectin's repeat domains neighboring the IF-binding site, and of the tail region on plectin-vimentin interaction	64

8.2.4. Plectin is a target for nitrosylation in vitro and in vivo	66
In vitro nitrosylation of cysteine 4 in plectin's repeat 5 domain	66
Nitrosylation of plectin in endothelial cell cultures	67
8.2.5. Effect of NO donor-mediated nitrosylation on the cytoskeleton of endothelial cell	67
Cytoarchitecture of vimentin networks	67
Effect of NO donor-mediated nitrosylation on microfilaments and focal adhesion contacts	69
8.2.6. Distribution, expression, and activity of eNOS in plectin-deficient endothelial cells	71
NO release from plectin-deficient compared to wild-type endothelial cells	71
Expression and activation (phosphorylation) levels of eNOS	73
Distribution of eNOS in endothelial cells	73
8.3. PHOSPHORYLATION OF PLECTIN AND ITS EFFECT ON THE FORMATION OF VIMENTIN NETWORKS AND IF INTERMEDIATES	75
8.3.1. Plectin and vimentin form globular complexes upon phosphorylation by Cdk1 in vitro	75
8.3.2. Plectin deficiency affects vimentin network dynamics during cell division and leads to multipolar spindles	78
8.3.3. Plectin-dependent formation of vimentin filament intermediates delays IF network assembly	83
8.3.4. Plectin-containing vimentin squiggles exhibit directional movement towards the cell periphery	86
9. DISCUSSION	90
9.1. Cysteines proximal to plectin's IF-binding site	91
Structural implications of repeat 5 domain cysteines	91
Functional implications of repeat 5 domain cysteines as a target for nitrosylation	92
Role of plectin in NO-induced IF collapse	94
Plectin deficiency affects NO production by eNOS	96
9.2. The role of plectin in the formation of vimentin intermediates	97
Vimentin network formation	97
Vimentin dynamics during mitosis and cytokinesis	98
Phosphorylation and formation of vimentin filament intermediates	100
10. REFERENCES	103
11. CURRICULUM VITAE	124

1. ACKNOWLEDGEMENTS

I would like to express my sincere gratitude to my supervisor, Professor Gerhard Wiche, Head of the Department of Molecular Cell Biology, Max F. Perutz Laboratories, University of Vienna. His understanding, encouraging and personal guidance have been of great value for me. I wish to thank Lubomir Janda for his guidance and help at the beginning of my work, and to Martin Gregor for his assistance in numerous ways. I also wish to thank Maria J. Castañón for her excellent advices. I am grateful to all members of the lab, namely Julius Kostan, Irmgard Fischer, and Patryk Konieczny for friendly atmosphere. I also want to express my gratitude to my family for their support and understanding. During my work I have collaborated with many colleagues for whom I have great regard, and I wish to extend my warmest thanks to all those who have helped me with my work.

2. ABBREVIATIONS

ABD	Actin binding domain
BCA	Bicinchoninic acid
BH4	Tetrahydrobiopterin
Biotin-HPDP	N-[6-(biotinamido)hexyl]-3'-(2'-pyridyldithio)propionamide
BPAG1	Bullous pemphigoid antigen 1
BSA	Bovine serum albumin
CaM	Calmodulin
cAMP	Cyclic 3', 5'-adenosine monophosphate
CAMK	Calmodulin-dependent kinase
Cdk	Cyclin-dependent kinase
CH	Calponin homology
Cys	Cysteine
DAG	Diacylglycerol
DTT	1,4-Dithiothreitol
EB	Epidermolysis bullosa
EBS	Epidermolysis bullosa simplex
EBS-MD	Epidermolysis bullosa with muscular dystrophy
eNOS	Endothelial nitric oxide synthase
FAC	Focal adhesion contact
FCS	Fetal calf serum
FMN	Flavin mononucleotide
GFAP	Glial fibrillary acidic protein
GFP	Green fluorescence protein
HD	Hemidesmosome
HRPO	Horse radish peroxidase
IF	Intermediate filament
IFAP	Intermediate filament associated protein
IPTG	Isopropyl thio- β -D-galatoside
MACF	Microtubule-actin crosslinking factor

MAP	Microtubule-associated protein
MMTS	Methyl methanethio-sulfonate,
MT	Microtubule
MTJ	Myotendinous junctions
MTOC	Microtubule-organizing center
NF	Neurofilament
NLS	Nuclear localization signal
NMJ	Neuromuscular junctions
NO	Nitric oxide
NOS	Nitric oxide synthase
OA	Oxaloacetic acid
PAGE	Polyacrylamide gel electrophoresis
PBS	Phosphate buffered saline
PI	Processive index
PKA	Protein kinase A (cAMP-dependent kinase)
PKC	Protein kinase C
PMA	Phorbol-12-myristate-13-acetate;
PPase	Protein phosphatase;
PS	Phosphatidylserine
R	Repeat
ROS	Reactive oxygen species
SDS	Sodium dodecylsulfate
SNAP	S-nitroso-N-acetylpenicillamine
ULF	Unit-length filament
wt	Wild type

3. SUMMARY

The cytolinker protein plectin plays a crucial role in maintaining the integrity of the cytoskeleton by interlinking intermediate filaments (IFs) with other cytoskeletal network systems, and anchoring them to the plasma membrane. It also serves as a scaffolding platform for signaling cascades, and may well have also a function in IF network assembly and dynamics. The plectin molecule, with its high molecular weight (>500,000), has a three-domain organization, where a central α -helical rod domain is flanked by two terminal globular domains. Harboring a unique phosphorylation site for protein kinase Cdk1 and binding sites for different IF proteins and for a variety of proteins involved in signaling, plectin's C-terminal domain consisting of six structural repeats (R1-6) is of strategic functional importance. Depending on the species, there are at least 13 cysteines in plectin's C-terminal domain, 4 of which reside in the repeat domain 5 (R5). Cysteines may play an important role in stabilizing the protein structure and conformation.

The first part of the thesis was focused on the purification and crystallization of the plectin fragments harboring the IF-binding site. All recombinant proteins were purified by at least one purification step and homogeneity of the proteins used for crystallization was confirmed by size exclusion chromatography. Extensive crystallization screening revealed that only a cysteine-free version of plectin R5 and a fragment corresponding to repeat domains R4-5 were able to form crystals. However, only small rod-shaped or clustered needle-shaped crystals occurred. Neither optimizing crystallization conditions nor macroseeding led to crystals with dimensions appropriate for collecting X-ray diffraction data.

In the second part, I investigated the structural and biological functions of R5 cysteines and the effects of plectin nitrosylation on vimentin-binding and involvement in IF collapse using biochemical and functional analyses. Performing cysteine to serine mutagenesis and biochemical analyses I showed that the four cysteines of R5 can form intra- and intermolecular disulfide bridges. In addition it could be shown that the single cysteine in vimentin as well as the cysteines in R5 formed disulfide bonds between each other. However, vimentin-binding was significantly more efficient when R5 was in its reduced form, probably reflecting distinct conformations of the reduced and the nonreduced forms.

Out of the four cysteines in R5 only one (Cys4) was found to be particularly reactive with respect to disulfide bridges formation ability and serving as a target for nitrosylation *in vitro*. Using immortalized endothelial cells, I could show that endogenous plectin is the target of S-nitrosylation *in vivo* and I found that NO donor-induced IF collapse proceeded dramatically faster in plectin-deficient compared to wild-type cells. Additionally, I observed that actin stress fibers accumulated in the center of the cells upon NO donor treatment. By measuring the amount of NO released from endothelial cells upon eNOS stimulation, I found that NO production was dramatically reduced in plectin-deficient compared to wild-type cells. NO release correlated with the expression level of eNOS and its activation status. Also the distribution of eNOS corresponded with its activation in both cell types, as it was localized at the cell periphery in plectin-deficient cells (inactive form) and diffusely distributed in wild-type cells (active form).

In a third part of my thesis I studied the effects of plectin phosphorylation on vimentin-binding and on IF network formation and dynamics. Using an *in vitro* binding assay I found that vimentin and plectin phosphorylation by Cdk1 (a typical mitotic event) influenced the interaction of both proteins. In particular, phosphorylated vimentin in the presence of phosphorylated plectin R5-6 led to the formation of globule-like structures of various sizes. Very similar structures, mainly in the form of granules and squiggles were observed in newly spreading postmitotic fibroblasts and in cells after trypsinization/replating. I could show that the formation of these vimentin intermediates were plectin dependent, as they showed association with plectin and were not observed in the absence of plectin. In addition in mitotic cells I observed multipolar spindles in plectin-deficient contrary to wild-type cells. Moreover, while the majority of wild-type cells undergoing cytokinesis showed an uneven distribution of the vimentin network to their daughter cells, a much more even distribution was observed in plectin knockout cells. Also I found that mitosis progressed faster in plectin knockout compared to wild-type fibroblasts. The data presented in my thesis suggest that plectin is not only a major organizing element of the IF network cyto-architecture, but also has an important function in IF network assembly and dynamics.

4. ZUSAMMENFASSUNG

Das Cytolinkerprotein Plectin spielt bei der Aufrechterhaltung der Integrität des Zytoskeletts eine entscheidende Rolle, indem es Intermediärfilamente (IFs) mit anderen zytoskelettären Netzwerksystemen verbindet und diese an der Plasmamembran verankert. Weiters dient es als strukturelles Grundgerüst für Signalkaskaden und dürfte ebenfalls eine Funktion in der Netzwerkanordnung und – dynamik haben. Das Plectinmolekül mit seinem hohen Molekulargewicht (>500,000), besitzt eine Drei-Domänen-Organisation, wobei eine zentrale α -helikale Stabdomäne von zwei terminalen globulären Domänen begrenzt wird. Indem es eine einzige Phosphorylierungsstelle für die Proteinkinase Cdk1 and Bindungsstellen für verschiedene IF-Proteine und eine Vielfalt an Proteinen, die im „Signaling“ involviert sind, besitzt, ist die C-terminale Domäne von Plectin (bestehend aus den sechs strukturellen Wiederholungen - R1-6) von strategisch wichtiger Bedeutung. Abhängig von der Spezies, gibt es zumindest 13 Cysteine in der C-terminalen Domäne von Plectin, vier davon befinden sich in der Repeatdomäne R5. Cysteine könnten einen wichtigen Beitrag zur Stabilisierung der Konformation von Proteinen leisten.

Der erste Teil der Arbeit ist auf die Aufreinigung und Kristallisation von Plectinfragmenten, in denen die IF-Bindungsstelle lokalisiert ist, fokussiert. Alle rekombinanten Proteine wurden durch mindestens einen säulenchromatographischen Schritt gereinigt und die Homogenität der Proben durch Größenausschluss-Chromatographie bestätigt. Umfangreiches Kristallisationsscreening zeigte, dass nur die cysteinfreie Version des Plectin R5 und ein Fragment, das die Repeat-Domäne R4-5 enthielt, in der Lage waren, Kristalle zu bilden. Aber auch in diesen Fällen traten nur kleine stabförmige oder sternförmig angeordnete nadelige Kristalle auf. Weder die Optimierung der Kristallisationsbedingungen noch Großansätze (Macroseeding) führten zu Kristallen mit Dimensionen, die für die Röntgenbeugungsanalysen geeignet waren.

Im zweiten Teil der Arbeit untersuchte ich strukturelle und biologische Funktionen der in R5 enthaltenen Cysteine und die Auswirkungen ihrer Nitrosylierung auf Plectins Vimentinbindung und den Kollaps von IFs. Mit Hilfe von Cystein-Mutagenese (zu Serinen) zeigte ich, dass vier der in der R5 Repeat-Domäne enthaltenen Cysteine intra- und intermolekulare Disulfidbrücken bilden konnten. Darüber hinaus, konnte gezeigt werden, dass das einzige in Vimentin enthaltene Cystein mit den R5-Cysteinen Disulfidbindungen eingehen

können. Dennoch war die Vimentinbindung signifikant effektiver wenn das R5-Fragment in reduzierter Form vorlag. Von den vier Cysteinen in R5 wurde nur eines (Cys4) gefunden, das besonders reaktiv hinsichtlich Disulfidbrückenbildung war und auch *in vitro* nitrosiliert werden konnte. Unter Verwendung immortalisierter Endothelzellen konnte ich zeigen, dass Plectin auch *in vivo* S-nitrosiliert wird, und außerdem zeigte sich, dass Stickoxid (NO)-Donor-induzierter IF-Netzwerkzerfall in Plectin-defizienten Zellen dramatisch schneller ablief als in Wildtyp-Zellen. Zusätzlich beobachtete ich, dass sich Aktin-Stressfasern durch NO-Donor-Behandlung im Zentrum der Zellen ansammelten. Die Messung des von Endothelzellen nach endothelialer Stickoxidsynthase (eNOS)-Stimulation freigesetzte NO ergab, dass die NO-Produktion in Plectin-defizienten im Vergleich zu Wildtyp-Zellen drastisch reduziert war. Die NO-Freisetzung korrelierte mit der Menge und dem Aktivierungsstatus von eNOS. Auch die Verteilung der eNOS entsprach ihrem Aktivierungszustand, wobei sie in Plectin-defizienten Zellen an der Zellperipherie lokalisiert (inaktive Form) war, während in Wildtyp-Zellen eine diffuse Verteilung (aktive Form) zu finden war.

Im dritten Teil meiner Arbeit untersuchte ich die Auswirkungen der Phosphorylierung von Plectin auf dessen Vimentinbindung, IF-Netzwerkbildung und Filamentdynamik. In Bindungsstudien fand ich heraus, dass die Phosphorylierung von Vimentin und Plectin durch die Mitose-spezifische Kinase Cdk1 deren Interaktion beeinflusste. Im speziellen führte phosphoryliertes Vimentin, in Gegenwart der phosphorylierten Bindungsdomäne Plectin R4-5, zur Bildung globulärer Strukturen unterschiedlicher Größe. Sehr ähnliche Strukturen, vorwiegend in Form von Granula und kurzen Filamenten, wurden in postmitotischen Fibroblasten und in Zellen unmittelbar nach der Trypsinierung beobachtet. Ich konnte zeigen, dass die Bildung dieser Vimentin-Filament-Zwischenstufen von Plectin abhängig war, da sie nur in Plectin-positiven Zellen zu beobachten war. Zusätzlich beobachtete ich in mitotischen Zellen multipolare Spindeln in Plectin-defizienten, jedoch nicht in Wildtyp-Zellen. Während der Großteil der Wildtyp-Zellen nach der Cytokinese eine ungleiche Verteilung des Vimentin-Netzwerks auf die Tochterzellen zeigte, wurde eine wesentlich gleichmäßigere Verteilung in Plectin-knockout Zellen beobachtet. Darüber hinaus zeigte sich, dass die Mitose in Plectin-knockout Fibroblasten schneller als in Wildtyp-Zellen ablief. Die in meiner Arbeit präsentierten Ergebnisse deuten darauf hin, dass Plectin nicht nur ein bedeutendes Organisationselement der IF-Netzwerk-Cytoarchitektur darstellt, sondern auch eine wichtige Rolle bei dynamischen Prozessen des IF-Netzwerks spielt.

5. INTRODUCTION

5.1. The cytoskeleton

Shapes and sizes of mammalian cells are fascinating and nearly as varied as the animals themselves. Cytoarchitecture is responsible for this diversity and also contributes to most functions of each cell type. The cytoskeleton is a fibrous meshwork of three major components – actin microfilaments, microtubules and intermediate filaments (IFs). Components of the cytoskeleton are assembled from soluble precursors, under the precise control of many different cellular processes and other proteins which crosslink the filaments. The cytoskeleton is found in all eukaryotic cells, provides the cell with mechanical strength, it is responsible for its shape and integrity and it is essential for the organization of cell movement in many aspects. It supports the fragile plasma membrane and provides mechanical linkages. It enables the cells to change their shape and to move from one place to another. Actin microfilaments play essential role in cell polarity and migratory or contractile processes. In contrast, IFs provide intracellular mechanical strength and are consequently abundant in tissues, such as epidermis and muscles that undergo physical stress. On the other hand, microtubules are essential for intracellular vesicle, organelle and protein delivery, whereas the mitotic spindle formed from microtubules plays a role in the chromosome alignment dynamics and segregation during mitosis. Many cellular functions, such as sperm cell swimming, neuronal axon and dendrite extension or the crawling of white blood cells are dependent on the cytoskeleton.

Interesting findings in the cytoskeleton research came from the family of cytoskeletal cross-linking proteins, known as cytolinkers or plakins, which were identified on the basis of IFs and membrane junctional complexes (Green et al., 1992; Ruhrberg and Watt, 1997; Wiche, 1998). These proteins are encoded by complex genes, which encode several isoforms, with potential unique functions and with varying abilities to associate with different cytoskeletal systems.

5.2. Actin microfilaments and microtubules

As essential components of the cytoskeleton, actin microfilaments and microtubules are polymers with structural polarity assembled from highly conserved globular proteins that have nucleotide-binding and hydrolyzing activity.

Microfilaments with a diameter of 5-9 nm are assembled from single subunits, called actin. In its monomer form, actin is usually referred to as G-actin. Each protein unit is about 42 kDa in size and contains an adenine nucleotide. When these monomers polymerize they associate head-to-tail to yield the F-actin. This process is usually accompanied by hydrolysis of bound ATP to ADP. Actin filaments are crosslinked and packed in the living cells together by different accessory proteins, making this abundant complex much stronger than single filaments. Actin exists in three different isoforms, α , β , and γ that partially differ in their amino acid sequence. While isoforms α and β were found together in nearly all non-muscle cells, γ actin is expressed only in muscle cells (Pollard and Cooper, 1986).

Microtubules are formed from heterodimeric protein subunits, α - and β -tubulin, each about 450 amino acids and 50 kDa in size, which are tightly bound together by non-covalent bonds. As in actin, each monomer contains a bound nucleotide, but tubulins use the GTP and GDP instead of ATP and ADP. Also as in actin, the dimers polymerize end to end, result in a polar filament. However, microtubules are composed of 13 parallel filaments (protofilaments) encircling the hollow core and they are much more rigid than the actin microfilaments. In contrast to actin microfilaments whose assembly is initiated at the cells periphery, microtubules are nucleated deep within the cytoplasm, from the structures near the nucleus called microtubule-organizing center (MTOC) (Kirschner and Mitchison, 1986).

5.3. Intermediate filaments

In contrast to microtubules and microfilaments, IF networks are formed from filamentous proteins, that have no enzymatic activity and form polymers without structural polarity. In most vertebrates, IFs form extensive networks throughout the cytoplasm, that extends from the nuclear surface to the cell periphery. As rope-like structures, able to resist deformation,

IFs are considered to be the most rigid component of the cytoskeleton and to be responsible for the maintenance of the cell shape. Thus, IFs are particularly prominent in cells that are exposed to mechanical stress.

5.3.1. Classification

Primary structure, gene structure, assembly properties or their developmentally regulated tissue specific expression patterns divide IF proteins into five distinct types (Strelkov et al., 2003). In contrast to keratins – IF protein types I and II that form obligatory heteropolymers – type-III IF proteins (vimentin, desmin, glial fibrillary acidic protein, and peripherin) form homopolymeric IFs. Vimentin has been found expressed in mesenchymal and some ectodermal cells during the early developmental stages, often forming a network before the expression of differentiation-specific IF proteins, such as desmin or neurofilament proteins. The three neurofilament protein subunits (NF-L, NF-M and NF-H), nestin, syncoilin and α -internexin comprise type-IV IF proteins. Finally, the nuclear IF protein lamin A and its splice variant lamin C, together with lamins B1 and B2, form the type-V group.

5.3.2. Domain structure and function

All cytoplasmic IFs have a common secondary structure. The central rod domain of about 310 amino acids is flanked by globular non- α -helical head and tail domains of variable size (Geisler and Weber, 1982). The α -helical central rod domain with a heptad repeat of hydrophobic amino acids is subdivided into the coil segments 1A, 1B, 2A, and 2B that are connected by short linkers (Parry and Steinert, 1999). The rod domain is the most conserved region among the different isoforms, but the N- and C-terminal globular domains can differ much.

Little is known about the functions of head and tail domains. While, N-terminal head domains are essential for IFs assembly, C-terminal tail domains might be involved in the lateral interactions and organization of the IF networks (Herrmann et al., 2003). Within these globular non- α -helical domains are present several phosphorylation sites that are involved in the regulation of their assembly/disassembly and subcellular organization (Kumar et al., 2002; Helfand et al., 2003).

5.3.3. IFs assembly

IFs are assembled in a three-step process, where gradual association of the dimers (Steinert, 1993) leads to the formation of tetramers (Herrmann and Aebi, 1999), which then rapidly associate laterally to form unit-length filaments (ULFs) (Strelkov et al., 2003). In particular, the vimentin ULFs appear to contain about sixteen ~46 nm long dimers (Herrmann et al., 1996). Subsequently, ULFs anneal longitudinally into loosely packed filaments. Finally, these filaments undergo an internal rearrangement of subunits resulting in the radial compaction of the filament (Strelkov et al., 2003). In general, the conditions for the *in vitro* polymerization and depolymerization of IFs are similar. *In vitro* polymerization of the vimentin into 10 nm filaments is determined by pH and ionic strength, increased ionic strength leads to the formation of the filaments from soluble subunits (Zackroff and Goldman, 1979; Strelkov et al., 2003).

In vivo studies of living cells by using rhodamine- and green fluorescent protein (GFP)-tagged vimentin, or immunofluorescence microscopy of fixed cells, have shown that type-III IF proteins exist in several intermediate states: non-filamentous granules, short filamentous structures that are known as squiggles, and longer filaments (Vikstrom et al., 1992; Prahlad et al., 1998; Yoon et al., 1998). The form of vimentin within the granules is unknown, although granules probably contain IF intermediates such as dimers, tetramers or ULFs. However, purified vimentin microinjected into living cells immediately forms non-filamentous granules before assembling into longer IFs (Vikstrom et al., 1989). On the basis of observations during the spreading process, it is evident, that IF granules and squiggles have an important role in the assembly of the IF network found in interphase cells. During the early stages of spreading of fibroblasts, a fraction of GFP-vimentin was found in non-membrane bound and non-filamentous forms, termed vimentin granules, which were most visible at the edge of the cells. These particles seemed to be replaced by the filamentous squiggles as the spreading progresses. Ultimately, the number of vimentin granules and squiggles decreases together with the appearance of extensive IF networks. This phenomenon is not vimentin-specific, as IF particles have also been observed in cultured nerve cells (Yabe et al., 1999b), spreading epithelial cells (Windoffer and Leube, 1999a) and in several types of mitotic cells (Rosevear et al., 1990).

In fact, the changes observed in IF network reorganization during different stages of mitosis resemble those seen in spreading cells. Both vimentin and keratin networks seem to

be converted into granules distributed through the cytoplasm during the transition from prophase to metaphase (Rosevear et al., 1990; Windoffer and Leube, 1999a). During cytokinesis, the majority of these granules are present at the centrosomal region of the daughter cells, where they form a perinuclear filamentous cap (Rosevear et al., 1990). From these observations, it is obvious that at least part of the IF network could be assembled sequentially in several distinct steps: non-filamentous granules, short fibrous squiggles and long fibrils (Prahlad et al., 1998; Chou and Goldman, 2000). The movement of these intermediates and the formation of IF networks in spreading cells have been shown to depend on microtubule integrity and require microtubule-based motors such as kinesin and dynein (Prahlad et al., 1998; Helfand et al., 2002).

5.4. Cytolinker proteins

Microfilaments, microtubules and IFs are the main components of the cytoskeleton responsible for maintaining the cell shape and resistance to the external oxidative or mechanical forces. In fact, these three cytoskeletal elements should be stabilized and interlinked together. The plakin protein family comprises large multifunctional proteins referred to as cytoskeletal linker proteins or cytolinkers that mediate such interactions (Wiche, 1998). Cytolinkers interlink different cytoskeletal networks and connect them to membrane-associated adhesive junctional complexes, such as desmosomes and hemidesmosomes. Seven members of the plakin family have been identified, including desmoplakin, plectin, bullous pemphigoid antigen 1 (BPAG1), ACF7, also called microtubule-actin crosslinking factor (MACF), envoplakin, periplakins and epiplakin (Fig. 1) (Leung et al., 2002). Plakin family members are defined by the presence of a plakin domain and/or one or more plectin repeat domains (plectin repeats) (Janda et al., 2001). There are also other domains that are common to some but not all members, such as a calponin-type actin-binding domain (ABD), a heptad repeat-containing coiled-coil rod domain, a spectrin-repeat-containing rod domain and a microtubule (MT)-binding domain.

The plakin domain, which consists of 4–8 spectrin repeats interrupted by an SH3 domain, has been predicted to comprise six α -helical segments that are organized as antiparallel α -helical bundles (Virata et al., 1992; Roper et al., 2002). All family members

except epiplakin contain the plakin domain, which is important in targeting plakins to specific cell junctions. Plakin or plectin repeat domains, which contain a module and linker region, comprise varying numbers of the repeat (R) domains, ranging from none in periplakin to 13 in epiplakin. Each repeat is composed of four complete and one partial highly conserved 38-residue motifs. These repeat domains can be categorized into A, B and C types. The linkers connecting the modules are less conserved and of variable lengths. The linker region between the repeat B- and C-type modules harbors the IF-binding site. The ABD which is homologous to the ABDs of the spectrin family members refer to spectraplakin family, consists of two calponin homology (CH) domains (Leung et al., 2002).

Desmoplakin, a component of desmosomes, besides plectin is the best plakin characterized. It is located in the innermost portion of the desmosomal plaque where it is thought to play a role in attaching IFs to the cell surface (Franke et al., 1987; Green et al., 1990). By anchoring IFs to the plasma membrane and forming a subcellular scaffold, it also contributes to the assembly and/or stabilization of desmosomes (Gallicano et al., 1998). There are two closely related splice forms of desmoplakin, DPI (322 kDa) and DPII (259 kDa) (Green et al., 1990; Virata et al., 1992). Both forms were found in all types of epithelia, but DPI was also found in heart muscle cells (Franke et al., 1987). Desmoplakin is a dumbbell-shaped molecule where the central rod domain is flanked by N-terminal and C-terminal globular domains (O'Keefe et al., 1989). The N-terminal part consists of the plakin domain, while the C-terminus is built from three repeat domains of the types A, B, and C (Green et al., 1990). The linker region between the repeats B and C is responsible for the direct binding to the various types of IFs (Stappenbeck et al., 1993; Kouklis et al., 1994). A mutation in the human desmoplakin gene causes autosomal dominant skin disorder called striated palmoplantar keratoderma, which is characterized by the hyperkeratosis of the palms and feet (Armstrong et al., 1999).

Bullous pemphigoid antigen 1 (BPAG1) is a plakin protein that is associated with the hemidesmosomal plaque. The BPAG1 gene encodes several structurally distinct proteins, which are differentially distributed over various tissues. BPAG1-a is produced in the pituitary primordial and in the dorsal root ganglia (Leung et al., 2001). BPAG1-b in the developing mouse embryos is restricted to the heart, skeletal muscle, and bone cartilage of the vertebrae. BPAG1-e is expressed in basal epithelial cells and was found associated with hemidesmosomes. The expression of BPAG1-n, also called dystonin, has been proposed to occur

in neuronal cells at a low level (Brown et al., 1995; Yang et al., 1996). The coiled-coil rod domain of the BPAG1-e is flanked by a N-terminal plakin domain and repeat domains of the type B and C at the C-terminal part. BPAG1-n is similar to BPAG1-e, except for an ABD at its N-terminus (Fig. 1). BPAG1-a has an ABD and a plakin domain, like BPAG1-n, but its rod domain is composed of 23 spectrin repeats, and the C-terminal domain is harboring a microtubule-binding site. These interaction domains are also present in BPAG1-b which contain additionally one repeat of the A type between its spectrin repeats and the plakin domain. BPAG1 deficiency in mice leads to degeneration of the sensory nervous system (Duchen, 1976; Dowling et al., 1997).

Microtubule-actin cross-linking factor (MACF), also known as ACF7, as a paralogue of BPAG1-a, contains an ABD, a plakin domain, a rod domain with 23 spectrin repeats, and an MT-binding domain. It coordinates and interlinks microtubules and actin filaments and is expressed ubiquitously in mouse embryos, with the highest level in the nervous system and intermediate to high levels in skeletal muscle and myocardium (Leung et al., 1999). Studies

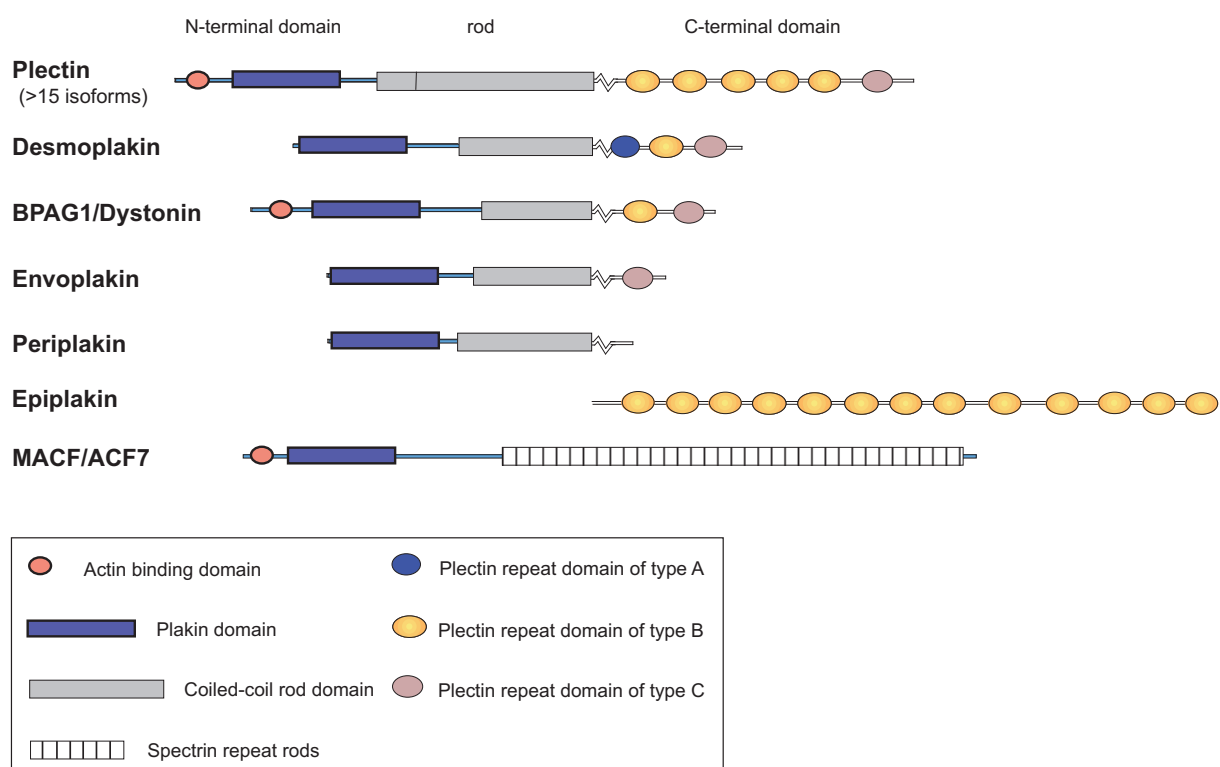


Figure 1. Schematic diagram of the plakin family cytolinker proteins. Various subdomains; actin binding domain (ABD), coiled-coil rod domain, spectrin repeats-containing rod domain and plectin repeat domains are specified in the legend. The homologous repeat domains of the A, B and C type consist of a 38 amino acid residues-long motif, tandemly repeated five times.

of its *Drosophila* homologue – kakapo – revealed that gene mutations result in defects in cell differentiation and development of the nervous system (Gregory and Brown, 1998).

Epiplakin was found as an epidermal autoantigene from a patient with a subepidermal blistering disease that resembled bullous pemphigoid (Fujiwara et al., 1996). In contrast to other plakin family members the whole molecule of epiplakin consists of sixteen repeats of the B type (Spazierer et al., 2003). It is expressed abundantly in skin, small intestine and salivary gland and at lower levels in lung, liver and uterus (Spazierer et al., 2003). Mutations causing disease have not been reported to date.

Periplakin and envoplakin are components of the cornified envelope in the outer layer of the stratified epithelium (Steinert et al., 1999). They were found in keratinizing and non-keratinizing stratified epithelia and in two-layered and transitional epithelia, such as the mammary gland and bladder (Simon and Green, 1984; Ruhrberg et al., 1996). They connect cytoskeletal structures with cell adhesion complexes. The rod domain of envoplakin is N-terminally flanked by a plakin domain, and C-terminally by C type repeat and a linker region (Fig. 1). While all proteins of the plakin family form two stranded coiled-coil homodimer (O’Keefe et al., 1989; Tang et al., 1996), the evidence suggests that envoplakin and periplakin might interact with each other via their rod domains forming heterodimers (Ruhrberg et al., 1997; DiColandrea et al., 2000). Up to date, there are no confirmed events of inherited diseases known which would arise from mutations in these proteins. Recent studies suggest, however, that envoplakin is not required for cornified envelope assembly (Määttä et al., 2001).

5.4.1. The cytolinker protein plectin

Plectin, as the most versatile cytoskeletal linker protein known, has a high molecular weight (>500,000) and is composed of a central ~200 nm long α -helical coiled coil rod domain flanked by globular domains. Plectin, which is expressed in a variety of mammalian tissues and cell types, was originally identified as a major component of IF-enriched extracts from rat glioma C6 cells (Pytela and Wiche, 1980). It interlinks IFs with microtubules and microfilaments and anchors them to the subplasma membrane skeleton and to plasma membrane-cytoskeleton junctional complexes (Wiche, 1998). The fact that plectin was found concentrated at hemidesmosomes (Reznicek et al., 1998), desmosomes (Eger et al., 1997), Z-disk structures and dense plaques of striated and smooth muscle, intercalated discs of

cardiac muscle and focal adhesion contacts (FACs) (Seifert et al., 1992; Andrä et al., 1997) implicates a role of the protein in linking the cytoskeleton to plasma membrane junctions. It is particularly prominent in stratified simple epithelia, various types of muscle, and cells forming the blood brain barrier (Wiche, 1989; Errante et al., 1994). In several tissues, plectin expression was found to be prominent in the cells forming the tissue layers at the interface between tissues and fluid-filled cavities, including the surfaces of kidney glomeruli, liver bile canaculi, bladder urothelium, gut villi, epidermal layers lining the cavities of brain, and endothelial cells of blood vessels (Wiche et al., 1983; Errante et al., 1994; Yaoita et al., 1996).

Molecular structure

The molecular mass of plectin was estimated as 300 kDa based on the co-migration of the protein with subcomponents of high molecular mass microtubule-associated proteins (MAPs) in SDS-PAGE (Pytela and Wiche, 1980). The precise size prediction of plectin isoforms varies from 507 to 527 kDa depending on several alternative first coding exons (Elliott et al., 1997). Rotary shadowing electron microscopy of purified plectin revealed a dumbbell-like structure, and its microscopic dimensions and gel permeation HPLC data indicated a molecular weight of over 1.1×10^6 , suggesting that plectin molecules in solution exist as dimers (Foisner and Wiche, 1987; Weitzer and Wiche, 1987). The interaction with IF involves a specific binding domain located in the C-terminal domain of the protein (Nikolic et al., 1996), whereas a functional actin-binding domain (ABD) is situated within the N-terminal domain (Elliott et al., 1997; Andrä et al., 1998) and binding sites for integrin $\beta 4$ are located at both ends (Rezniczek et al., 1998) (Fig. 2).

The building block of plectin's C terminus is a repeat domain, known as the plakin or plectin repeat domain, from now referred to as repeat domain (Janda et al., 2001; Leung et al., 2002). Repeat domains consist of a conserved core domain, or module, built from 4.5 tandemly repeated copies of a 38-amino acid motif (the "PLEC repeat", according to databases SMART, <http://smart.embl-heidelberg.de/> and Pfam, <http://www.sanger.ac.uk/cgi-bin/pfam/>) (Sonnhammer et al., 1997; Schultz et al., 1998). The modules are separated from each other by linker sequences of variable lengths. The concept of the module as the basic structure of the C-terminal domain of plakin proteins has been validated by the crystal structure determination of the two desmoplakin repeat domains (Choi et al., 2002). The C-

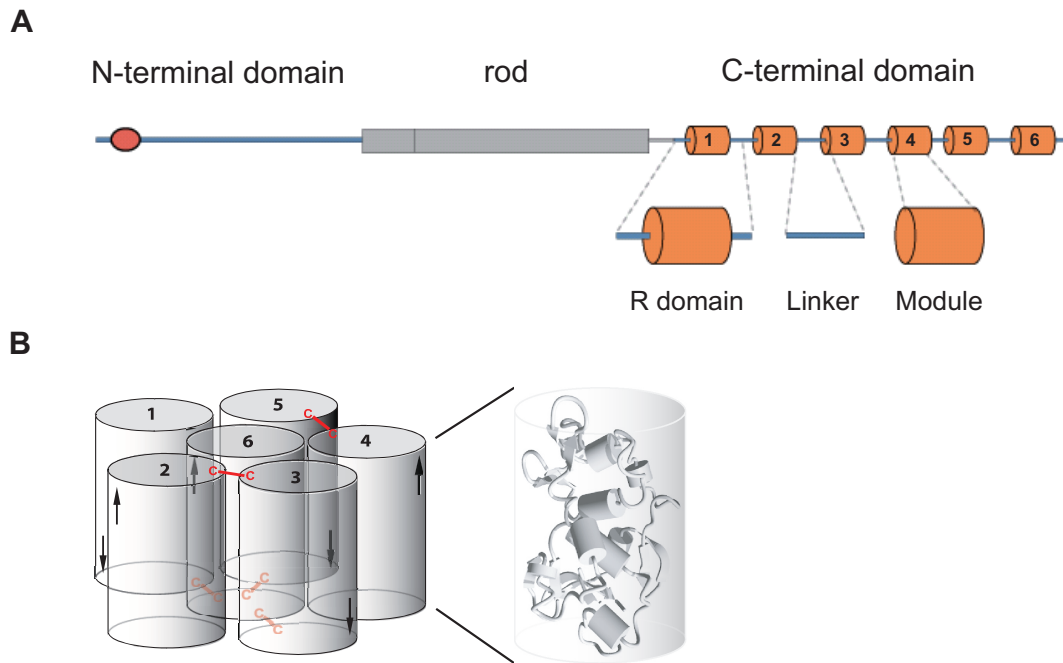


Figure 2. Schematic diagram of plectin's subdomain structure and plectin repeat domains 1-6. (A) N-terminal domain with its ADB, central rod and C-terminal domain consisting of six repeats connected by linker regions of different lengths. (B) Schematic hypothetical diagram of plectin repeats arranged as a compact 6-cylinder structure stabilized by disulfide bridges and a schematic structure of one repeat, showing the module's cylindrical shape predicted on the basis of known 3D structure of desmoplakin (modified from Janda et al., 2001).

terminal part of plectin (~1900 amino acids) represents six highly homologous repeat domains (R1-R6) of about 300 amino acids each, with five of the B type and one of the C type. The linker region between modules 5 and 6 contains the IF-binding site, whereas the tail of module 6 harbors a putative MT-binding site. Secondary structure analysis revealed that plectin repeats are similar to the ankyrin repeat motif (Janda et al., 2001), having a hairpin-helix-loop-helix ($\beta 2\alpha 2$) structure (Sedgwick and Smerdon, 1999; Kobe and Kajava, 2000). Accommodation of the six repeat plectin domains within the globular C-terminal plectin domain, which has an estimated diameter of 9 nm (Foisner and Wiche, 1987), requires tight packing. Janda et al. (2001) proposed a circular arrangement of antiparallel-oriented plectin repeat 1-5 domains with the repeat 6 domain in their center. Such a structure could be stabilized by hydrophobic interactions between residues on the surface of each repeat domain and/or through cysteines via disulfide bond formation upon oxidative stress.

Molecular interactions

Plectin has been characterized as an essential component of cytoarchitecture. Due to its multiple functions in many cellular processes, plectin can be defined as a universal cytolinker

protein. Several studies have shown that plectin interacts with all of the fundamental cytoskeletal filament systems, the plasma membrane, desmosomes and hemidesmosomes. Plectin has been identified as a direct interaction partner of vimentin (Pytela and Wiche, 1980; Wiche et al., 1982) and of other cytoplasmic IF subunit proteins, including GFAP, epidermal cytokeratins, neurofilament triplet proteins, and desmin (Foisner et al., 1988) as well as the nuclear IF protein, lamin B (Foisner and Wiche, 1991). The IF-binding site of plectin linking the C-terminal repeat 5 and 6 domains has been mapped to a stretch of ~50 amino acid residues (Nikolic et al., 1996). A basic amino acid residue cluster within a typical bipartite nuclear localization sequence (NLS) motif was identified as a crucial element of this site. In vitro experiments showed that the plectin repeat 5 domain bound to type III IF proteins (vimentin) with preference over type I and II cytokeratins 5 and 14 (Steinböck et al., 2000).

The evidence from both in vitro and in vivo experiments indicates that plectin's interaction with IFs is differentially regulated by phosphorylation involving different types of protein kinases (Foisner et al., 1991; Foisner et al., 1996). Plectin's interaction with lamin B was found to be significantly decreased upon phosphorylation of either binding partner by cAMP-dependent protein kinase (PKA) or Ca²⁺/phosphatidyl-dependent protein kinase C (PKC), while its binding to vimentin was increased upon PKA phosphorylation but decreased upon PKC phosphorylation (Foisner et al., 1991).

In the light of plectin's role as a cytoskeletal linker element, a specific regulation of its binding properties could have particular importance during mitosis, when the IF network is dramatically reorganized (Malecz et al., 1996). Plectin, as a target of cyclin-dependent kinase 1 (Cdk1), during mitosis becomes phosphorylated at a unique site (threonine 4542), which resides in plectin's C-terminal repeat 6 domain, not far from the IF-binding site (Malecz et al., 1996).

Functions beyond cytolinking

Examination of cultivated plectin-deficient fibroblasts revealed a new aspect of plectin functions. After short-term adhesion these cells showed a dramatic increase in the number of actin stress fibers and focal adhesion contacts, compared to wild-type cells (Andrä et al., 1998). Plectin seemed to destabilize actin filaments instead of favoring the formation of stable adhesion complexes, as one could expect based on its stabilizing effect on hemi-

desmosomal junctions (Andrä et al., 1998). Thus, plectin seems to act not only as a mechanical linker of different structural elements but also as a regulator of their dynamic rearrangements. According to this hypothesis, plectin was proposed to act as a cytoskeletal scaffolding platform for proteins involved in signaling and cytoskeletal reorganization. Its enormous surface area and multidomain structure would ideally be suited to facilitate such a task (Janda et al., 2001). This notion is also supported by the high number of different plectin-binding proteins that have been identified (Steinböck and Wiche, 1999). Among several interaction partners linked to signaling the nonreceptor tyrosine kinase Fer binds to plectin's N-terminal globular domain and the absence of plectin leads to an elevation of its kinase activity (Lunter and Wiche, 2002). The finding of a high affinity interaction between an N-terminal plectin peptide (residues 95-117) and the ubiquitin E₃ ligase Siah, suggested a potentially new regulatory role of plectin in the selective degradation of proteins (House et al., 2003). Using yeast two hybrid screening, RACK1, the receptor for activated C kinase, and the regulatory γ 1 subunit of AMP-activated protein kinase (AMPK), the key regulatory enzyme of energy homeostasis, have been identified as a binding partners of plectin (Osmanagic-Myers and Wiche, 2004; Gregor et al., 2006). Finally, plectin was found to play a role in the regulation of keratin filament dynamics. It has been shown that upon incubation of keratinocytes with the protein phosphatase inhibitor okadaic acid (OA), collapse of keratin networks proceeds significantly faster in plectin-deficient compared with wild-type cells (Osmanagic-Myers et al., 2006).

Plectin deficiency

Defects in plectin expression lead to epidermolysis bullosa simplex (EBD)-MD, a severe hereditary skin blistering disease combined with muscular dystrophy (Gache et al., 1996; Chavanas et al., 1996; McLean et al., 1996; Pulkkinen et al., 1996; Smith et al., 1996). The skin pathology is due to defects in hemidesmosomes, which show disrupted anchorage of keratins. In addition, a number of studies reported that some EBS-MD patients additionally suffer from inspiratory stridor and respiratory distress involving laryngeal obstruction and urethral strictures (Mellerio et al., 1997; Dang et al., 1998). A form of an inherited autosomal dominant skin disease known as EBS-Ogna, linked to chromosome 8q24, has also been linked to defects in the plectin gene (Koss-Harnes et al., 1997; Koss-Harnes et al., 2002). Schröder et al. (2002) reported an EBS-MD patient with a novel homozygous 16-bp insertion

mutation in plectin's C-terminal domain residing in close proximity to the IF-binding site. The latter mutation results in marked subsarcolemmal and intermyofibrillar desmin filaments accumulation in muscle tissues that can be attributed to faulty protein-protein interaction between the mutated plectin molecules and desmin IFs.

Plectin-null mice, generated by targeted gene inactivation (Andrä et al., 1997) showed that while structures of desmosomes and hemidesmosomes seem to be unaffected, the number of hemidesmosomes was significantly reduced and their mechanical stability impaired. Skeletal muscle biopsies of plectin-deficient mice revealed an increased number of necrotic muscle fibers, focal disruptions of sarcomeres and aberrant Z-disk formations.

Conditional gene targeting in mice revealed that in striated muscle plectin deficiency results in progressive degenerative modifications, including detachment of the contractile apparatus from the sarcolemma, decreased number and dysfunction of mitochondria, and partial loss and aggregation of IF networks in distinct cytoplasmic compartments, depending on the missing isoform (Konieczny et al., 2008). Plectin 1d and 1f, two major plectin isoforms expressed in muscle, integrate fibers by specifically targeting and linking desmin IFs to Z-disks and costameres, whereas plectin 1b establishes a linkage to mitochondria. Additionally, mouse fibroblasts and myoblasts that selectively lack this isoform but express all others showed extensive elongation of mitochondrial networks, while other mitochondrial properties remained largely unaffected (Winter et al., 2008). Mice with conditionally deleted plectin in stratified epithelia died early after birth with signs of starvation, growth retardation, and blistering on their extremities. The epidermis of this knockout was very fragile and showed focal epidermal barrier defects caused by the presence of small skin lesions (Ackerl et al., 2007).

5.5. S-Nitrosylation and oxidation

All proteins residing in the cytoplasm are directly exposed to oxidative stress, which leads to formation of disulfide bridges between at least two cysteines that can contribute to maintaining the structure of such proteins. Disulfides maintain the conformational integrity of proteins. In their reduced state, proteins without disulfide bonds tend to be unfolded, because they lack the stabilizing influence of these bonds. This depends however on the

intrinsic stability of the folded conformation and upon the stabilizing contribution of any disulfide bonds (Creighton, 1986). The formation of disulfide bonds is necessary for many proteins, especially for their cellular function and conformational stability.

The C-terminal part of plectin contains from 13 (mouse) to 17 (human) cysteines (Liu et al., 1996; Fuchs et al., 1999). Four of these generally highly conserved residues are clustered in the repeat 5 domain harboring also the IF-binding site. This tempting localization might have a functional purpose, as these cysteines could form intra- and inter-repeat disulfide bridges, thereby providing more structural rigidity to the protein itself. Intracellular disulfide bridge formation is likely to be of particular importance in situations where cells have to respond to mechanical, oxidative or other types of stress. Reversible *in vivo* modifications of cysteines by local redox changes could lead either to cysteine oxidation through reactive oxygen species or to S-nitrosylation through reactive NO. In addition, reactive oxygen species could convert NO into higher oxides of nitrogen and radicals, such as peroxynitrite, which efficiently oxidize thiol groups (Lane et al., 2001).

5.5.1. Oxidative stress and vascular NO release

NO is a reactive molecule that can rapidly diffuse throughout the whole cell, which can react with sulfur groups on cysteine residues that are present in an acid–cysteine–base motif. This results in reversible S-nitrosylation and in the presence of reducing enzymes, such as GSNO-reductase, may also lead to the formation of disulfide bridges between cysteine residues (Kim et al., 2002; Liu et al., 2004). The rapid access of NO to different parts of the endothelial cell and reactivity with a broad scale of biological molecules makes NO very appropriate for the coordination of cellular processes through posttranslational protein modification. Redox reactive molecules may play a role in integrating signaling events and determine the duration and strength of signaling (Nathan, 2003). One important function of NO in oxidative phosphorylation may be its competition with oxygen as an electron acceptor in respiratory complex IV (Moncada and Erusalimsky, 2002). As a consequence, with decreasing oxygen availability, NO will predominate as an electron acceptor and reduce oxidative phosphorylation thus limiting energy expenditure.

Like for NO, reactive oxygen species may also provide permissive signaling. The H₂O₂ is the predominant reactive oxygen component in the intracellular environment where superoxide dismutase is present (Finkel, 1998). H₂O₂ can also react with cysteine residues

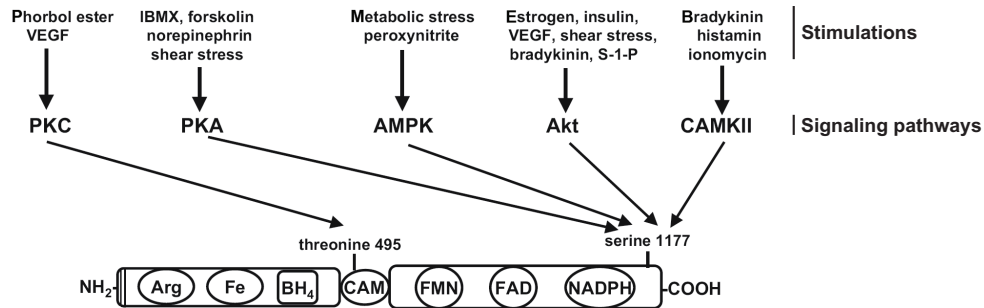


Figure 3. Regulation of endothelial NO synthase (eNOS). eNOS consists of a C-terminal reductase domain containing binding sites for the nicotinamide adenine dinucleotide phosphate (NADPH), flavin adenine dinucleotide (FAD), and flavin mononucleotide (FMN), and of an N-terminal oxygenase domain with binding sites for heme (Fe), tetrahydrobiopterin (BH₄), and L-arginine (Arg). Both domains are linked by a recognition site for calmodulin (CAM). Several amino acid residues of eNOS undergo posttranslational phosphorylation controlling the enzyme activation. Threonine 495 is a negative regulatory site (phosphorylation is associated with a decrease in enzyme activity). Serine 1177 combines several signaling pathways upon cell stimulation and promotes the activation of eNOS. AMPK, 5'-AMP-activated kinase; CAM, calmodulin; CAMKII, calmodulin-dependent kinase II; IBMX, isobutylmethylxanthine; PKA, protein kinase A; PKC, protein kinase C; S-1-P, sphingosine-1-phosphate; VEGF, vascular endothelial growth factor (modified from Heller et al., 2006)

leading to the formation of sulfenic acid (SOH) and disulfide modifications (Stuehr et al., 2004). Similarly to NO, H₂O₂ can also rapidly diffuse throughout the cell. However, the cellular events are different from that induced by NO, H₂O₂ results in the phosphorylation of transcription factors such as NF- κ B, AP1, and CREB1 e.g. (Finkel, 1998).

5.5.2. Regulation of eNOS activation

Endothelium-derived NO is generated from L-arginine by the endothelial isoform of NO synthases under remarkably complex regulation (Fleming and Busse, 2003). eNOS consists of a C-terminal reductase domain containing binding sites for the reduced form of NADPH and the flavin cofactors FAD and flavin mononucleotide (FMN), and of an N-terminal oxygenase domain with binding sites for heme, tetrahydrobiopterin (BH₄) and L-arginine (Fig. 3). Both terminal domains are connected by a recognition site for calmodulin (CaM). Activation of eNOS occurs upon an increase of intracellular Ca²⁺ and binding of the subsequently formed Ca²⁺/CaM complex which then permits the electron flux required for NO generation (Alderton et al., 2001). Alternatively, eNOS can be activated by the phosphorylation of the amino acid residue serine 1177 (human eNOS sequence), which then enhances electron flux through the reductase domain and improves Ca²⁺ sensitivity of the enzyme (Fleming and Busse, 2003). Several protein kinases including Akt/protein kinase B,

protein kinase A (PKA), AMPK, and calmodulin-dependent kinase II (CAMKII) have been shown to phosphorylate serine 1177 and to participate in the eNOS activation. On the other hand, most probably PKC basally phosphorylates the threonine 495 residue (human eNOS sequence), which may be dephosphorylated upon stimulation of cells and its response to bradykinin (Fleming and Busse, 2003).

In endothelial cells eNOS colocalizes with caveolae and lipid rafts of the plasma membrane (Shaul et al., 1996; Sowa et al., 2001) and have been also found on the cytoplasmic face of the Golgi complex (O'Brien et al., 1995; Fulton et al., 2002; Fulton et al., 2004). Proper subcellular localization seems to be critical for the phosphorylation and activation of the enzyme, as mislocalization of eNOS leads to the attenuation of both, agonist-stimulated NO release and eNOS phosphorylation (Sakoda et al., 1995; Sessa et al., 1995; Fulton et al., 2004; Jagnandan et al., 2005).

As well as the other NOS isoforms, eNOS is an NADPH-consuming enzyme, which ensures electron flow from the reductase domain of the enzyme toward the heme-containing oxygenase domain. The cofactor CaM is an important checkpoint required for the shuttling of electrons toward the heme group (Stuehr et al., 2004). In the presence of oxygen a very reactive superoxy ferrous–peroxy ferric complex is formed. Another important checkpoint, the eNOS cofactor BH₄, facilitates the reaction of L-arginine with the electrons and oxygen, which leads then to the formation of L-citrulline and NO (Werner et al., 2003). However, if either BH₄ or the substrate L-arginine are lacking, the superoxy ferrous–peroxy ferric complex may dissociate and result in the formation of superoxide (if BH₄ is lacking) or H₂O₂ (if L-arginine is lacking) (Werner et al., 2003; Berka et al., 2004). This state of eNOS known as “uncoupled state”, has been regarded as an abnormality of eNOS function and was found to be associated with risk factors for atherosclerosis. Uncoupled state of eNOS indicates that the endothelial cell can switch from a quiescent state (NO) into a state adapted for the host defense (H₂O₂). In this respect, formation of the reactive oxygen species by uncoupled eNOS could be considered as a physiological signalization during injury and infection, and in fact it may be an essential mechanism in the host defense response.

6. MAJOR GOALS

As described above, plectin's C-terminal domain consists of 6 repeat domains connected by linker regions, and the linker between repeat domains 5 and 6 is harboring the binding site for IFs. Plectin contains at least 13 cysteines, 4 of which reside in repeat 5, and a unique Cdk1 phosphorylation site resides in repeat 6.

Initially, the goal of my thesis was to resolve the 3D crystal structure of the repeat domains containing plectin's IF-binding site. In particular, the focus was on repeat domain 5 in its singular form, and in forms combined with either repeat domain 4 or 6. As crystallization requires proteins of high purity and may not always be successful, another goal to be approached in parallel was to study biochemical and cell biological aspects of plectin's interaction with vimentin. In this context it was of particular interest to study the question, whether the binding of vimentin to plectin was affected upon oxidation of cysteines located near the IF-binding site of plectin. To gain insight into the location and accessibility of the cysteine residues within the repeat 5 domain, one of my goals was to generate a 3D model of the plectin repeat 5 domain by homology modelling based on the recently solved crystal structure of the desmoplakin repeat domain B. As the localization of cysteines in the repeat 5 domain might serve a functional purpose I was interested if these cysteines could form intra- and/or inter-repeat disulfide bridges and if the binding affinity of the repeat 5 domain to vimentin was affected by their oxidative state. S-Nitrosylation has a potential role in the regulation of protein function in response to oxidative stress and therefore my next goal was to test whether some of the cysteines are targets for nitrosylation and whether S-nitrosylation has any effects on the structure or functions of IFs. If S-nitrosylation was found to have consequences on plectin-regulated cellular functions the question would be whether eNOS and/or NO production were affected.

In a third part of my thesis several questions concerning the Cdk1 phosphorylation site near the IF-binding site were to be addressed. The first questions were whether the binding of vimentin to plectin was affected upon phosphorylation by mitotic Cdk1 and whether phosphorylation had an influence on IF cytoarchitecture. As a major organizing element of IF network cytoarchitecture plectin may well affect also IF network assembly dynamics. Therefore another question to be addressed was whether plectin deficiency has an

influence on IF network formation in spreading cells after replating and during reformation of IF networks after cell division. If such an influence could be found one of my goals was to study the dynamics of this network formation in live cells using time-lapse microscopy.

7. MATERIALS AND METHODS

7.1. Homology modeling

A model was generated by an automated homology modeling server (ExpASY proteomics server using SWISS-MODEL-ProModII) running at the Swiss Institute of Bioinformatics (Geneva), and GENO3D (Lyon). The structural template used for modeling was the crystal structure of human desmoplakin repeat domain B (PDB Identifier 1LM7) (Choi et al., 2002), which shares 73% sequence identity with plectin's repeat 5 domain. Modeling by satisfaction of spatial restraints was performed by the method of Combet et al. (2002). The alignment of the target (plectin repeat 5 domain) and the template (desmoplakin B domain) was obtained using Needleman-Wunsch global alignment algorithm on EMBL-EBI server (<http://www.ebi.ac.uk/emboss/align/>). Restraints on various distances, angles, and dihedral angles in the sequence were derived from the alignment of the target with the template structure. Finally, the three-dimensional (3D) model was refined by applying distance geometry, simulated annealing and energy minimization procedures. Visualization of the 3D structure was performed using the molecular-graphics package Yasara (<http://www.yasara.com>).

7.2. cDNA constructs, plasmids, and site directed mutagenesis

Plectin's repeat 4 and 5 domains comprise residues 3780-4024 and 4025-4367 (SwissProt accession number P30427), respectively. The domains were amplified by PCR, using as template a mouse plectin cDNA (exons 31 and 32; Fuchs et al., 1999), and subcloned into pBN120, a pET15b derivative (Nikolic et al., 1996). Mutagenesis was carried out by an overlap extension approach, or by using the QuickChange site-directed mutagenesis kit (Stratagene) with primers designed to substitute cysteines with serines. All constructs were verified by automated DNA sequencing. Wild-type repeat 5 domain and its cysteine mutants were cloned by K. Abdoulrahman (PhD thesis, 2004).

For bacterial expression, full-length mouse vimentin cDNA (GenBank accession

number M26251), including the stop codon at position bp 1879-1881, was excised from mammalian expression vector pMCV21 and subcloned in several steps into a modified version of plasmid pET23a (Novagen), yielding plasmid pFS129 (Steinböck et al., 2000). Tagless vimentin encoded by pFS129 was used in all in vitro experiments.

For transfection of cells in culture (chapter 7.42), plasmid pMG3, encoding GFP-tagged vimentin, was generated (by M. Gregor) by subcloning mouse vimentin cDNA (a generous gift of P. Traub; plasmid pMC-V21) (Steinböck et al., 2000) into vector pEGFP-C1 (BD Biosciences Clontech).

7.3. Proteins

7.3.1. Expression of recombinant proteins in *E. coli*

Recombinant proteins were expressed in the *E. coli* strain BL21 (DE3) after induction with 1 mM IPTG, when culture reached an OD₆₀₀ of 0.5 to 0.7, at 30°C in 1000 ml of LB-amp medium. Cells harvested by centrifugation at 5000 rpm, 10 min, 4°C were either frozen in liquid nitrogen or resuspended in 1/20 of volume of lysis buffer (10 mM piperazine, pH 11.0, 1% Triton X-100).

7.3.2. Purification of recombinant plectin repeat domains

Disruption of the cells was performed by incubation with lysozyme (0.1 mg/ml) for 30 min followed by sonication (Bandolin Sonopuls). The procedure was repeated twice keeping the cells on ice and then lysates were centrifuged at 12000 rpm, 30 min, 4°C prior to next purification procedures. His-tagged recombinant proteins were then affinity-purified on ÄKTA FPLC™ using 5ml HisTrap HP columns following the protocol of the manufacturer, using the binding, washing, and elution column buffers (20 mM Tris-HCl, pH 9.0, containing 5, 20, and 500 mM imidazole, respectively). Only purification of R4-5 was followed then by ion-exchange chromatography on 15 ml Source 30Q column; after loading sample column was washed (20 mM Tris-HCl, pH 9.0) and protein eluted with a 0-2 M NaCl. Gel filtration on HiLoad Superdex 75 column (20 mM Tris-HCl, pH 9.0, 150 mM NaCl) was used as a last purification step. Proteins were kept in elution buffer at 4°C, and dialyzed against the required buffer prior to be assayed.

7.3.3. Purification of recombinant full length vimentin

Recombinant full length mouse vimentin was purified by sequential ion-exchange column chromatography on Q-sepharose and S-sepharose (ÄKTA FPLC™) as described previously (Nagai and Thogersen, 1987). Following expression, bacterial cell pellets were resuspended in 1/20 volume lysis buffer (5 mM Tris-HCl, pH 7.5, 1 mM EDTA), incubated with lysozyme (10 µg/ml, 30 min) and disrupted in a dounce homogenizer. MnCl₂ (1 mM), MgCl₂ (10 mM) and DNase I (10 µg/ml) were added to the cell suspension to digest the DNA. This mixture was incubated 30 min at room temperature, then 4 volumes of detergent buffer (20 mM Tris-HCl, pH 7.5, 200 mM NaCl, 1% Deoxycholic acid, 1% Nonidet P40) was added, and finally the suspension was centrifuged (7500 rpm, 10 min, 4°C). The recovered pellet was dissolved in 15 ml binding buffer (9 M Urea, 5 mM Tris-HCl, pH 7.5, 1 mM EDTA, 0.4 mM PMSF, 0.1% β-ME) and centrifuged again (19000 rpm, 15 min, 8°C). The supernatant was then used for ion-exchange chromatography on 15 ml Q-Sepharose column using ÄKTA FPLC™. The column was washed with Q-sepharose column buffer (8 M Urea, 5 mM Tris-HCl, pH 7.5, 1 mM EDTA, 0.4 mM PMSF, 10 mM β-ME) and the protein eluted with a 0-0.5 M NaCl gradient. Fractions with the highest protein concentration were combined, diluted with 7 volumes of SP-Sepharose column buffer (8 M Urea, 50 mM Na-formate, pH 4.0, 0.4 mM PMSF, 10 mM β-ME), and loaded onto 15 ml SP-Sepharose column. The column was washed with 5 volumes of SP-Sepharose column buffer and eluted with a 0-0.5 M KCl gradient. Purified vimentin was kept in elution buffer at 4°C, and dialyzed stepwise against the required buffer prior to be assayed. All proteins were analyzed by SDS-PAGE and concentrations were estimated by the Bradford or the bicinchoninic acid (BCA) method (Pierce).

7.3.4. Determination of protein concentration

Bradford method: Protein content of samples was measured with Bradford Reagent (100 mg Coomassie G-250 dissolved in 50 ml ethanol, followed by addition of 100 ml 85% H₃PO₄, and distilled water to 1000 ml). Protein samples were mixed with the Bradford Reagent and incubated for 5 minutes at room temperature. Subsequently absorbance was measured at 595 nm. Concentrations of protein samples were calculated using a bovine serum albumin (BSA) standard curve.

Bicinchoninic acid (BCA) method: BCA reagent mix was prepared immediately

before use by mixing BCA-reagent A with BCA-reagent B (Pierce) in a 50:1 ratio. 50 µl of protein sample were added to 1 ml BCA reagent mix, and incubated for 30 minutes at 37°C. The samples were cooled to room temperature and absorbance at 562 nm was measured. The protein concentration was calculated from standard curve.

7.3.5. Crystallization of plectin repeat domains

The purified proteins were dialyzed against 20 mM Tris-HCl, pH 9.0 and concentrated to 10 or 20 mg/ml for crystallization. Crystallization trials were performed at 4 and 20 °C using the sitting- and hanging-drop vapor diffusion method (McPherson, 1982). Drops were prepared by mixing 1 µl protein solution prepared as described above with 1 µl reservoir solution. The initial screenings for crystallization conditions was performed using the Crystal Screens from Hampton Research and JBScreens from Jena BioScience.

7.3.6. SDS-PAGE and immunoblotting

Protein samples (10 µg in 20 µl) were analyzed by SDS-10% PAGE under reducing and nonreducing conditions. The reduction of samples before application to the gel was achieved by addition of 0.2 M dithiothreitol (DTT) to 2x sample buffer. After electrophoresis, the gels were stained with Coomassie Blue (0.25% Coomassie Brilliant Blue, 45% methanol, 10% acetic acid) and scanned in HP ScanJet 8250. Densitometric analysis was performed with the Gel Doc 2000 (Bio-Rad Laboratories) gel documentation system and the QuantityOne image analysis software (Bio-Rad Laboratories).

Transfer to nitrocellulose membranes (Schleicher & Schuell, Portan® 0.2 µm) and immunoblotting were done using standard procedures. Following electrophoretic transfer of proteins to nitrocellulose, the membranes were blocked for 60 minutes with 5% milk powder in phosphate-buffered saline containing 0.05% Tween (PBST), incubated with primary antibodies diluted in PBST for 60 minutes, washed extensively in PBST, and then incubated with peroxidase-coupled secondary antibodies for 60 minutes. For detection of immunoreactive bands, the Super Signal System (Pierce) was used. Signal intensities were quantified using the program Quantiscan.

7.3.7. Oxidative cross-linking

For oxidative cross-linking of plectin repeats, purified recombinant proteins at a

concentration of 0.5 mg/ml were dialyzed against 10 mM Tris-HCl, pH 7.9, overnight at 4°C, while concurrently exposed to oxidation by air. The reaction was quenched by addition of iodoacetamide (final concentration 50 mM) to block free sulfhydryl groups. Samples were then resolved by SDS-10% PAGE under nonreducing or reducing conditions. Alternatively, aliquots of two different recombinant proteins were mixed 1:1 at a concentration of 0.5 mg/ml each, dialyzed against 10 mM Tris-HCl, pH 7.9, 6 M urea, and 1 mM DTT, for 1.5 h at room temperature, and subsequently oxidized by air while dialyzed at 4°C into 10 mM Tris-HCl, pH 7.9, without urea. The reactions were then quenched and analyzed as described above.

For oxidative cross-linking of plectin repeat 5 domain and vimentin, polymerized vimentin was incubated with His-tagged plectin R5 wt, or R5 Cys-free, and then oxidized by 100 μ M SNAP for 2 hours. Samples were dissolved in gel loading buffer supplemented with 6M urea, subjected to SDS-10% PAGE under nonreducing conditions, and immunoblotted using anti-His-tag or anti-vimentin antibodies.

7.3.8. Europium overlay binding assay

Recombinant vimentin was dialyzed stepwise against 50 mM NaHCO₃, pH 8.5, and labeled with Eu³⁺ overnight at room temperature, using 10 μ l of Eu³⁺-labeling reagent per 100 μ l of protein samples (0.5-1.5 mg/ml) according to the protocol of the manufacturer (Wallac, Turku, Finland). When vimentin was labeled with Eu³⁺, it was subsequently Cdk1-phosphorylated in some samples as described later. For binding assays, 96-well microtiter plates were coated (overnight at 4°C) with 100 μ l of 100 nM recombinant non-phosphorylated or Cdk1-phosphorylated plectin R5-6, or BSA type H1 (Gerbu Biotechnik, Gaiberg, Germany), all in 25 mM Na₂B₄O₇, pH 9.3. Coating was followed by blocking with 4% BSA in PBS, for 1 hour at room temperature. After washing with PBS, plates were overlaid with dilutions of Eu³⁺-labeled proteins (10-500 nM) in 100 μ l of PBS, 1 mM EGTA, 2 mM MgCl₂, 1 mM DTT, and 0.1% Tween 20, for 90 minutes at room temperature. Plates were washed six times with PBS, and protein bound was then determined by releasing the complexed Eu³⁺ with enhancement solution and measuring fluorescence with a Delfia time-resolved fluorometer (Wallac; excitation wavelength 340 nm, emission wavelength 615 nm). Further details of this assay have previously been described (Nikolic et al., 1996; Steinböck et al., 2000). The Scatchard method was used for analysis of binding data and

fluorescence values converted to concentrations by comparison with a Eu^{3+} standard.

7.3.9. S-nitrosylation biotin-switch assay

S-nitrosylated proteins were detected using the biotin-switch assay as described by Jaffrey and Snyder (Jaffrey and Snyder, 2001). For in vitro assays purified R5 wt and R5-C4S (80 μg each) in 250 mM HEPES, pH 7.7, 1 mM EDTA, 0.1 mM neocuproine (HEN solution) were incubated in the dark with 100 μM SNAP for 2 h at room temperature, and the NO donors were then removed by passing the samples twice through a desalting column (Micro BioSpin P6, BioRad). Proteins in the flowthrough were blocked with 20 mM methyl methanethio-sulfonate (MMTS, Sigma) for 20 min at 50°C, precipitated with acetone for 20 min at -20°C, and collected by centrifugation at 10,000xg for 10 min at 4°C. Pellets were resuspended in 500 μl HENS (HEN solution containing 1% SDS), and incubated with 1 mM ascorbic acid to release NO from thiol groups, which were subsequently biotinylated with 1 mM biotin-HPDP (Pierce). Proteins were again acetone-precipitated, resuspended in 300 μl HENS solution, and biotinylated proteins recovered by streptavidin-affinity chromatography. Eluted proteins were separated by SDS-10% PAGE, transferred to nitrocellulose membranes and analyzed by immunoblotting using antibodies and visualized by chemiluminescence.

For the identification of S-nitrosylated proteins in cultured cells, confluent mouse renal endothelial cells ($\sim 2.5 \times 10^7$) were incubated with 100 μM SNAP for 2 h in the dark, or with 100 nM PMA for 20 h, washed thoroughly with PBS, scraped off, and lysed in 350 μl

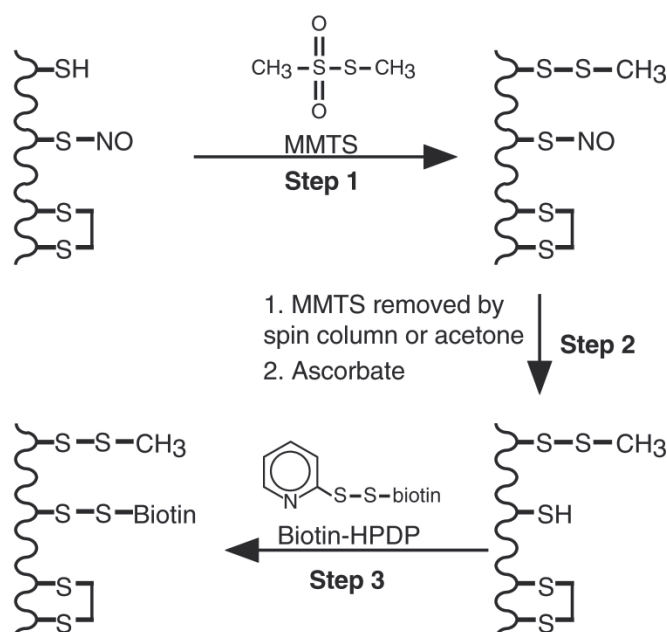


Figure 4. Schematic diagram of the Biotin switch assay for the detection of the S-nitrosylated proteins. A protein is indicated with cysteines in the free thiol, disulfide or nitrosothiol form. In the first step of this assay free thiols are blocked by methylthiolation with MMTS, and this modification can be reversed by β -ME reduction. Remaining MMTS is then removed in the next step either by acetone precipitation of protein mixture or by passing through the spin column. In the final step nitrosothiols are selectively reduced by the ascorbate to thiols form, which are then biotinylated by biotin-HPDP. Note that biotinylated proteins could be detected directly with antibodies or recovered by streptavidin-affinity chromatography (Jaffrey and Snyder, 2001).

HEN solution supplemented with 2.5% SDS, blocked with MMTS, and subjected to the biotin-switch assay as described above.

7.3.10. Phosphorylation of proteins by Cdk1

10 µg of the proteins (plectin R5-6 or vimentin) were resuspended in 20 mM Tris-HCl, pH 7.4, 100 mM MgCl₂, 1 mM EGTA, 1 mM NaF, and 0.1 mM ATP, and incubated (30 min at 37°C) with 1 unit of recombinant Cdk1/cyclinB (Vermeulen et al., 2002), kindly provided by V. Krystof (Palacky University, Olomouc, Czech Republic). The reaction was stopped by adding EDTA to a final concentration of 10 mM.

7.3.11. IFs assembly in vitro

To prepare filaments, recombinant vimentin was dialyzed stepwise at room temperature against 5 mM Tris-acetate, pH 8.3, 1 mM EDTA, and 10 mM β-ME, with decreasing concentrations of urea (6-0 M). The dialyzed vimentin solution was centrifuged in a Beckmann benchtop ultracentrifuge (Optima™ TLX) at 100,000xg for 30 min at room temperature. Soluble non-phosphorylated or Cdk1-phosphorylated vimentin was mixed with (either unphosphorylated or phosphorylated) plectin domain R5-6 at different concentrations (molar ratios of vimentin:plectin 1:1-10:1) and polymerized in 20 mM HEPES, pH 7.5, 150 mM NaCl, 1 mM EDTA, and 0.1% (v/v) Tween-20, for 1 h at 37°C.

7.3.12. Electron microscopy

For staining with uranyl acetate, 7 µl of protein samples (final concentrations 10 µM) were loaded onto Formvar/carbon-coated and glow-discharged 400 mesh-copper grids and stained 8 times (40 s each) with 1% uranyl acetate. Specimens were visualized in a JEOL 1210 electron microscope operated at 80 kV.

7.4. Mammalian cell culture

7.4.1. Cell culture

The immortalized endothelial cell line used in this study was generated by Kerstin Andrä Marobela. Primary mouse kidney endothelial cells isolated by standard procedures from

wild-type and plectin^{-/-} neonatal (1 day old) mice were transduced with a polyoma middle T (PymT)-expressing retrovirus that confers growth advantage to endothelial cells over other types of cells (Williams et al., 1988). The kidneys from one mouse were excised, rinsed 3x with PBS, minced, and digested with 0.1 mg/ml collagenase (type XI, Sigma) for 30 min with gentle shaking at 37°C in 5 ml DMEM. After centrifugation, the cell pellet was resuspended in DMEM supplemented with 10% heat-inactivated fetal calf serum and seeded onto two 9.6 cm² 0.2% gelatin-coated plates (2 wells of a 6 well plate). Two days later the cell monolayers were infected with PymT as described previously (Golenhofen et al., 2002). In brief, after a 2 h exposure to the virus, the medium was exchanged, cells were cultured for 48 h and then selected with G418 (0.8 µg/ml). Stable cell lines were obtained 4-5 weeks later. Cultures were subsequently expanded and characterized for several endothelial marker proteins such as von Willebrand factor, VE-cadherin, and PECAM-1 (CD31). Cells were negative for cytokeratins, GFAP, and the tight junction protein zona occludens 1 (ZO-1). Immortalized cells lines were routinely maintained on gelatin (Spurny et al., 2007).

Immortalized mouse dermal fibroblasts were derived from plectin^{+/+}/p53^{-/-} (wild-type) and plectin^{-/-}/p53^{-/-} (knockout) mice as previously described (Andrä et al., 2003). Primary cells were derived in a similar manner from plectin^{+/+} and plectin^{-/-} mice. Experiments with immortalized cells were performed with cells from passages 8 to 15 after isolation. Cells were grown at 37°C in Dulbecco's modified Eagle's medium supplemented with 10% fetal calf serum. Confluent cultures grown on plastic dishes were trypsinized, dispersed into culture medium, and the cells replated onto coverslips at densities of 10⁴-10⁵/cm² (Prahlad et al., 1998).

7.4.2. Preparation of cell lysates

Confluent cells were washed twice with phosphate-buffered saline. Cells were lysed directly with 50 mM Tris-HCl, pH 6.8, 100 mM DTT, 2% SDS, 0.1% bromphenol blue, 10% glycerol (sample buffer). Aliquots of cell lysates containing equal amounts of total proteins were separated by SDS 5% PAGE and, after immunoblotting protein bands were visualized by exposure to x-ray film as described above.

7.4.3. NO donor mediated nitrosylation of endothelial cells

Endothelial cells were grown on gelatin-coated glass coverslips, treated with NO donor-

mediated nitrosylation 100 μ M SNAP in the dark for 2, 4, or 6 h, washed with PBS, and then fixed with cold methanol at -20°C for 90 sec prior to processing for immunofluorescence microscopy (Gregor et al., 2006). After incubation with primary and secondary antibodies, specimens were viewed in a Zeiss Axiophot fluorescence microscope and confocal images were obtained using an LSM 510 module (Carl Zeiss).

7.4.4. Spectrofluorimetric determination of NO released from endothelial cells

NO release by endothelial cells was measured using the DAF-2 fluorescence assay, as described previously (Leikert et al., 2001; Rathel et al., 2003). Endothelial cells were grown until confluence and for selected experiments stimulated with protein kinase A activator PMA (100 nM) for 20 hours. Cells were washed twice with PBS containing arginine (100 μ M) and incubated with 2 ml of this buffer with or without the irreversible eNOS inhibitor L-NAA (200 μ M). After 10 minutes of equilibration at 37°C , the NO-sensitive fluorescent probe DAF-2 as well as calcium ionophore A23187 were added into the buffer. Following another 30 minutes of incubation at 37°C , the supernatant was taken off into reaction tubes, cells were washed with 1 ml of ice cold PBS, and stored at 4°C until further processing. Fluorescence was measured in quartz cuvettes at 515 nm (excitation: 492 nm) in a Shimadzu fluorometer. Then the cells were trypsinized and counted automatically in a ViCell cell counter (Beckman Coulter). Fluorescence units were normalized to the number of cells.

7.4.5. Synchronization by double thymidine block

Fibroblast cell synchronization was performed by double thymidine block followed by nocodazole treatment. For the first block, exponentially growing cells were incubated with 2 mM thymidine for 16 h. This was followed by a 9-h release in which cells were washed and incubated in fresh medium, and a second block for another 16 h. Cells were then washed and cultivated for an additional 24 h in growth medium containing 400 ng/ml nocodazole. Mitotic cells that rounded up and detached from the petri dish were harvested by mechanical shake-off (Merrill, 1998), washed thoroughly to remove nocodazole, replated on polylysine-coated glass coverslips and then incubated at 37°C to allow for cell cycle progression. At different time intervals, cells were fixed in 4% formaldehyde and processed for immunofluorescence microscopy.

7.4.6. Immunofluorescence microscopy

Endothelial cells grown on gelatin-coated glass coverslips in DMEM supplemented with 10% fetal calf serum and a standard complement of antibiotics were rinsed rapidly in PBS, and fixed in methanol for 90 seconds at -20°C. Fibroblasts, plated on glass coverslips, were fixed in 100 mM Pipes, 2 mM EGTA, 1 mM MgSO₄, pH 6.9 (PEM), supplemented with 4% formaldehyde for 6 min at room temperature; after fixation, cells were permeabilized in 0.1% NP-40 in PEM for 3 min at room temperature, and then briefly washed in PEM for 3 min. BSA (5%) was added to the fixed cells to block non-specific binding sites, and cells were then washed five times for 5 minutes with PBS. Samples were incubated with primary antibodies for 1 hour at room temperature. Coverslips were then washed thoroughly with PBS, incubated with secondary antibodies for 1 hour at room temperature, washed again with PBS, and finally rinsed with water and mounted in mowiol. For actin-staining, phalloidin-Texas Red (dilution 1:150) was used in the mixture with secondary antibodies. Specimens were viewed in a Zeiss Axiophot fluorescence microscope and confocal images were obtained using an LSM 510 module (Carl Zeiss).

7.4.7. Cell transfection

For live cell observations, a cDNA construct (pMG3) encoding GFP-tagged vimentin was transfected into wild-type and plectin-null fibroblasts using Fugene (Roche Applied Science) following the instructions of the manufacturer. Briefly, 6 µl Fugene reagent was incubated with 100 µl of serum free DMEM and 2 µg DNA for 30 minutes at room temperature. Then an appropriate volume (final volume 50 µl) of Opti-MEM was added, and this mix was subsequently added to the medium of a sub-confluent cell culture (culture dish 5 cm in diameter). After 24-48 h of transfection, cells were trypsinized and replated onto glass coverslips for live cell observations.

7.4.8. Live-cell imaging

Time-lapse video microscopy was implemented on a Zeiss Axiovert S100TV microscope equipped with phase-contrast and epi-illumination optics. Cells were spread on glass coverslips at a density of 2.8×10^5 cells/cm² and kept in phenol red-free DMEM during the whole period of observation. Cells were monitored in a closed POCmini cultivation system (Carl Zeiss MicroImaging, Inc) under 5% CO₂ and at 37°C. Recordings of squiggle motility

started 14 h after plating, and frames were taken with a 100x lens in 10-sec intervals over a period of 15 min. Images were obtained using a back-illuminated, cooled charge-coupled device camera (Princeton Research Instruments) driven by a 16-bit controller. The whole video microscopy system was automated by Metamorph 6.3 (Universal Imaging Corporation). The length of trajectories of moving squiggles was measured by tracking their ends. For statistical evaluation 20–30 squiggles per genotype were monitored.

7.5. Antibodies

Lists of antibodies used for immunoblotting (A) and immunofluorescence microscopy (B):

A

Immunoblotting					
Primary antibody (Anti-)	Source	Dilution	Secondary antibody	Source	Dilution
Plectin #46	Andrä et al., 2003	1:4000	goat anti-rabbit HRPO	Jackson Laboratories	1:50,000
Plectin #9	Andrä et al., 2003	1:2500	goat anti-rabbit HRPO	Jackson Laboratories	1:50,000
Plectin 10F6	Foisner et al., 1994	1:100	goat anti-mouse HRPO	Jackson Laboratories	1:50,000
Plectin exon 1	Abrahamsberg et al., 2005	1:1000	goat anti-rabbit HRPO	Jackson Laboratories	1:30,000
Plectin exon 1f	Abrahamsberg et al., 2005	1:1000	goat anti-rabbit HRPO	Jackson Laboratories	1:30,000
Vimentin	Giese and Traub, 1986	1:10,000	donkey anti-goat HRPO	Jackson Laboratories	1:50,000
Actin	A-2066; Sigma-Aldrich	1:1000	goat anti-rabbit HRPO	Jackson Laboratories	1:30,000
HIS tag	34660; Qiagen Inc.	1:1000	goat anti-mouse HRPO	Jackson Laboratories	1:20,000
eNOS	610297; BD Trans. Lab.	1:1000	goat anti-rabbit HRPO	Jackson Laboratories	1:20,000
eNOS Thr495	9574; Cell Signaling	1:1000	goat anti-rabbit HRPO	Jackson Laboratories	1:20,000
eNOS Ser1177	9571; Cell Signaling	1:1000	goat anti-rabbit HRPO	Jackson Laboratories	1:20,000
Akt	9272; Cell Signaling	1:1000	goat anti-rabbit HRPO	Jackson Laboratories	1:20,000
Akt Ser473	9271; Cell Signaling	1:1000	goat anti-rabbit HRPO	Jackson Laboratories	1:20,000

B

Immunofluorescence microscopy					
Primary antibody (Anti-)	Source	Dilution	Secondary antibody	Source	Dilution
Plectin #46	Andrä et al., 2003	1:500	Cy5 donkey anti-rabbit	Jackson Laboratories	1:1000
Plectin 10F6	Foisner et al., 1994	1:2	RRX donkey anti-mouse	Jackson Laboratories	1:1000
Plectin exon 1	Abrahamsberg et al., 2005	1:1000	Cy5 donkey anti-rabbit	Jackson Laboratories	1:1000
Plectin exon 1f	Abrahamsberg et al., 2005	1:50	Cy5 donkey anti-rabbit	Jackson Laboratories	1:1000
Vimentin	Giese and Traub, 1986	1:1000	Cy2 donkey anti-goat	Jackson Laboratories	1:1000
α -Tubulin	B-512; Sigma-Aldrich	1:1000	RRX donkey anti-mouse	Jackson Laboratories	1:1000
eNOS	610297; BD Trans. Lab.	1:1000	CY5 donkey anti-rabbit	Jackson Laboratories	1:1000
Vinculin	V-4505; Sigma-Aldrich	1:100	RRX donkey anti-mouse	Jackson Laboratories	1:1000

8. RESULTS

The results are organized into three parts. The first part focuses on the purification and crystallization of plectin fragments containing the IF-binding site. The second part describes the effects of cysteine oxidation on vimentin-binding of plectin and on intra- and inter-repeat disulfide bridge formation of the plectin molecule. It also describes nitrosylation of plectin's cysteines and its involvement in IF collapse. The third part describes the effects of plectin phosphorylation on vimentin-binding and on IF network formation and dynamics.

8.1. PURIFICATION AND CRYSTALLIZATION OF PROTEINS

To crystallize plectin fragments containing the IF-binding site, to study the vimentin-binding to plectin, to study the disulfide bridges formation and nitrosylation in vitro, and to study IF architecture, several recombinant proteins were purified. Originally most of the purification procedures were developed for crystallography. As the information gained in these studies could be useful for future research on the structure of plectin molecules, the first part of Results is entirely devoted to the description of these procedures.

8.1.1. Expression and purification

Since full-length plectin (>500 kDa) or even entire subdomains, such as the C-terminal globular domain with its six repeat domains (>200 kDa) are too large to be recombinantly expressed for biochemical analyses, our study was restricted to single plectin repeat domains or combinations of two repeat domains.

To assess the potential of individual repeat 5 domain cysteines to form disulfide bridges, recombinant versions of the repeat 5 domain were used (K. Abdoulrahman, PhD Thesis, 2004), where all four cysteines were replaced by serines, either individually, or in different combinations. Cys1 and Cys4 were mutated alone and in various combinations with Cys2 and Cys3, including a mutant without any cysteine (R5 Cys-free). In addition, a

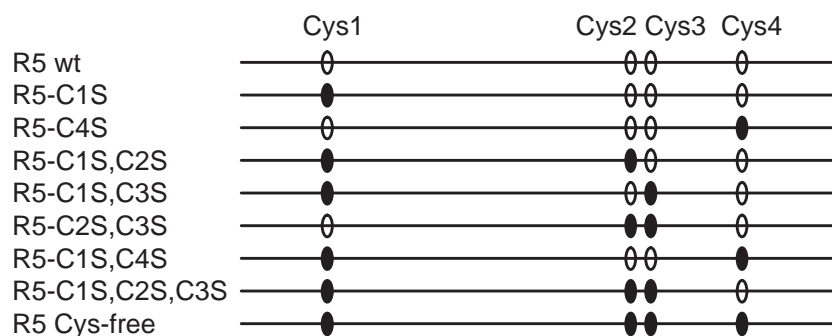


Figure 5. Schematic representation of wild-type and mutated versions of the repeat 5 domain used in this study. The name of each mutant is indicated on the left hand side. Mutants are named according to the numbers of the mutated cysteines; wt, wild-type. Only cysteine residues (open ellipsoids) and their serine replacements (filled ellipsoids) are shown. Cysteine residues Cys1-4 of repeat 5 domain correspond to residues 4074, 4248, 4257, and 4316 in full length plectin (SwissProt accession number P30427).

mutant with native Cys1 and Cys4, but without Cys2 and Cys3 (R5-C2S, C3S) and its counterpart with Cys2 and Cys3, but without Cys1 and Cys4 (R5-C1S, C4S) were used (K. Abdoulrahman, PhD Thesis, 2004). Schematics of R5 wt and the eight mutant versions used and their assigned names are shown in Fig. 5. In addition to the single repeat 5 domain, protein fragments consisting of two repeat domains were used. Fragment R4-5 contained the repeat 4 domain linked to the repeat 5 domain and the following linker domain containing the IF-binding site. Fragment R5-6 contained repeats 5 and 6 connected by their linker domain (containing the IF-binding site), and R5-6tail resembled R5-6 but contained also the terminal tail region.

R5 wt

The wild-type version of plectin's R5 domain which was quite soluble was purified using nickel ion affinity chromatography (Fig. 6A). After loading the sample onto the column and washing, by which a fair amount of protein impurities were removed, the protein bound was eluted with 0.5 M imidazole. The fractions corresponding to the protein peaks in the chromatogram were analyzed by SDS-PAGE. As shown in Fig. 6B, fractions B9-B13 contained high concentrations of a protein with an apparent molecular mass of ~41 kDa. Homogeneity of the eluted protein was further tested using size exclusion chromatography, where a single peak was observed (Fig. 6C), showing that the protein was homogeneous and formed just one conformation.

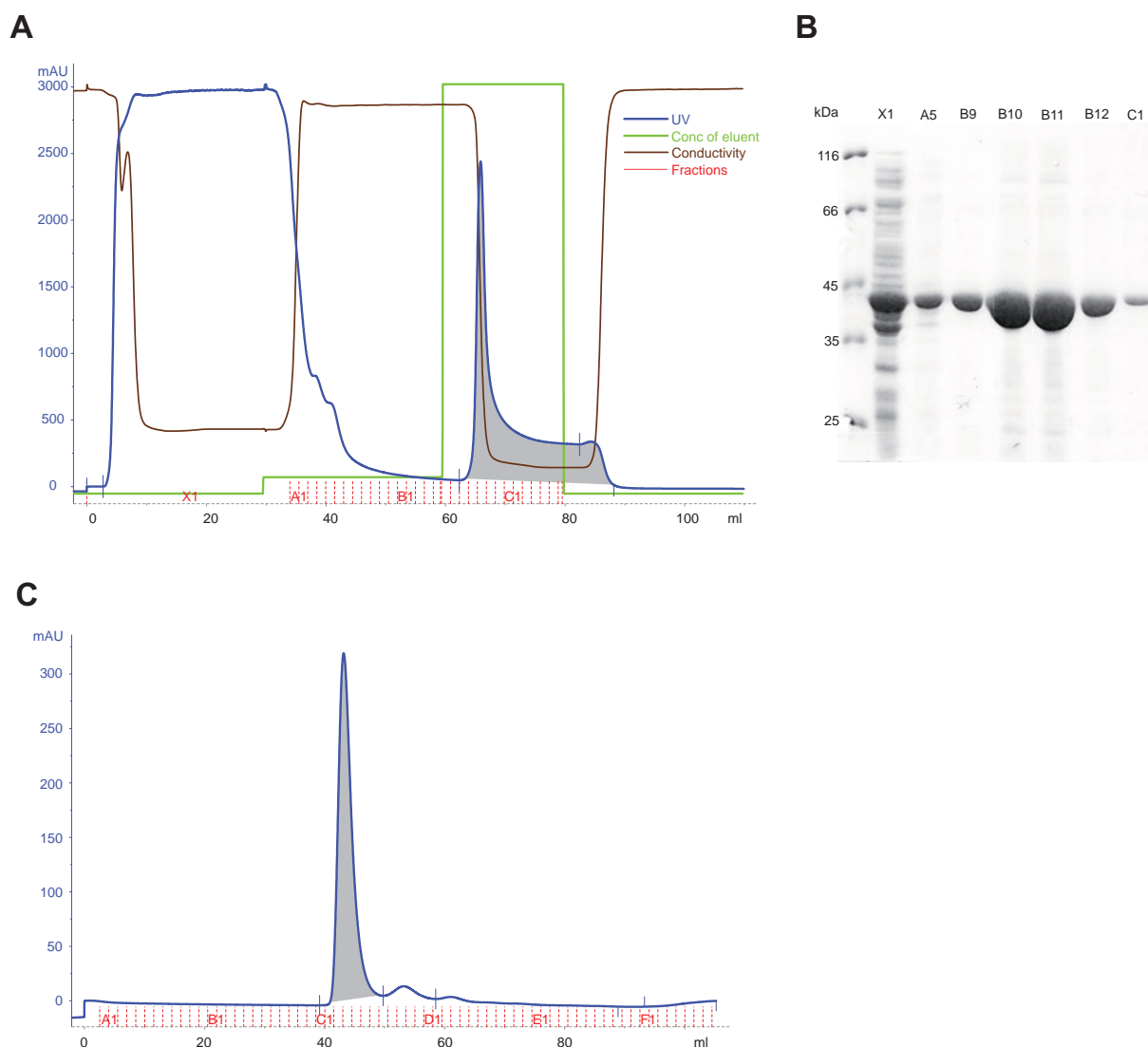


Figure 6. Purification of plectin fragment R5 wt by affinity chromatography. (A) Elution profile of R5 wt from a HisTrap column using the ÄKTA FPLC™ system. Pure protein was eluted from the column by 500 mM imidazole and fractions with the highest absorbance were collected. Grey colored area corresponds to fractions containing eluted R5 wt. Blue (UV), absorbance of the sample; green, concentration of eluent; brown, conductivity; red, fractions. (B) 10% SDS-PAGE (Coomassie staining). Lanes correspond to indicated fractions in A; lane X1 represents unbound proteins in fraction X1, lane A5 corresponds to proteins contained in one of the fractions collected during the washing step, and lanes B9-C1 correspond to eluted fractions. (C) Size exclusion chromatography on a HiLoad Superdex 75 column. Note, the single peak indicated that the protein existed in a single conformation.

R5 Cys-free

Standard purification procedure used for R5 wt resulted in low solubility and yields of R5 Cys-free, therefore purification of this particular protein was modified. After cells lysis and centrifugation, most of the R5 Cys-free protein was present in the pellet in an insoluble form. Protein pellets were solubilized by increasing the pH of the solution to 11. By this treatment most of the protein was solubilized and could then be subjected to HisTrap affinity

column chromatography (Fig. 7A). The purification procedure was then continued in the same way like in the case of R5 wt. This one-step affinity chromatography purification yielded protein of greater than 90% purity (Fig. 7B). Homogeneity of the R5 Cys-free sample was confirmed by size exclusion chromatography (Fig. 7C).

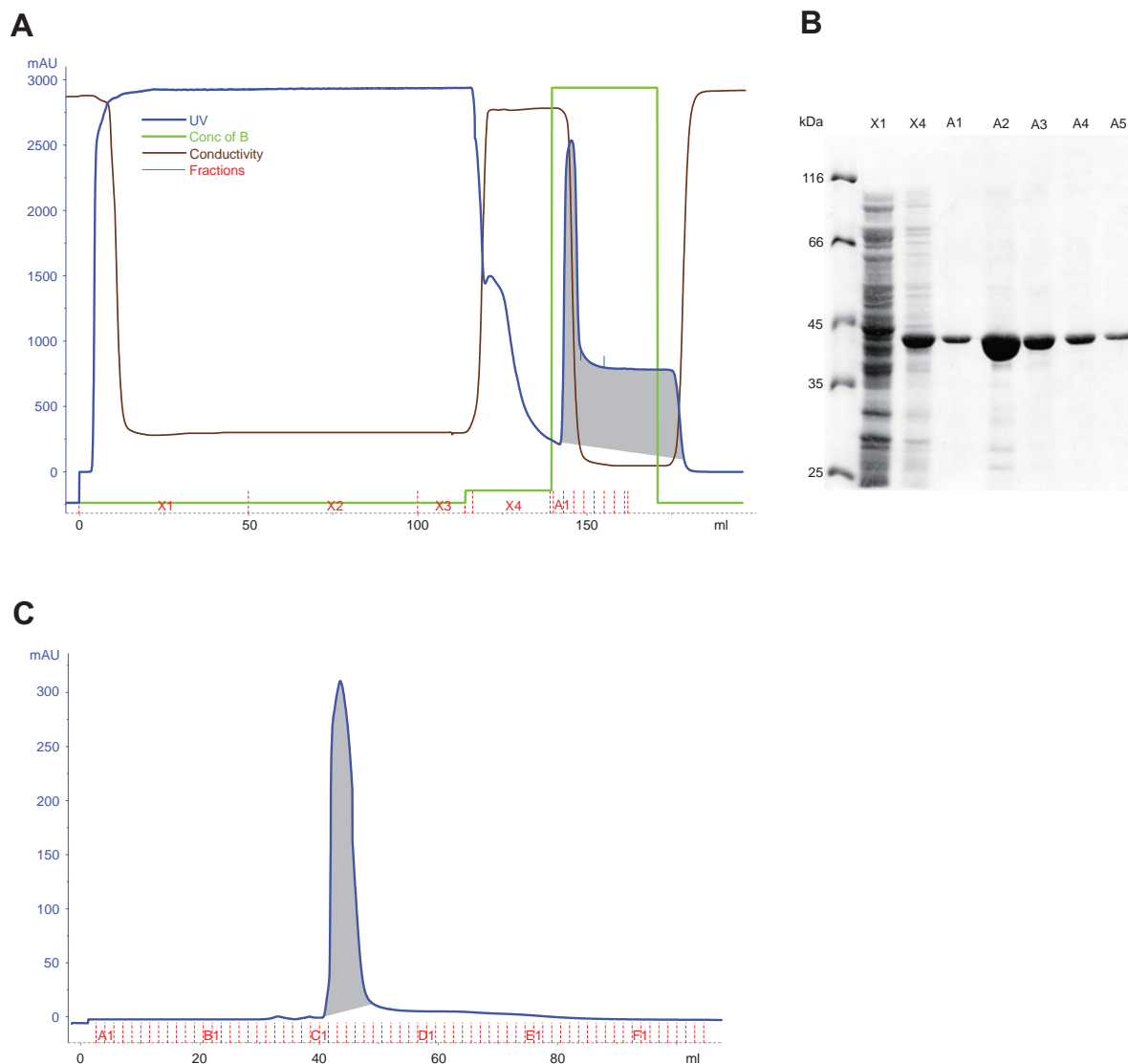


Figure 7. Purification of plectin fragment R5 Cys-free by affinity chromatography. (A) Elution profile of R5 Cys-free from a HisTrap column using the ÄKTA FPLC™ system. Pure protein was eluted from the column by 500 mM imidazole and fractions with the highest absorbance were collected. Grey colored area corresponds to fractions containing eluted R5 Cys-free. Blue (UV), absorbance of the sample; green, concentration of eluent; brown, conductivity; red, fractions. (B) 10% SDS-PAGE (Coomsie staining). Lanes correspond to indicated fractions in A; lane X1 represents unbound proteins in fraction X1, lane X4 corresponds to proteins contained in one of the fractions collected during the washing step, and lanes A1-A5 correspond to eluted fractions. (C) Size exclusion chromatography on a HiLoad Superdex 75 column. Note, the single peak indicated that the protein existed in a single conformation.

All other recombinant versions of the repeat 5 domain where cysteines were replaced, (either individually or in different combinations) by serines, were expressed to an extent similar to that of R5 wt and displayed similar solubilities. They, too, were purified by one-step affinity chromatography on a HisTrap column, as described in detail in Materials and Methods.

R4-5

In purifying R4-5 by affinity chromatography on a HisTrap column, the washing steps removed most of the protein impurities (Fig. 8A). However, the purity of eluted R4-5 was still insufficient. Therefore two additional purification steps were performed, one of which was ion-exchange chromatography using a SourceQ column, where R4-5 mostly eluted at 250 mM NaCl (Fig. 8B). Peak fractions from the ion-exchange chromatography were collected and subjected to gel filtration on a Superdex column. R4-5 eluting as a single major peak was homogeneous as verified by SDS-PAGE (Fig. 8C).

R5-6 and R5-6tail

To purify R5-6 and R5-6tail one-step purification schemes using nickel ion affinity chromatography were applied (Figs. 9A and 10A). Both proteins were expressed to a similar extent and were of similar solubility, as assessed by SDS-PAGE (Fig. 9B and Fig. 10B) and gel filtration chromatography (Fig. 9C and Fig. 10C).

Recombinant vimentin

Recombinant full-length (untagged) vimentin was purified in two steps by ion-exchange chromatography as described previously (Nagai and Thogersen, 1987). After the first step (anion-exchange purification on Q-sepharose columns, Fig. 11A), eluted protein peaks were analyzed by SDS-PAGE and fractions of highest purity were used for cation-exchange chromatography on SP-sepharose columns (Fig. 11B). The purity of salt-eluted vimentin protein samples was verified by SDS-PAGE and in vitro assembly of IFs (shown in part 7.3. of Results, Fig. 26 A).

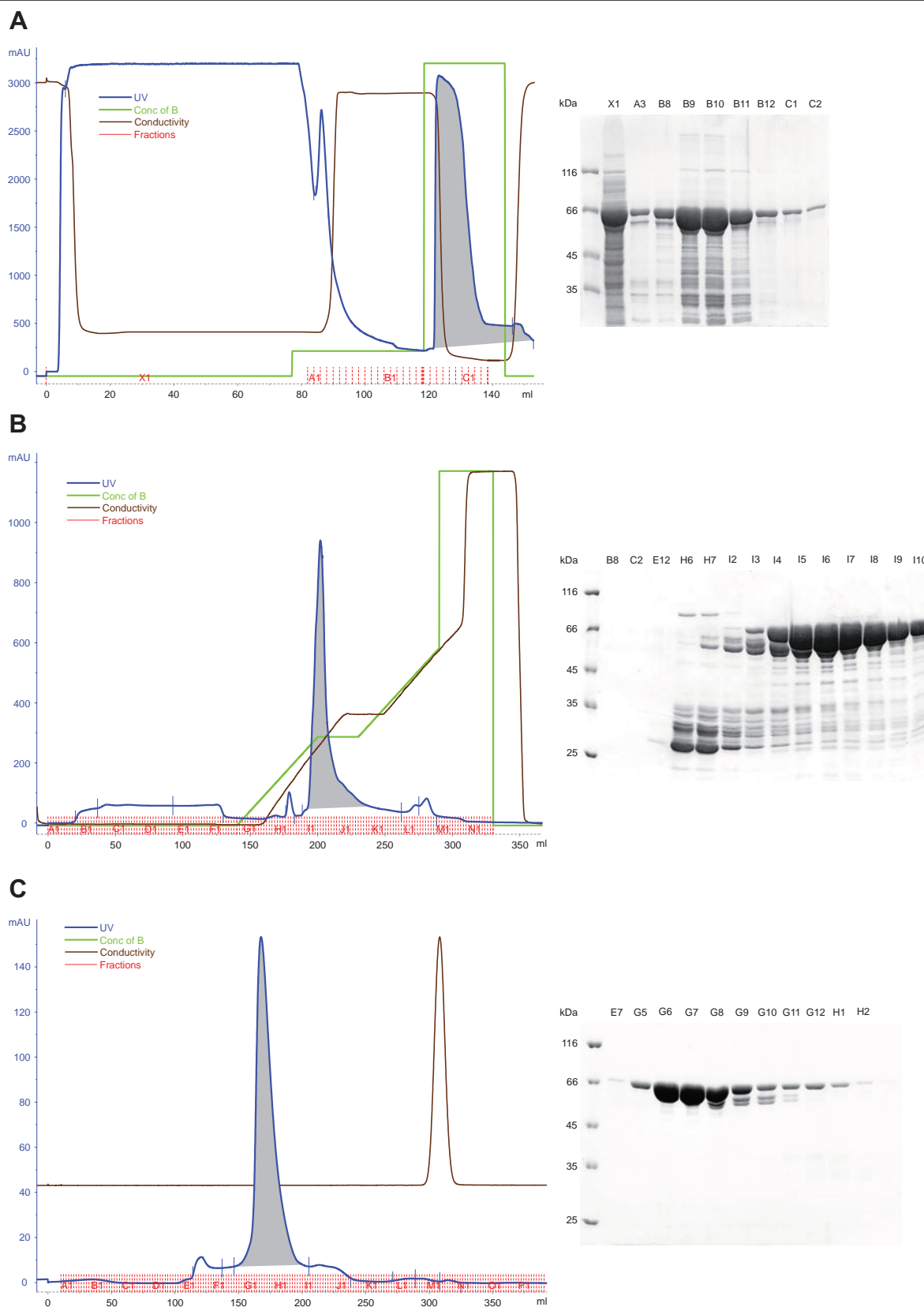


Figure 8. Purification of plectin fragment R4-5 by a three-step purification. Elution profiles of R4-5 from affinity HisTrap (A), ion exchange Source Q (B), and gel filtration Superdex 75 (C) columns using the ÄKTA FPLC™ system. Protein corresponded to R4-5 eluted from the columns and fractions with the highest absorbance were collected. Grey colored area corresponds to fractions containing eluted R4-5. Blue (UV), absorbance of the sample; green, concentration of eluent; brown, conductivity; red, fractions. 10% SDS-PAGE (Coomassie staining): Lanes correspond to indicated fractions in chromatogram.

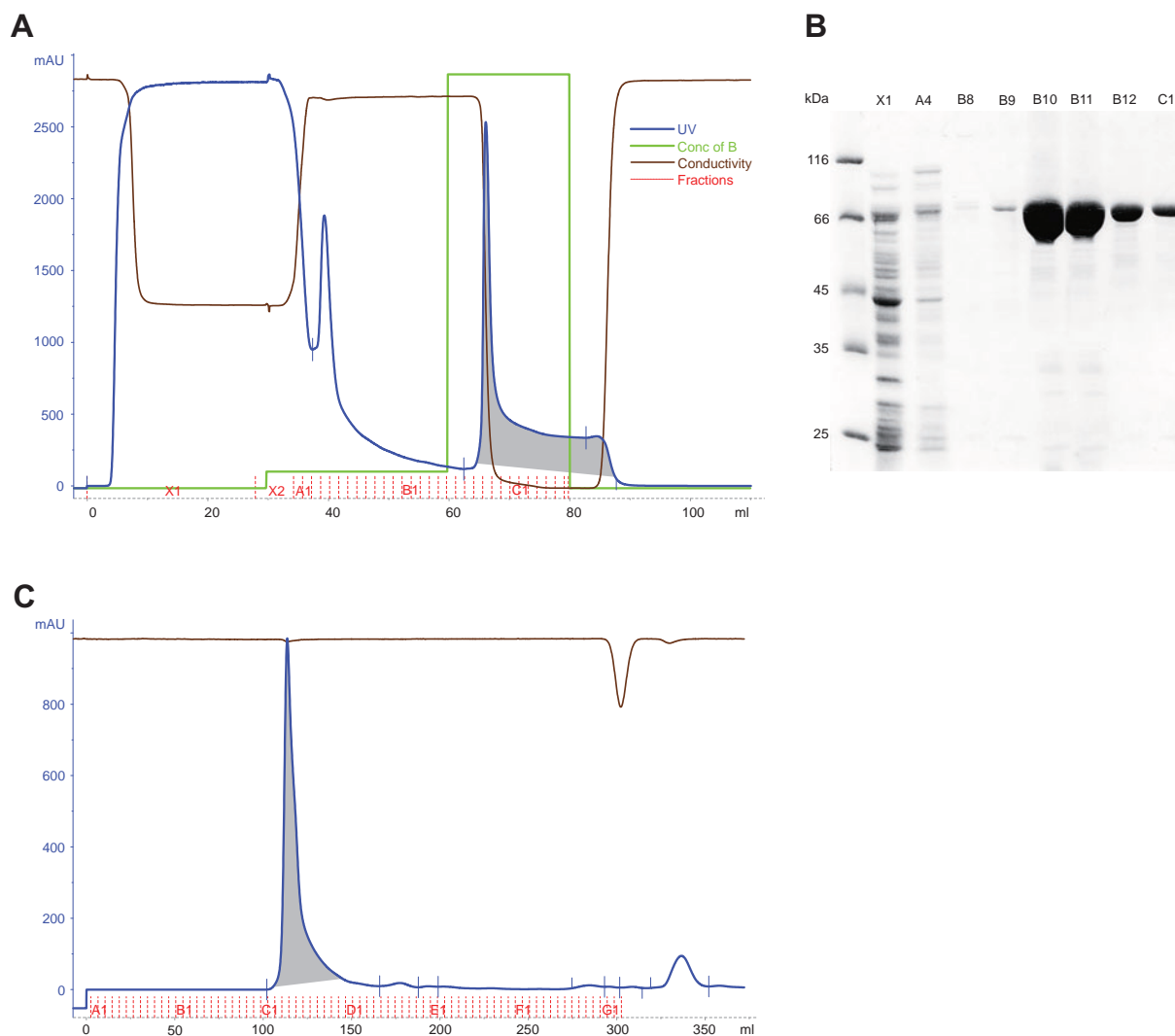


Figure 9. Purification of plectin fragment R5-6 by affinity chromatography. (A) Elution profile of R5-6 from a HisTrap column using the ÄKTA FPLC™ system. Pure protein was eluted from the column by 500 mM imidazole and fractions with the highest absorbance were collected. Grey colored area corresponds to fractions containing eluted R5-6. Blue (UV), absorbance of the sample; green, concentration of eluent; brown, conductivity; red, fractions. (B) 10% SDS-PAGE (Coomasie staining). Lanes correspond to indicated fractions in A; lane X1 represents unbound proteins in fraction X1, lane A4 corresponds to proteins contained in one of the fractions collected during the washing step, and lanes B8-C1 correspond to eluted fractions. (C) Size exclusion chromatography on a HiLoad Superdex 75 column. Note, the single peak indicated that the protein existed in a single conformation.

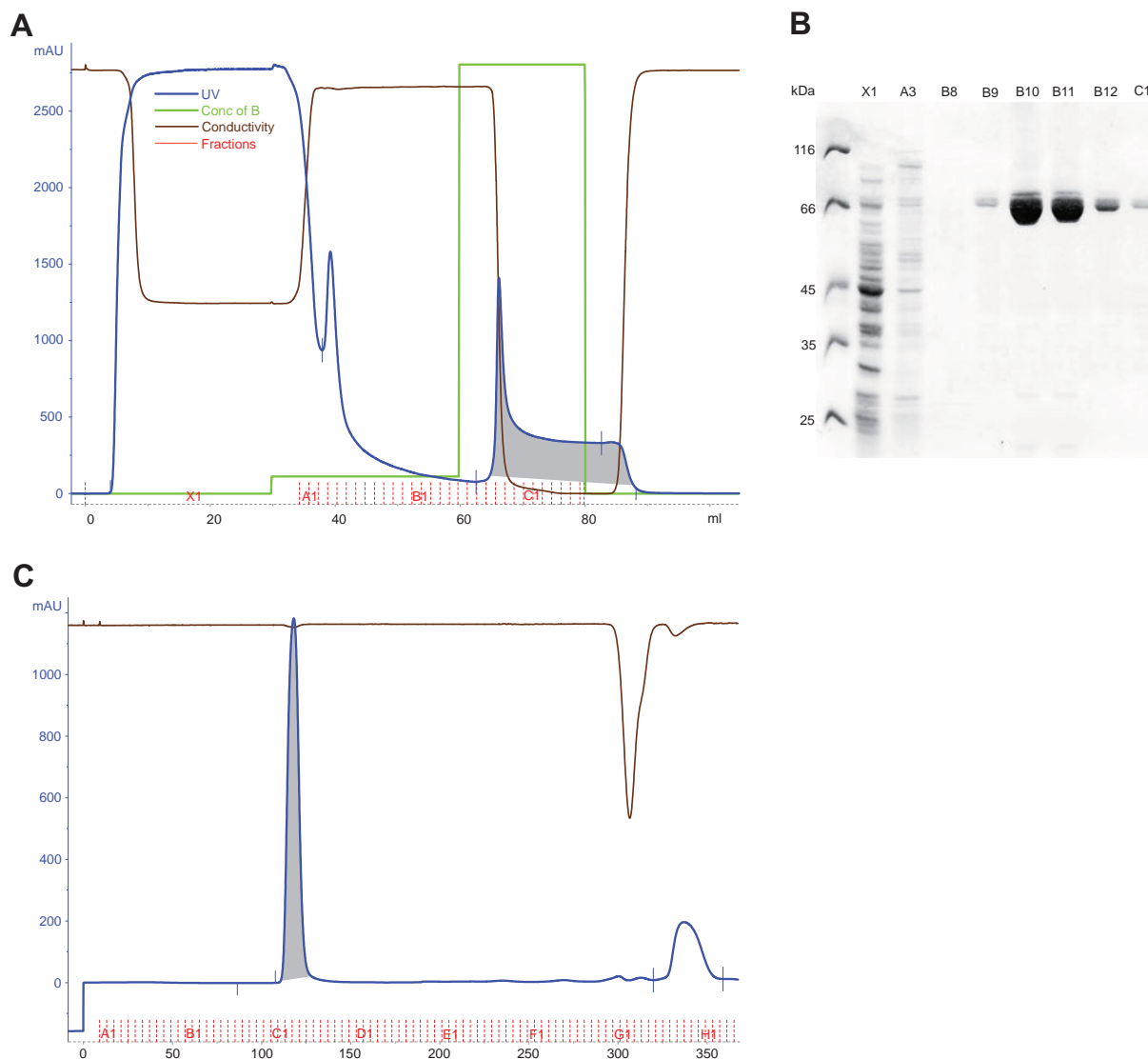


Figure 10. Purification of plectin fragment R5-6tail by affinity chromatography. (A) Elution profile of R5-6tail from a HisTrap column using the ÄKTA FPLC™ system. Pure protein was eluted from the column by 500 mM imidazole and fractions with the highest absorbance were collected. Grey colored area corresponds to fractions containing eluted R5-6tail. Blue (UV), absorbance of the sample; green, concentration of eluent; brown, conductivity; red, fractions. (B) 10% SDS-PAGE (Coomassie staining). Lanes correspond to indicated fractions in A; lane X1 represents unbound proteins in fraction X1, lane A3 corresponds to proteins contained in one of the fractions collected during the washing step, and lanes B8-C1 correspond to eluted fractions. (C) Size exclusion chromatography on a HiLoad Superdex 75 column. Note, the single peak indicated that the protein existed in a single conformation.

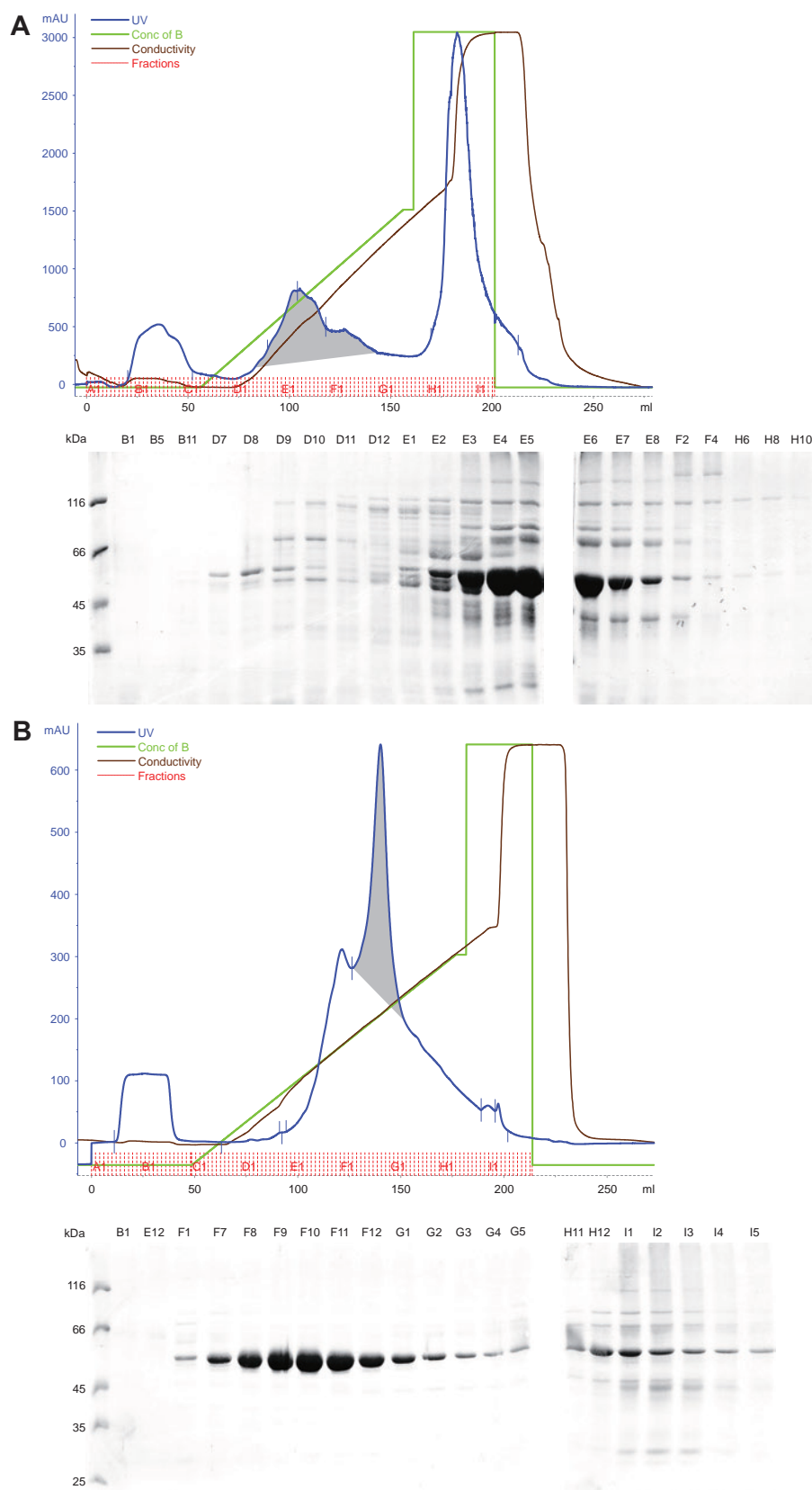


Figure 11. Purification of recombinant vimentin by a two-step purification. Elution profiles of vimentin from an anion-exchange Q-sepharose (A) and cation-exchange SP-sepharose (B) columns using the ÄKTA FPLC™ system. Protein corresponded to vimentin eluted from the columns and fractions with the highest absorbance were collected. Grey colored area corresponds to fractions containing eluted vimentin. Blue (UV), absorbance of the sample; green, concentration of eluent; brown, conductivity; red, fractions. 10% SDS-PAGE (Coomassie staining). Lanes correspond to indicated fractions in chromatogram.

8.1.2. Crystallization

In the course of my thesis I attempted to crystallize the following plectin constructs: R5 wt, R5 Cys-free, R4-5, R5-6 and R5-6tail. Purified protein samples were concentrated to ~10 mg/ml and centrifuged prior to crystallization assays. Crystallization trials were performed by hanging and sitting drop vapour diffusion. Of all the samples tested only plectin R5 Cys-free and R4-5 were forming crystals.

R5 Cys-free

Crystallization screening, consisting of more than thousand different solutions, varying mostly in pH and concentration of the precipitant, resulted in mostly amorphous precipitates or phase separation. After approximately 14 days, small, clustered, needle-shaped crystals occurred in 0.2 M $MgCl_2$, 0.1 M Tris-HCl, pH 8.5, 15% PEG 4000 (Fig. 12A). In order to obtain crystals with appropriate dimensions I tried to optimize the conditions for crystallization by employing a process called macroseeding. For this method the clustered needle crystals were broken to single crystals and to avoid crystal bending, the longer needle crystals were further split into shorter fragments. Unfortunately, macroseeding again resulted in the formation of only small clustered needle crystals. I then tried to optimize

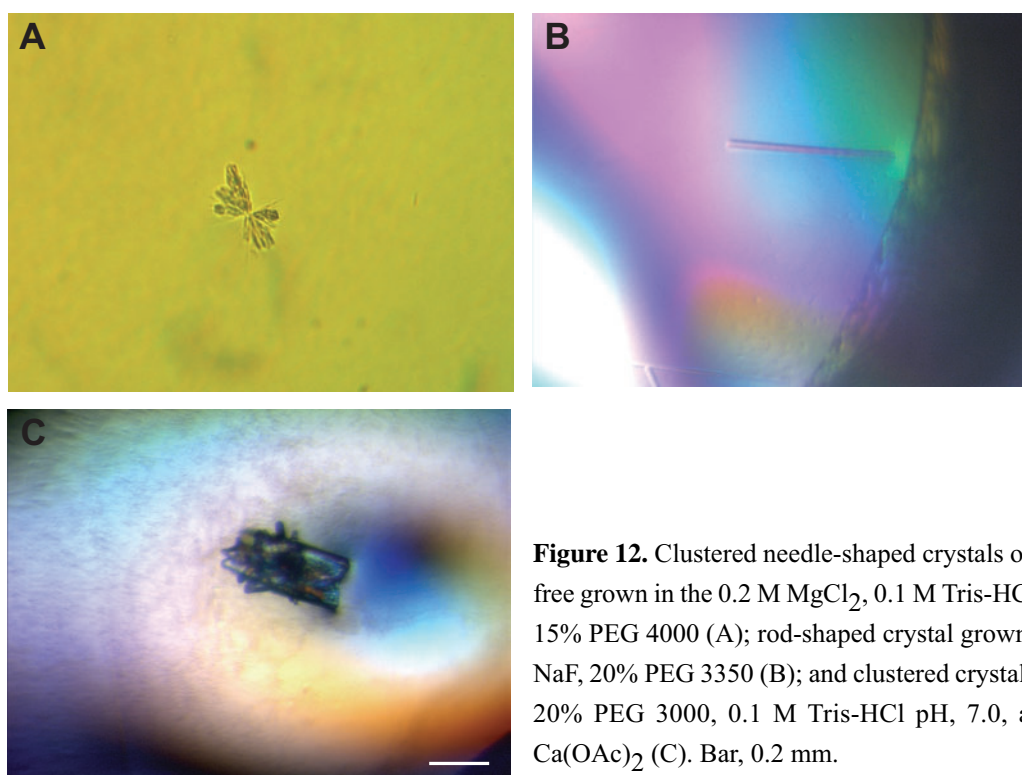


Figure 12. Clustered needle-shaped crystals of R5 Cys-free grown in the 0.2 M $MgCl_2$, 0.1 M Tris-HCl, pH 8.5, 15% PEG 4000 (A); rod-shaped crystal grown in 0.2 M NaF, 20% PEG 3350 (B); and clustered crystal grown in 20% PEG 3000, 0.1 M Tris-HCl pH, 7.0, and 0.2M $Ca(OAc)_2$ (C). Bar, 0.2 mm.

crystallization by employing conditions varying only slightly from those of the initial successful crystallization attempt. In particular, I varied the pH and the concentrations of MgCl_2 and PEG. However, R5 Cys-free continued to form amorphous precipitates or clustered needle-shaped crystals. Also, when a screening with detergents as additives was carried out, in the presence of 0.2 mM sucrose monolaurate or 2.5 mM n-decanoylsucrose, only the formation of small clustered needle crystals was observed.

Two other conditions (0.2 M NaF and 20% PEG 3350; and 20% PEG 3000, 0.1 M Tris-HCl pH 7.0, and 0.2M $\text{Ca}(\text{OAc})_2$) gave rise to minuscule crystals, smaller than 0.05 mm in size (Fig 12B and C, respectively), without any increase in size over time. To obtain larger crystals, again I tried to optimize the conditions for crystallization by varying the pH and the concentrations of salt and PEG, as well as by adding detergents. Unfortunately none of these conditions resulted in formation of aptly bigger crystals.

R4-5

Within approx. 14 days of the crystallization trials, R4-5 yielded very small crystals (Fig. 13A), or clustered needle-shaped crystals (Fig. 13B), in several drops containing PEGs of different molecular weights and/or different concentrations. Figs. 13A and B show examples in 20 mM Tris-HCl, pH 9.0, 20% PEG 20K, and sucrose monolaurate; and 20 mM Tris-HCl, pH 9.0, 10% PEG 1000, and sucrose monolaurate, respectively. However, optimization attempts of crystallization through modification of the pH, the concentration of PEGs, the addition of detergent, or the macroseeding of needle crystals did not result in improved crystals with appropriate dimensions suitable for the collection of X-ray diffraction data.

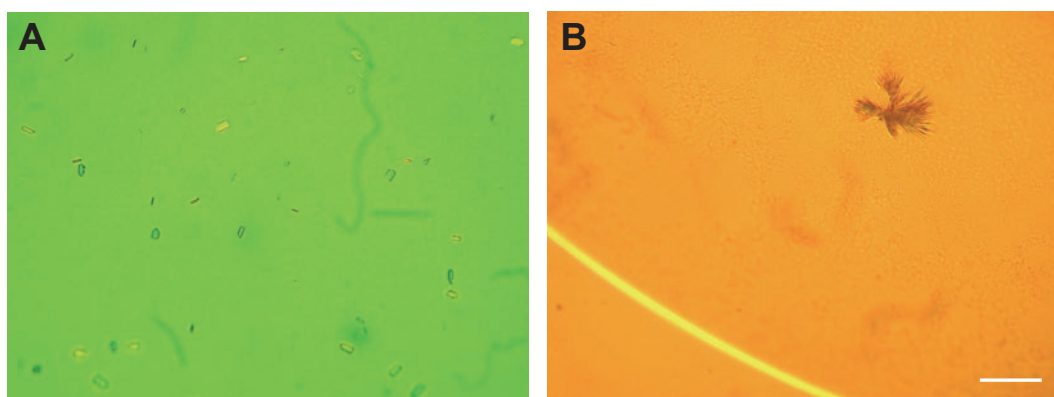


Figure 13. Very small crystals of R4-5 grown in 0.2 M MgCl_2 , 0.1 M Tris-HCl, pH 8.5, 15% PEG 4000 (A) and clustered needle-shaped crystals grown in 0.2 M NaF, 20% PEG 3350, 20% PEG 3000, and 0.1 M Tris-HCl, pH 7.0, 0.2M $\text{Ca}(\text{OAc})_2$ (B). Bar, 0.3 mm.

8.2. NITROSYLATION OF PLECTIN: EFFECTS ON VIMENTIN-BINDING AND INVOLVEMENT IN IF COLLAPSE

8.2.1. Structure prediction for plectin repeats and implications for cysteine residue exposure

The C-terminal repeat domains of plakin protein family members have been classified as type A, B, and C (Green et al., 1992). Desmoplakin has three such domains (one of each type), while five of the six plectin repeat domains are of the B-type (repeat domains 1-5) and one of the C-type (repeat domain 6) (Wiche et al., 1991). Within the repeat regions, plectin and desmoplakin share a high sequence similarity and all but one of the cysteines present in plectin's repeat domains 4-6 are present in desmoplakin's repeat domains A-C. I chose the repeat 5 domain for structure prediction, which contains four cysteines and one of them resides in the linker region containing the IF-binding site. As an additional option, I selected the repeat 1 domain, which contains only one cysteine corresponding to cysteine 2 in repeat domain 5. This repeat 1 domain also harbors the point mutation E2798K (substitution of glutamic acid 2798 by lysine), which has been shown to be responsible for skin blistering, therefore this mutation is likely to affect the package of the repeats.

3D structure of plectin's repeat 5 domain and localization of cysteines

To gain insight into the location and accessibility of the cysteine residues within the repeat 5 domain, I generated by an automated homology modeling server (SWISS-MODEL, GENO3D) a 3D model of plectin's repeat 5 domain based on the recently solved crystal structure of the desmoplakin B-type repeat domain (Choi et al., 2002; Protein Data bank 1LM7). The alignment of the target (plectin repeat domain 5) and the template (desmoplakin's B domain), obtained using the Needleman-Wunsch global alignment algorithm on EMBL-EBI server (<http://www.ebi.ac.uk/emboss/align/>), is shown in Fig. 14A and C.

The overall topology of the 3D structure of plectin's repeat 5 domain (Fig. 14B) was found to be similar to that of the model template, yet small differences are likely to confer unique properties to plectin. Like desmoplakin's B-type repeat domain, plectin's repeat 5 domain comprises 5 homologous copies of a 38 amino acid-long structural subunit, called

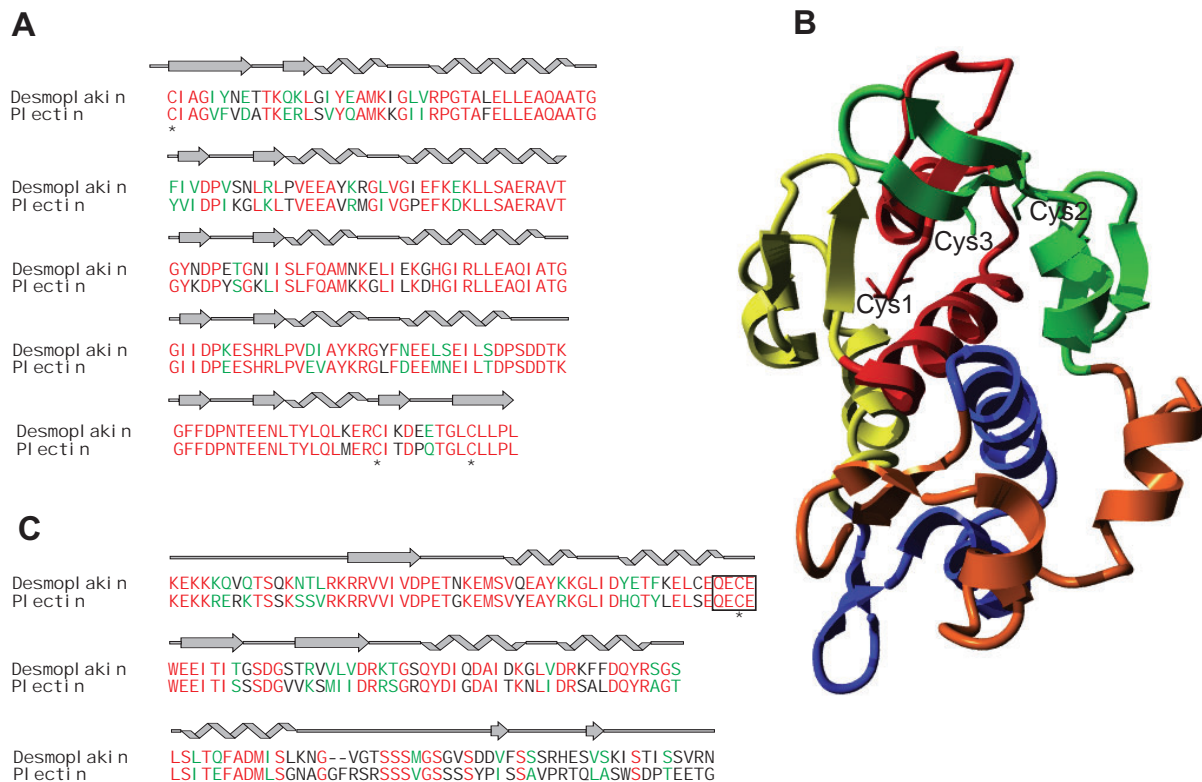


Figure 14. Proposed structural model of plectin's repeat 5 domain. (A) Sequence alignment of the template (desmoplakin B domain) and plectin's repeat 5 domain with secondary structure assignments derived from the homology model. Arrows and ribbons indicate β -strands and α -helices, respectively. Residues in red, green and black are identical, similar, or different, respectively. Cysteine residues are marked by asterisks. (B) Homology model of plectin's repeat 5 domain based on the structure of the desmoplakin B-type repeat domain, represented as a ribbon diagram. PLEC repeats 1-5 are highlighted in red, yellow, blue, orange, and green, respectively. The PLEC fold is characterized by two antiparallel β -sheets that form a β -hairpin and two antiparallel α -helices. Cysteine residues (Cys1-3) are numbered sequentially according to their position in the polypeptide chain. (C) Sequence alignment of the linker region connecting repeat domains B and C of desmoplakin and repeat 5 and 6 domains of plectin. The position of Cys4 is marked by an asterisk. The nitrosylation consensus sequence is boxed.

the PLEC repeat (SMART accession number SM00250). Each of the five PLEC repeats adopts a fold that, similar to the one described for desmoplakin, is dominated by two antiparallel β -sheets (forming a β -hairpin) and two antiparallel α -helices (Fig. 14, A and B). The fold is remarkably similar to a structure referred to as ankyrin repeat, as it was predicted by threading analysis (Janda et al., 2001). Conserved hydrophobic residues in the β -hairpin contribute to the packing within each PLEC repeat and promote the adoption of a globular, cylinder-like structure that is 45 Å long with a diameter of 25 Å. Cys1 is located in the β -hairpin of the first PLEC repeat, while Cys2 and Cys3 are in the terminal part of the fifth PLEC repeat, which is in close vicinity of the first PLEC repeat (Fig. 14B). Cys2 and Cys3 are on the surface of the structure, whereas Cys1 is partially buried in a groove. The

crystallized desmoplakin fragment did not include the linker region containing the corresponding Cys4. There is evidence, however, that this cysteine, residing in the loop connecting the B-type with the C-type repeat domains, is exposed, as partial chymotryptic digestion of the bacterially expressed C-terminal domain of desmoplakin resulted in cleavage of the polypeptide within this repeat domain linker region (Choi et al., 2002). Secondary structure predictions for this region suggest that Cys4 is located in a short unstructured sequence connecting an α -helical segment and a β -sheet (Fig. 14A). This linker region is also the one of highest sequence conservation amongst different plakin family members (Määttä et al., 2000). An alignment of the corresponding linker regions of plectin and desmoplakin is shown in Fig. 14C.

3D structure of plectin's repeat 1 domain and of plectin mutant E2798K

In order to localize and assess the accessibility of the E2798K mutation within the repeat 1 domain through homology modelling, 3D models of the wild-type and mutant repeat 1 domains were generated, again based on the crystal structure of the human desmoplakin repeat B domain (Choi et al., 2002). The alignment of plectin's repeat 1 domain and the template showed 69% identity and 82% sequence similarity. The 3D model was obtained with Modeller 8v1 (<http://salilab.org/modeller/>) and refined using Swiss-Pdb Viewer v3.7 (<http://www.expasy.org/spdbv/>). The overall topology of the 3D structure of plectin's repeat 1 domain (Fig. 15A) was found to be very similar to that of the model template as well as to the predicted model of plectin's repeat 5 domain (Fig. 14B). The mutation E2798K lies in the 4th helix of the repeat 1 domain. By superimposing the mutated and the wild-type forms no differences in the positions of the C α atoms of both proteins chains were observed (Fig. 15A). The only detectable alteration was in regard to the secondary structure at the site of the mutation, as in the mutated form the helix was prolonged by one amino acid residue (Fig. 15, A and B).

The calculation and the visualization of the electrostatic potential were performed using the program PyMOL v0.98 (<http://pymol.sourceforge.net/>). The wild-type repeat 1 domain has a negatively charged glutamic acid at position 2798 and therefore bears a negative electrostatic potential. In the mutated form the glutamic acid is replaced by lysine resulting in a large region of positive electrostatic potential (Fig. 15C). The electrostatic potential of proteins caused by charged side chains plays an important role in protein folding

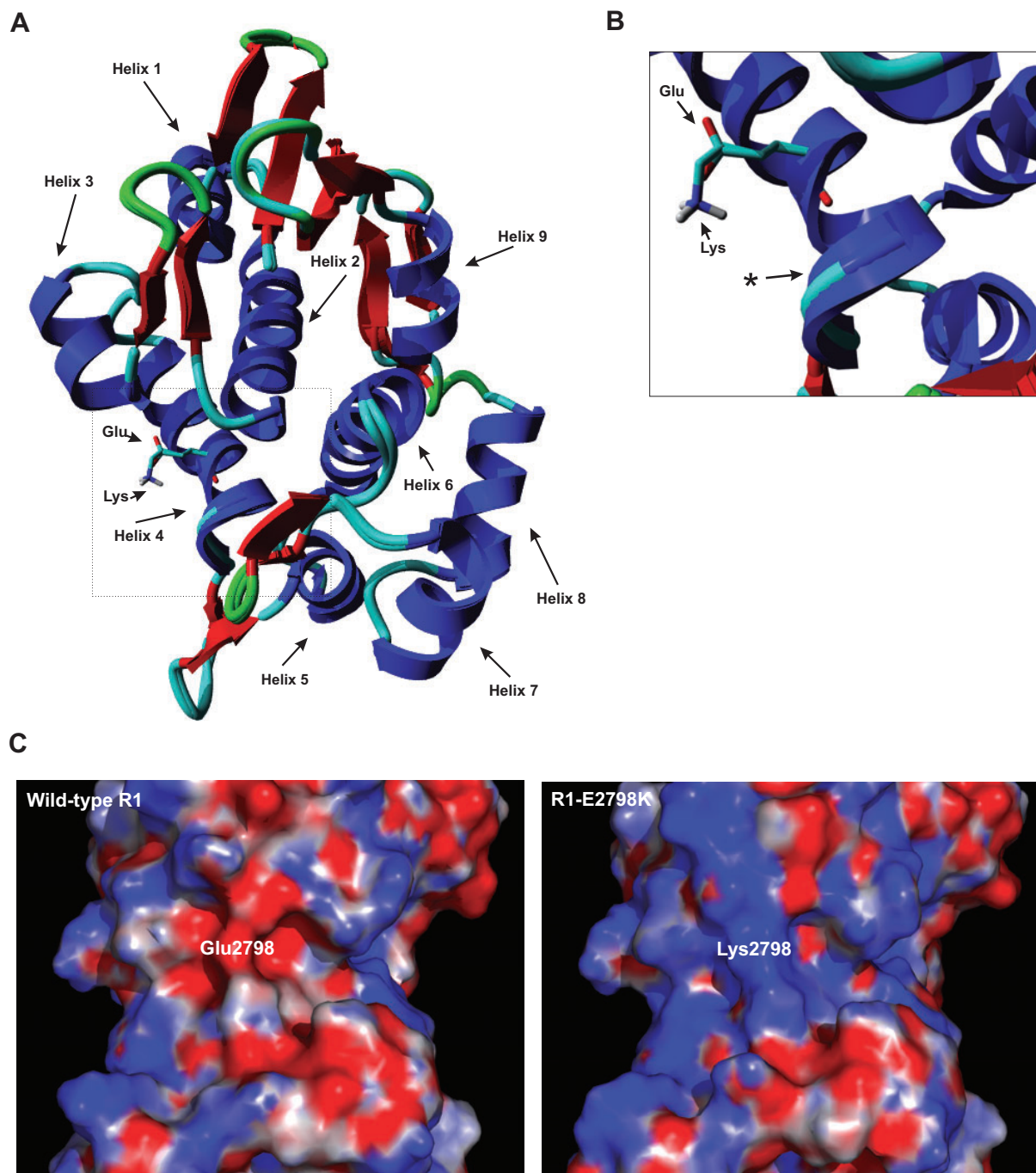


Figure 15. Proposed structural model of superimposed plectin's wild-type repeat 1 domain and mutant R1-E2798K. (A) Homology model of the plectin repeat 1 domain based on the structure of the desmoplakin B-type repeat domain represented as a ribbon diagram. The mutation E2798K lies in the 4th helix of the repeat 1 domain. The helices in PLEC repeats 1-5 are indicated as well as the wild-type glutamic acid (Glu) and the mutant lysine (Lys). (B) Detail of the superposition shown in A. Note, that in the mutated form the helix is prolonged by one amino acid residue (asterisk). (C) Electrostatic potential of the wild-type repeat 1 and R1-E2798K calculated and visualized using PyMOL. The surface of the repeat 1 domain molecule is color coded according to its electrostatic potential. Blue and red, positive and negative regions, respectively (contoured at 6 kT/e).

and stability and in protein-protein recognition. Therefore this change in the electrostatic potential of the wild-type repeat 1 domain and repeat 1-E2798K could affect the proper folding and function of the protein.

8.2.2. Disulfide cross-linking within and between plectin repeats, and between plectin and vimentin

Intramolecular disulfide bridges within the repeat 5 domain

To identify cysteine residues within the repeat 5 domain with reactive thiol groups that could engage in disulfide bridge formation, the repeat 5 domain and the cysteine mutants were tested for changes in their electrophoretic mobility due to disulfide-linked dimer or higher oligomer formation. For this purpose, purified recombinant proteins were oxidatively crosslinked by exposure to air at 4°C to promote disulfide bond formation, subsequently treated with iodoacetamide to block free cysteine residues, and then subjected to SDS-PAGE in the presence or absence of the reducing agent DTT. In the presence of DTT, the wild-type version of the repeat domain 5 fragment and all mutant proteins occurred in the monomeric form characteristic of the R5 wt fragment, migrating with an apparent molecular mass of 41 kDa (Fig. 16A, lane 10). In contrast, in the absence of DTT, several proteins bands corresponding to monomeric, dimeric, and higher order oligomeric forms were observed (Fig. 16A, lanes 1-9). The R5 wt fragment occurred as reduced (~41 kDa) and oxidized monomers (~38 kDa), and was able to form dimers, trimers, tetramers, and other oligomers (Fig. 16A, lane 1). Faster migration of the oxidized form compared to the reduced form of the monomer is typical for intramolecular disulfide bonding, resulting in a more tightly folded structure (Rogers et al., 1996; Locker and Griffiths, 1999). R5-C2S,C3S gave a cross-linking pattern similar to that of R5 wt (Fig. 16A, lane 8). Since the only cysteines available in the R5-C2S,C3S mutant are Cys1 and Cys4, I concluded that the oxidized forms of the monomer were presumably formed by disulfide bond formation between these two residues. Mutants R5-C1S and R5-C1S,C2S,C3S displayed two prominent bands corresponding to the reduced form of the monomer (~41 kDa) and dimers with an abnormal mobility of ~100 kDa (Fig. 16A, lanes 2 and 5). Probably these dimers were formed by disulfide pairing of two Cys4 residues in two different repeat 5 domain molecules. Cys4 resides in the linker

region between the repeat domains 5 and 6 at a relatively large distance from the core region of the repeat 5 domain. Disulfide bond formation between two Cys4 residues may therefore generate dimers with a larger hydrodynamic dimension, thus migrating slower (apparent molecular mass of ~100 kDa instead of ~82 kDa) in SDS-PAGE due to their extended conformation (Peitsch et al., 2001; Uversky, 2002). In contrast, cross-linked R5-C4S formed a dimer migrating with the expected mobility of a ~82 kDa protein (Fig. 16A, lane 7). R5 Cys-free occurred only as the reduced form of the monomer (~41 kDa) (Fig. 16A, lane 6). In addition to a protein band with an apparent molecular mass of ~100 kDa, mutant R5-C1S, C3S yielded a band corresponding to a higher oligomer (Fig. 16A, lane 3). The rest of the mutants, R5-C1S,C2S, and R5-C1S,C4S remained in the monomeric form after oxidation (~41 kDa; Fig. 16A, lanes 4, and 9).

These results provided evidence for the formation of an intra-repeat domain disulfide bridge between Cys1 and Cys4. When either Cys1 or Cys4 were not available, oxidative conditions promoted inter-repeat crosslinking (i.e. between distinct repeat 5 domain molecules) and yielded two different types of dimers depending on the cysteine residue engaged in the disulfide bridge. Inter-repeat domain crosslinking via Cys1 delivered dimers in the regular conformation, migrating with the expected apparent molecular mass of 82 kDa (see lane 7), while inter-repeat domain crosslinking via Cys4 delivered dimers with an extended conformation that migrated slower. Bridges between the other cysteines were unlikely to have occurred, because of distance restrictions between the cysteine residues (the 5.691 Å distance between the SH groups of Cys2 and Cys3 is beyond the optimum of 2.4 Å for creating a disulfide bridge). This assumption is supported by the fact that in the crystal structure of desmoplakin's domain B obtained in the absence of reducing agents (Choi et al., 2002), disulfide bonding between cysteine residues 2259, 2433 and 2442, which are equivalent to Cys1, Cys2 and Cys3 was not observed. Since the available high resolution structural data on desmoplakin do not include the region where Cys4 resides, from structural homology no information could be obtained regarding the putative disulfide bridge formation between Cys1 and Cys4.

Intermolecular disulfide bridges between repeat domains 4 and 5

It has been speculated earlier that plectin's repeat domains may bind to each other not only due to hydrophobic and electrostatic interactions, but also due to disulfide bond formation

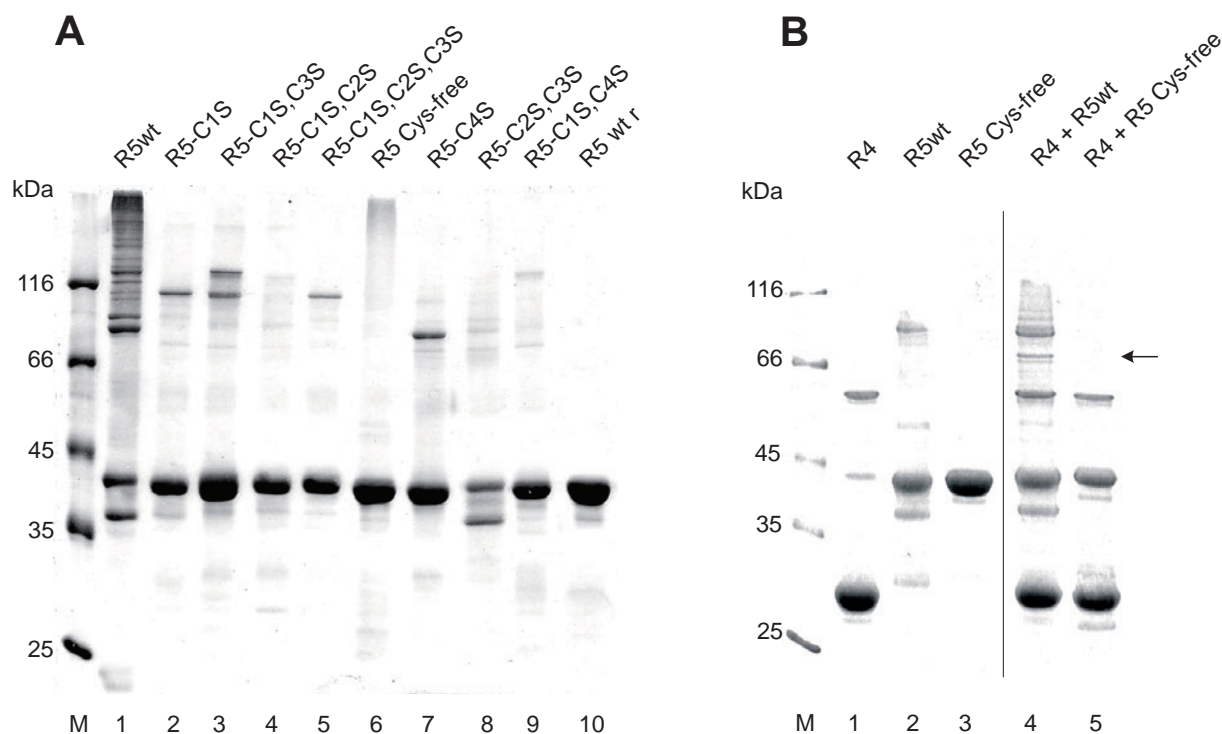


Figure 16. Disulfide cross-linking within and between plectin repeat 5 and 4 domains. (A) Analysis of cross-linked products formed by wild-type and mutant versions of repeat 5 domain. Proteins oxidized by air were subjected to SDS-10% PAGE under nonreducing (lanes 1-9) or reducing (lane 10) conditions. For reducing conditions, 0.2 M DTT was added to 2x sample buffer to achieve a final concentration of 0.1 M. r, reduced. (B) Cross-linking of R4 with wild-type and cysteine-free repeat 5 domain. Lanes 1-3, cross-linked products of indicated single repeat domains. Conditions similar to A except that 6M urea was added to the sample buffer. Lanes 4 and 5, cross-linked products of two repeat domains. R4 was mixed with either R5 wt, or R5 Cys-free, and air-oxidized. Samples were resolved by SDS-10% PAGE under nonreducing conditions. Molecular masses of monomers and dimers of R4 are ~30 and ~60 kDa; of repeat 5 domain ~38, ~41 and ~82 kDa. Arrow indicates the heterodimer band (~66 kDa) formed between R4 and R5 wt. Lanes M, molecular mass markers.

between the repeats (Janda et al., 2001). To test this hypothesis I first examined whether the single cysteine residue present in R4 was able to form a disulfide bond between two R4 molecules. When R4 oxidatively crosslinked under nonreducing conditions was analyzed, two bands were found, one corresponding to the monomer, the other to the dimer, both with the expected mobilities (Fig. 16B, lane 1), while a single monomeric band was observed under reducing conditions. Next, I tested whether repeat domains 4 and 5 could be linked via a disulfide bridge. Heterodimer formation was examined by incubating fragments R4 with R5 wt under reducing conditions for 1.5 h in the presence of 6 M urea, followed by dialysis (to remove urea) and SDS-PAGE, both without reducing agents. Due to the size difference of repeat domains 4 and 5 (~30 and ~41 kDa, respectively), a band of a size between that of the homodimers (~61 and ~82 kDa, respectively) would be indicative of

heterodimer formation. Such a band was indeed observed (Fig. 16B, lane 4). This band was absent when R4 was incubated with the R5 Cys-free mutant (Fig. 16B, lane 5). Thus the single cysteine in R4 as well as cysteines in repeat 5 domain, formed disulfide bonds not only between their own molecular entities (R4-R4 and R5-R5 homodimers), but also between each other (R4-R5 heterodimers).

Disulfide cross-linking between plectin's repeat 5 domain and vimentin

As plectin's repeat 5 domain could form intra- and inter-molecular disulfide bridges, the question arose whether inter-molecular disulfide cross-linking between plectin's repeat 5 domain and the unique cysteine of vimentin was possible. The assumption was that this type of cross-linking could stabilize the association of vimentin with plectin.

To assess this hypothesis, polymerized vimentin was incubated with the R5 wt fragment of plectin, or the R5 Cys-free fragment and then oxidized using the NO donor reagent SNAP. Samples were analyzed by immunoblotting using antibodies that recognized plectin's repeat 5 domain or vimentin. Plectin R5 wt and R5 Cys-free alone detected by anti-His-tag antibodies showed patterns corresponding with the ones observed by SDS-PAGE. Anti-vimentin antibodies revealed two bands typical for vimentin, one corresponding to the monomer, the other to the dimer. When it was tested whether plectin's repeat 5 domain and vimentin could be cross-linked via a disulfide bridge, anti-His-tag as well as anti-vimentin antibodies revealed some additional bands (Fig. 17A, lane 4; and B, lane 4). The observation

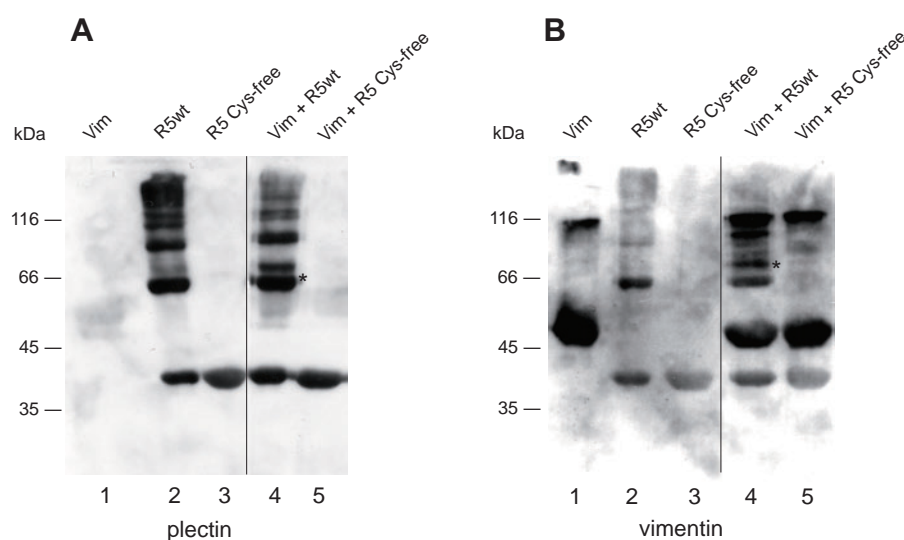


Figure 17. Disulfide cross-linking between plectin's repeat 5 domain and vimentin. Polymerized vimentin was incubated with His-tagged plectin fragments R5 wt, or R5 Cys-free, and oxidized by SNAP. Samples were then subjected to SDS-10% PAGE under nonreducing conditions, and immunoblotted using anti-

His-tag (A), or anti-vimentin (B) antibodies. Lanes 1-3, vimentin, plectin R5 wt, and R5 Cys-free alone, respectively. Lanes 4 and 5, cross-linked products of vimentin and repeat domain 5, respectively. Asterisks indicate plectin-vimentin heterodimers identified by superposition of immunoblots.

of additional bands immunoreactive with both antibodies to plectin and vimentin would indicate heterodimeric disulfide bond formation between plectin and vimentin. Such a band was indeed observed (Fig. 17A, lane 4; and B, lane 4, asterisk). This band was absent when vimentin was incubated with the cysteine-free mutant R5 Cys-free (Fig. 17A, lane 5; and B, lane 5). Thus the single cysteine in vimentin as well as the cysteines in repeat domain 5 formed disulfide bonds between each other, which may lead to the stabilization of the plectin-vimentin interaction.

8.2.3. Effects of plectin's cysteine residues, of repeat domains neighboring the IF-binding site, and of the tail region on plectin-vimentin affinity

Increased vimentin-binding affinity of plectin's repeat domain 5 in its reduced form

Plectin's major vimentin-binding site is located in the linker region connecting the repeat domains 5 and 6. Since this region harbors also Cys4 of plectin's repeat 5 domain (see Figure 14C), it was of special interest to examine whether this cysteine plays any role in the interaction of the repeat 5 domain with vimentin. Therefore I measured the vimentin-binding affinities of the fragment R5 wt and its cysteine-free variant R5 Cys-free, using a quantitative non-radioactive binding assay based on Eu^{3+} -labeled proteins (Soini and Kojola, 1983; Nikolic et al., 1996). The two plectin fragments to be assessed, were coated under reducing or nonreducing conditions onto 96-well microtiter plates and overlaid with increasing concentrations of Eu^{3+} -labeled vimentin. The amount of vimentin bound to microtiter plate-immobilized plectin's repeat 5 domain was determined by measuring released Eu^{3+} by time-resolved fluorometry, using microtiter plate-bound BSA as control for non-specific binding. The obtained dissociation constants showed that R5 wt bound to vimentin with 2-times higher affinity under reducing ($K_d=0.155 \mu\text{M}$) compared to nonreducing conditions ($K_d=0.312 \mu\text{M}$), while an even higher binding affinity ($K_d=0.096 \mu\text{M}$) was observed for the mutant protein (Fig. 18). These differences in binding affinities probably reflected distinct conformations of the reduced and the nonreduced forms of fragment R5 wt, on the one hand, and of this fragment and its cysteine-free mutant, on the other.

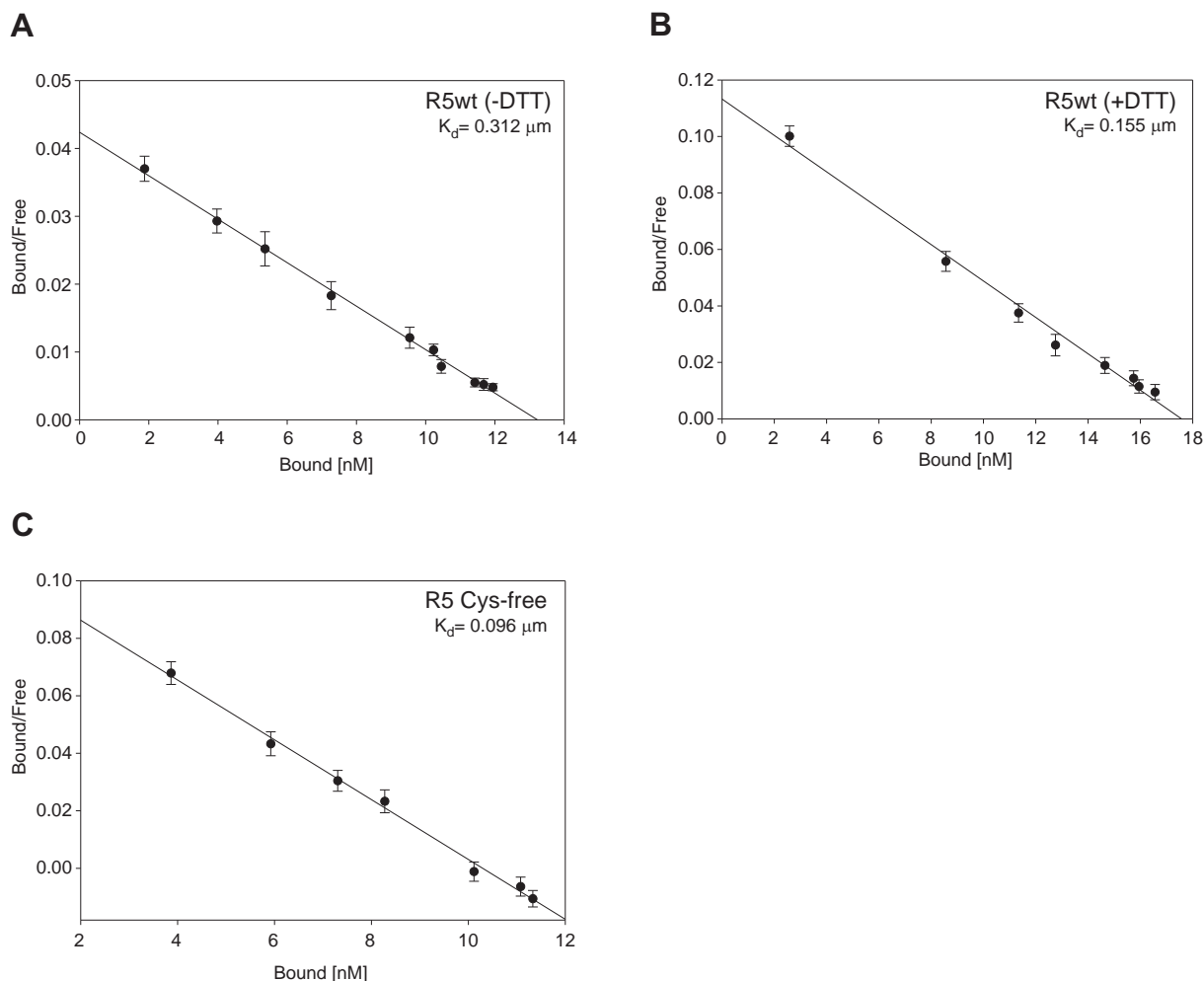


Figure 18. Concentration-dependent binding of Eu^{3+} -labeled vimentin to immobilized wild-type and cysteine-free repeat domain 5. Fragments R5 wt in the absence (A), or presence of 1 mM DTT (B), and R5 Cys-free (without DTT) (C) were coated onto microtiter plates at concentrations of 100 nM, and overlaid with Eu^{3+} -labeled recombinant vimentin at concentrations of 0.05-2 μM . Eu^{3+} -labeled vimentin bound to the different versions of the repeat 5 domain was measured. Scatchard plots of the binding data are shown.

Effects of plectin's repeat domains neighboring the IF-binding site and of the tail region on plectin-vimentin interaction

The neighboring repeats 4 and 6 of plectin's repeat 5 domain, contain one and three cysteines, respectively; and their presence may affect the binding affinity to vimentin. Therefore purified fragments R5-6, R5-6tail, and R4-5 were immobilized (under non-reducing conditions) and overlaid with increasing amounts of Eu^{3+} -labeled vimentin (Fig. 19). Scatchard transformation of the binding data showed that fragment R5-6 ($K_d = 0.174 \mu\text{M}$) (Fig. 19A) bound to vimentin with an affinity that was very similar to that of fragment R5 wt under reducing conditions ($K_d = 0.155 \mu\text{M}$). However, the presence of the terminal tail

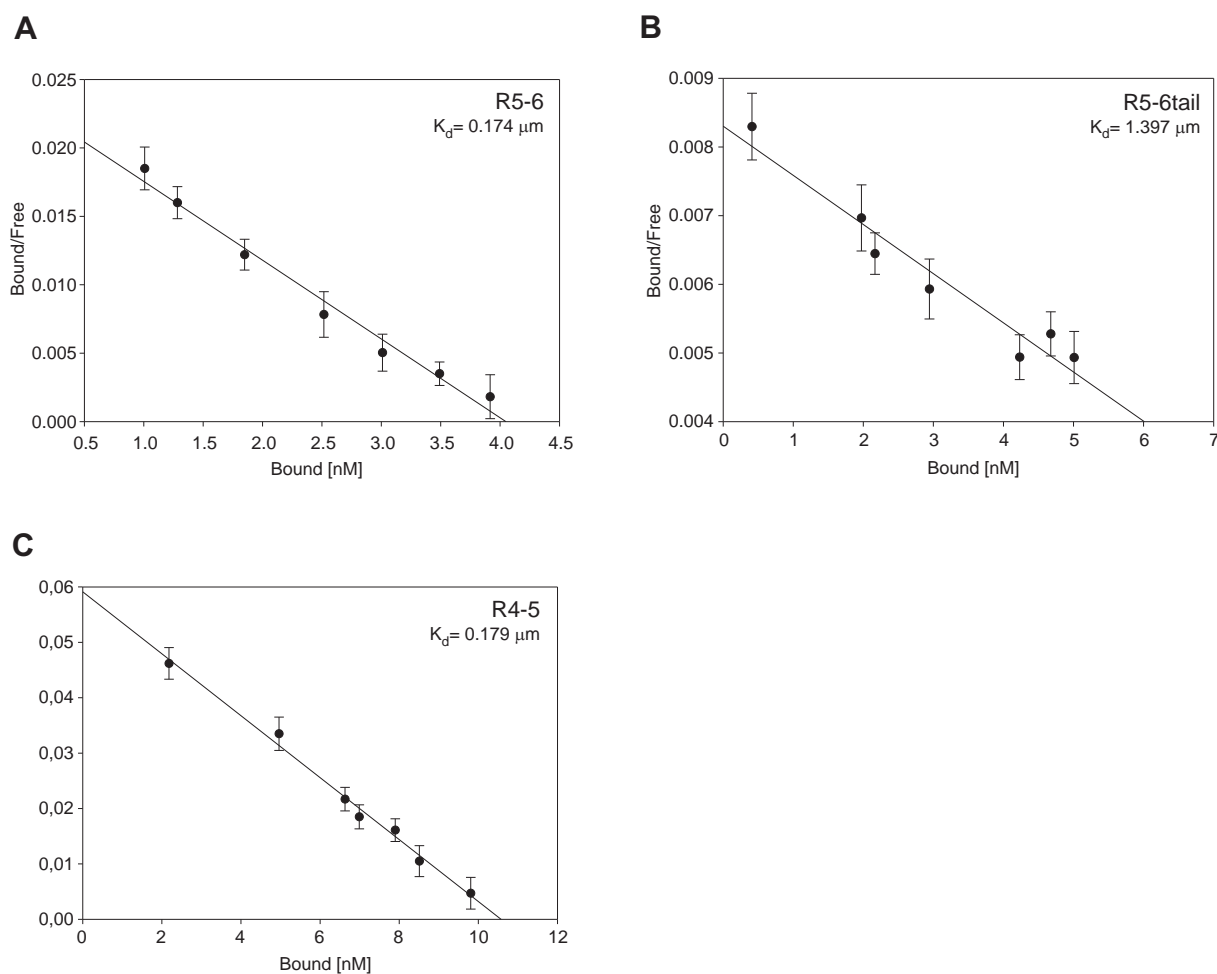


Figure 19. Concentration-dependent binding of Eu^{3+} -labeled vimentin to immobilized fragments R5-6, R5-6tail, and R4-5. R5-6 (A), R5-6tail (B), and R4-5 (C) were coated onto microtiter plates at concentrations of 100 nM, and overlaid with Eu^{3+} -labeled recombinant vimentin at concentrations of 0.05–2 μM . Eu^{3+} -labeled vimentin bound to the different versions of the repeat 5 domain was measured. Scatchard plots of the binding data are shown.

region partially decreased the affinity ($K_d = 1.397 \mu\text{M}$) (Fig. 19B). Interestingly, fragment R4-5 ($K_d = 0.179 \mu\text{M}$) displayed a vimentin-binding affinity that was very similar to that of fragment R5-6 (Fig. 19C). The binding affinities of fragments R5-6 and R5-6tail resembled the affinity of the R5 wild-type domain under reducing conditions ($K_d = 0.174 \mu\text{M}$, $0.179 \mu\text{M}$, and $0.155 \mu\text{M}$, respectively).

These results suggested that the neighboring repeats of repeat 5 have a positive effect on its binding to vimentin, reaching the affinity levels measured for the wild-type version of R5 in its reduced form. These findings led me to suggest, that plectin's intra-repeat disulfide bridges decreased the affinity to vimentin, while the inter-repeat disulfide bridges increased it.

8.2.4. Plectin is a target for nitrosylation in vitro and in vivo

In vitro nitrosylation of cysteine 4 in plectin's repeat 5 domain

S-nitrosylation is a reversible posttranslational modification with a potential role in the regulation of protein function in response to oxidative stress. Mechanistically, S-nitrosylation is the reversible covalent binding of NO to an SH-group of a reactive cysteine, and it is precisely targeted to residues in hydrophilic protein domains that contain consensus acid-basic motifs consisting of a core of three residues, K/R/H/D/E-C-D/E (Stamler et al., 1997). As the fourth cysteine (Cys4) in repeat domain 5 meets these criteria, an in vitro S-nitrosylation assay was carried out, using fragments R5 wt and R5-C4S as the protein substrates, SNAP as the NO donor, and the biotin switch method for detection of S-nitrosylated cysteines. In this assay, after blocking non-nitrosylated free thiol groups by methylation, S-nitrosylated cysteines are selectively identified by the cleavage of S-NO by ascorbate followed by biotinylation of the free thiols, pull down of biotinylated proteins with streptavidin beads, and immunoblotting of eluates. As shown in Fig. 20A, extensive nitrosylation of fragment R5 wt preincubated with SNAP was observed, while hardly any signal was detected with R5-C4S.

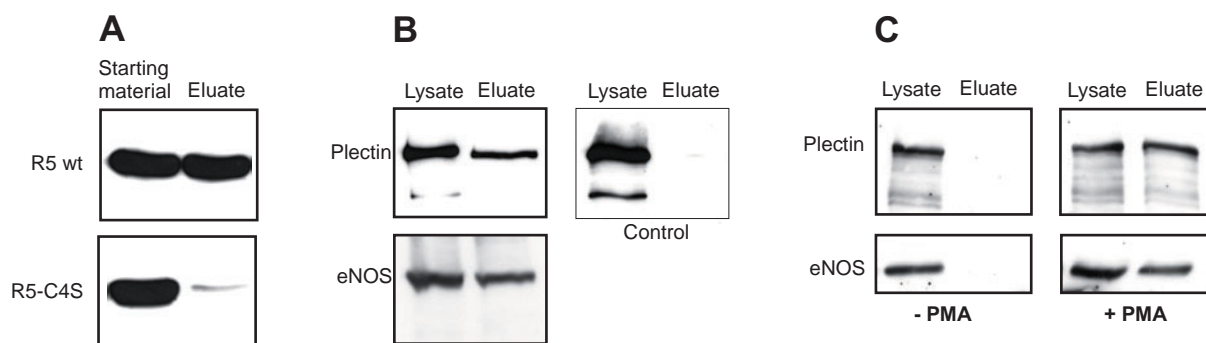


Figure 20. Nitrosylation of fragment R5 Cys4 in vitro and of plectin in cultured endothelial cells in vivo. (A) Nitrosylation in vitro. Purified samples (80 μ g) of R5 wt and mutant R5-C4S were incubated with 100 μ M SNAP, and S-nitrosylated proteins detected by the biotin switch method. Biotinylated proteins were purified on streptavidin beads, eluted with β -ME, immunoblotted (SDS-10% PAGE), and probed with antibodies to HIS-tag. (B) NO donor-mediated S-nitrosylation of plectin in cultured mouse renal endothelial cells. Cells preincubated with 100 μ M SNAP were lysed in blocking buffer (see text) and processed as described in A. Eluted proteins were subjected to immunoblotting (SDS-5% PAGE) and probed with antibodies to plectin (upper panels). Control, ascorbate added prior to blocking free thiols. Lower panel, membranes were stripped and reblotted with anti e-NOS antibodies. (C) S-nitrosylation of plectin in cultured mouse renal endothelial cells after stimulation of endogenous eNOS. Cells, kept untreated or incubated with 100 nM PMA for 20 h, were lysed and processed as described in B. In A, 0.8% of the starting material and 25% of the eluates were loaded onto the gels; in B and C, 3.3% of the cell lysates and 50% of the eluates.

Nitrosylation of plectin in endothelial cell cultures

Nitric oxide plays a key regulatory role in endothelial cell function (Hess et al., 2005). To investigate whether plectin S-nitrosylation occurs in vivo, I incubated immortalized mouse renal endothelial cells in culture with SNAP and assayed plectin S-nitrosylation by the biotin-switch assay. As shown in Fig. 20B, a strong signal corresponding to full length plectin could be detected in the streptavidin-bead eluate, indicating S-nitrosylation of endogenous endothelial cell plectin. When ascorbate (1 mM) was added to the samples prior to blocking free (non-nitrosylated) thiol groups, no plectin signal was detectable in the eluate (Fig. 20B, control), validating the assay. As an additional control, the membrane was stripped and overlaid with antibodies to eNOS, which itself is a target of nitrosylation (Ravi et al., 2004), revealing, as expected, the presence of the enzyme in both, the starting cell lysate and the eluate recovered from the streptavidin beads (Fig. 20B, eNOS).

Next, I examined whether plectin can be S-nitrosylated by an endogenous mechanism of NO generation. For this purpose I treated cultured endothelial cells with PMA and subjected the cell lysates to the biotin-switch assay. PMA, an agonist of PKC, has been shown to increase expression and enzymatic activity of eNOS in endothelial cells (Li et al., 1998; Shen et al., 2001). As shown in Figure 20C, plectin was indeed S-nitrosylated by endogenously generated NO, whereas at basal NO levels (no PMA treatment), neither plectin nor eNOS were nitrosylated.

8.2.5. Effect of NO donor-mediated nitrosylation on the cytoskeleton of endothelial cell

Cytoarchitecture of vimentin networks

To assess whether S-nitrosylation induced by NO donors had any effects on IF network cytoarchitecture, subconfluent cultures of immortalized mouse renal endothelial cells were subjected to immunofluorescence microscopy after exposure to the NO donor SNAP for 2, 4, or 6 h. Visualizing vimentin, the major constituent protein of endothelial IF networks, well spread cellular networks were observed at all time points, with no detectable differences becoming apparent between untreated and 6 hour-treated cells (compare Fig. 21, A-D). In contrast, when a similar experiment was carried out with immortalized plectin-deficient

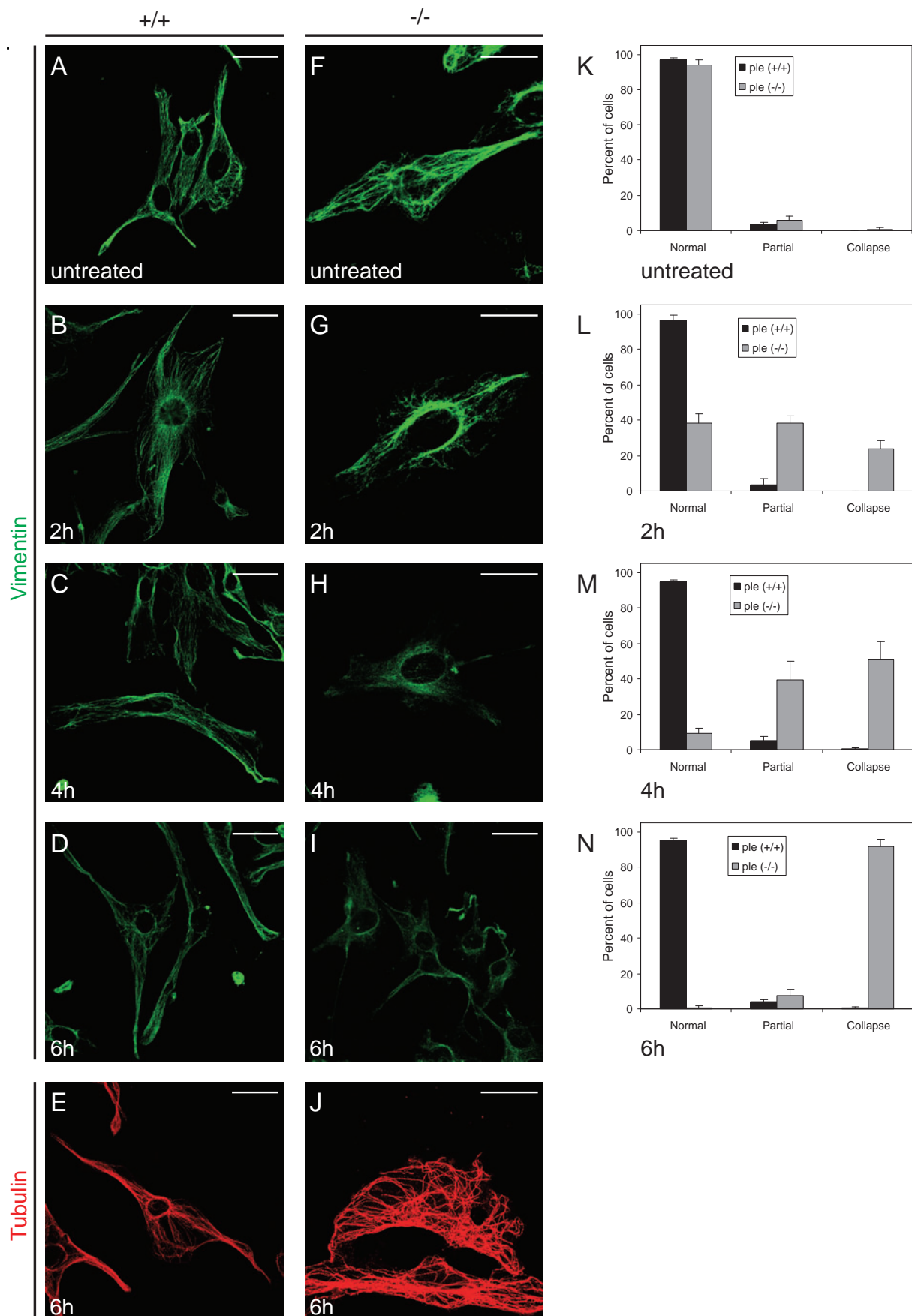


Figure 21. Immunofluorescence microscopy of wild-type and plectin-deficient endothelial cells after nitrosylation with SNAP. (A-J) Cells were untreated, or treated with SNAP for 2h, 4h, or 6h, prior to immunostaining, using antibodies to vimentin, or tubulin as indicated. Bars, 30 μm (A-E, I), and 20 μm (F-H, J). (K-N) Bar diagrams showing statistical evaluation of cells with normal, partially collapsed, and completely collapsed vimentin networks. Data shown represent mean values (\pm SEM) of three independent experiments (>100 cells per experiment were counted from randomly chosen optical fields).

endothelial cells, a progressive collapse of vimentin filament networks into perinuclear bundles was observed. A partial collapse was visible in some cells already at the 2 hour time point (Fig. 21G), while after 6 hours hardly any of the cells contained intact filaments (Fig. 21 I). In contrast, microtubules appeared unaffected by the SNAP treatment (Fig. 21, E and J). A statistical evaluation of over 100 wild-type and mutant cells, each, per time point (Fig. 21, K-N), revealed that while in wild-type cells the proportions of cells with intact (normal), partially collapsed, and fully collapsed IF networks were ~97:3:0 in untreated cells, compared to ~95:4:1 in 6 hours SNAP-exposed cells, in plectin-deficient cells the corresponding values were ~93:6:1 and ~1:8:91, respectively (Fig. 22, K-N). This strongly suggested an antagonistic role of plectin in S-nitrosylation-mediated vimentin filament collapse.

Effect of NO donor-mediated nitrosylation on microfilaments and focal adhesion contacts

A major biological significance of plectin's interaction with actin was revealed in studies on primary fibroblasts and astroglial cell cultures obtained from plectin^{-/-} mice. Andr a et al. (1998) found that the actin cytoskeleton, including focal adhesion contacts (FACs), was more extensively developed in plectin-deficient compared to wild-type cells. To investigate whether nitrosylation had any effects on microfilament network structure, endothelial cells deficient in plectin and corresponding cells from wild-type littermates were incubated with the NO donor SNAP and then subjected to immunofluorescence microscopy using antibodies to actin and to vinculin. As previously shown, untreated plectin-deficient fibroblasts showed a significant increase in the number of actin stress fibers and of vinculin-positive FACs compared to wild-type cells (compare Figs. 22 A-C with G-I). Upon treatment with the NO donor, several interesting phenomena were observed. First of all, in wild-type cells, actin stress fibers became restricted to regions in the cell centers (Fig. 22D), paralleled by the relocalization of vinculin-positive FACs (Fig. 22E) to the ends of the stress fibers in the same regions (Fig. 22, E and F). Interestingly, plectin-deficient endothelial cells did not show this retraction effect of microfilaments to the cell center upon SNAP treatment. Instead, I observed an increased number of stress fibers extending all the way to the periphery of cells, accompanied by an accumulation of FACs at the cell edges (Figs. 22, J-L). While NO donor-mediated nitrosylation caused the collapse of vimentin networks in the absence of plectin, the actin filament network in plectin^{-/-} cells did not show any significant changes.

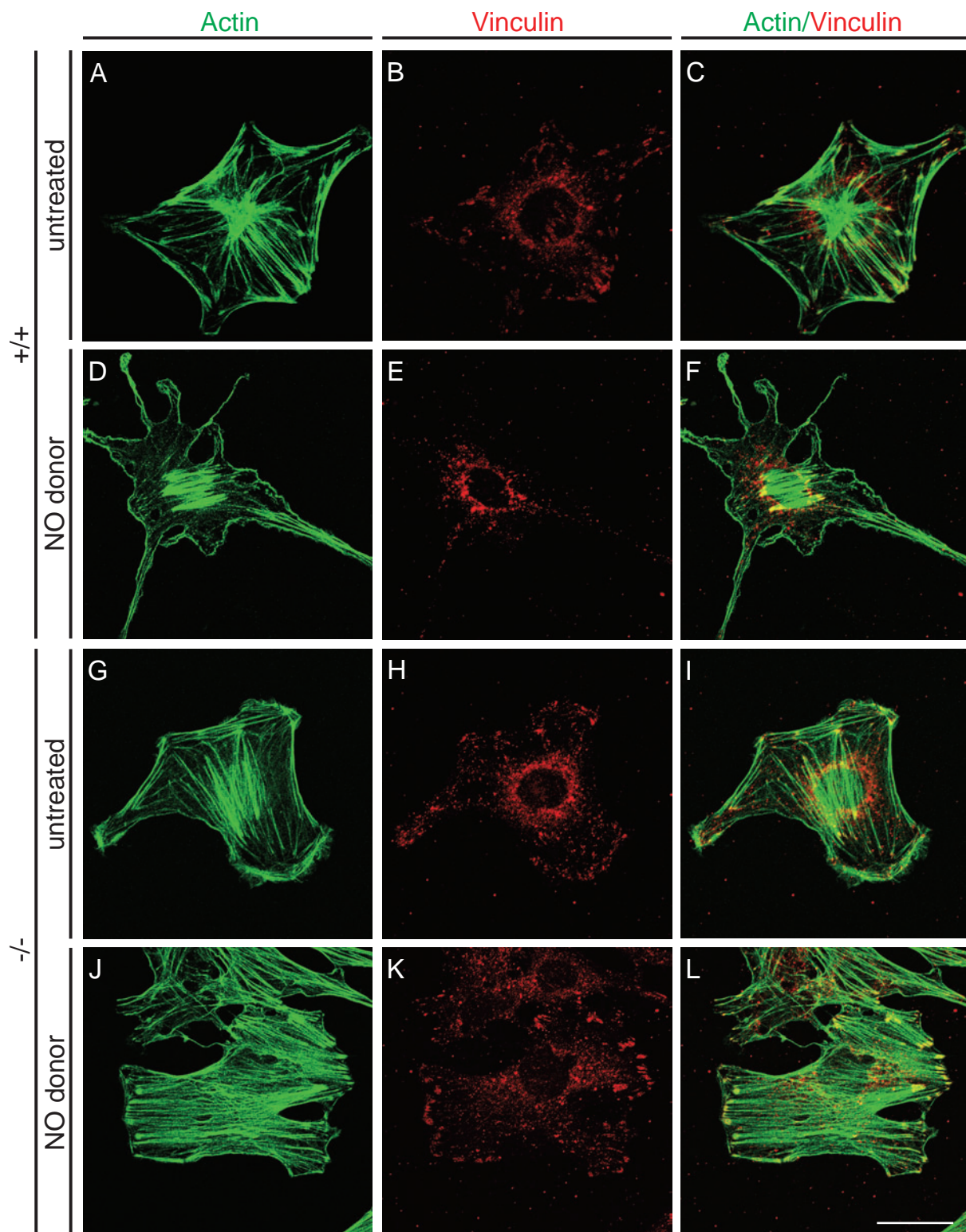


Figure 22. Immunofluorescence microscopy of wild-type (+/+) and plectin-deficient (-/-) endothelial cells before (untreated) and after nitrosylation using SNAP. Cells were immunostained using antibodies to actin or vinculin as indicated. Bar, 20 μ m.

8.2.6. Distribution, expression, and activity of eNOS in plectin-deficient endothelial cells

NO release from plectin-deficient compared to wild-type endothelial cells

After having shown that NO differentially affects cytoskeletal filament systems in plectin-deficient and wild-type cells, it was of interest to assess whether plectin was involved in NO-based signaling pathways. To address this question, I tested the influence of plectin deficiency on the NO levels released from endothelial cells. In cooperation with V. Dirsch & C. Schmitt (Department of Pharmacognosy, University of Vienna) NO production was quantified using the fluorescent probe DAF-2 in cell culture supernatants of endothelial cells

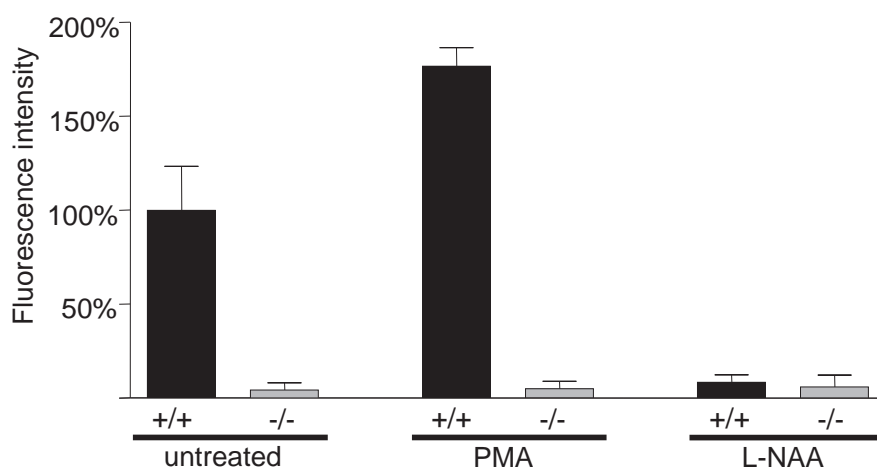


Figure 23. NO release from endothelial cells. Plectin^{+/+} or plectin^{-/-} endothelial cells were untreated or treated with either the protein kinase A activator PMA, or the irreversible eNOS inhibitor L-NAA. NO was quantified in cell culture supernatants using the fluorescent probe DAF-2. Fluorescence units were normalized to the number of cells. Data shown represent mean values (\pm SEM) of three independent experiments, each performed at least in triplicates.

that had previously been stimulated by the eNOS activator PMA (Leikert et al., 2001; Rathel et al., 2003). As a result of eNOS stimulation, NO released from endothelial cells increased to levels of 160% in comparison to unstimulated cells (100%) (Fig. 23). Interestingly, when unstimulated, plectin-deficient endothelial cells showed very low NO production, and even when eNOS was stimulated, NO production stayed unchanged. When a similar experiment was carried out with cells treated with the eNOS inhibitor L-NAA, NO production in wild-type cells significantly decreased, reaching a level comparable to that detected in the untreated plectin-deficient cells; NO production in plectin^{-/-} cells remained unchanged (Fig. 23). These results suggested that plectin was important for NO production by eNOS, as in its absence the production of NO was considerably lower, if not brought to a stop.

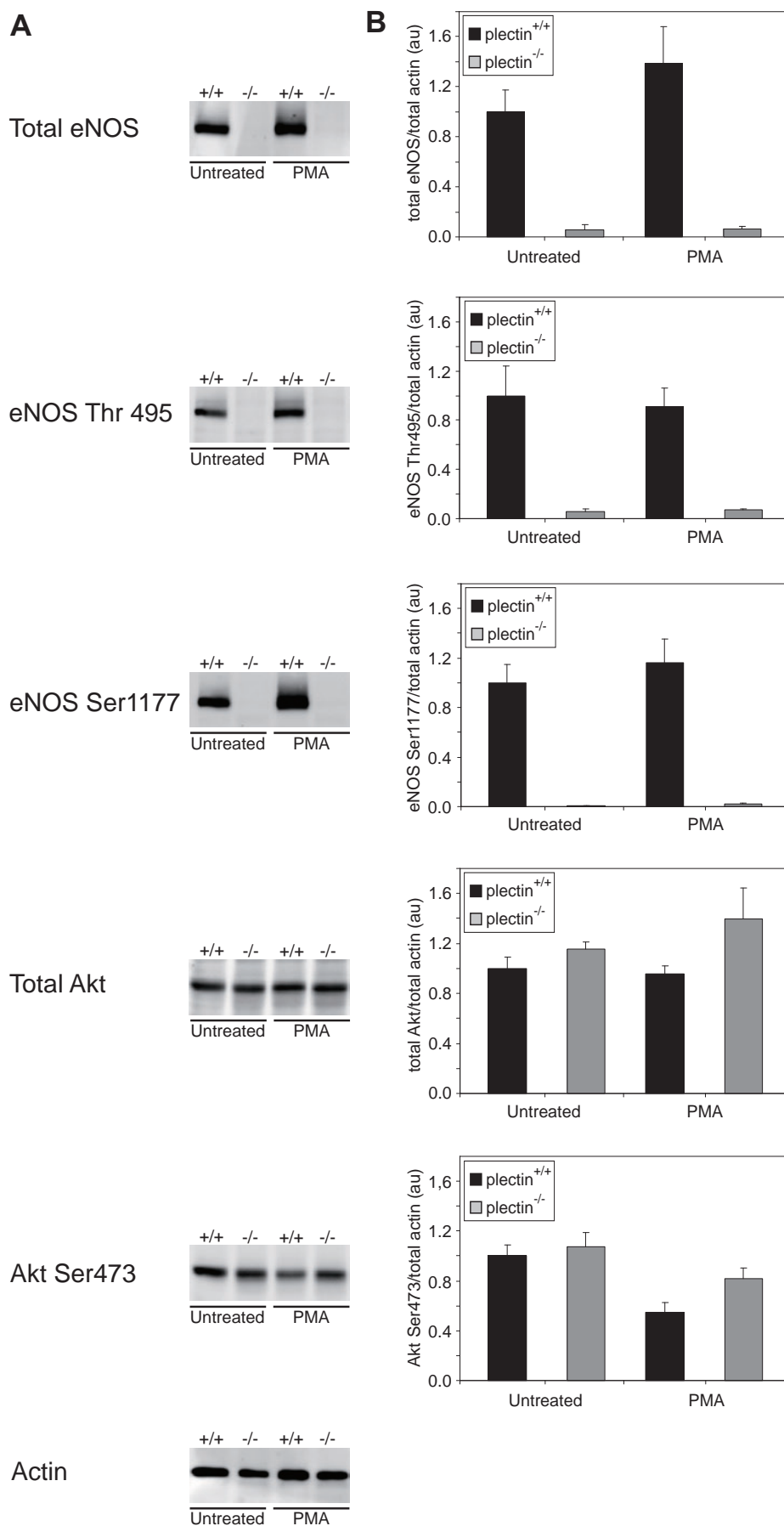


Figure 24. Expression and activation (phosphorylation) levels of eNOS. (A) Endothelial cells were either left untreated or treated with eNOS activator. Lysates from these cells were subjected to electrophoresis and immunoblotting was performed using antibodies to total eNOS, eNOS phosphoepitopes threonine 495 and serine 1177, Akt/protein kinase B, and its phosphoepitope serine 1177. Actin was used as a loading control. (B) Signal intensities of the bands, which were densitometrically determined in three independent experiments, were normalized to actin (mean \pm SEM). au, arbitrary units.

Expression and activation (phosphorylation) levels of eNOS

In order to determine whether the decreased NO production in plectin-deficient endothelial cells was due to decreased eNOS protein levels or activation, cell lysates from plectin^{+/+} and plectin^{-/-} endothelial cells were analyzed by immunoblotting. Cell lysates prepared from endothelial cells treated with eNOS activator, were analyzed using antibodies recognizing either all forms of eNOS (activated and inactivated) or only the phosphoepitopes characteristic of activated eNOS, such as phosphorylated threonine 495 and serine 1177 (Fleming and Busse, 2003; see details in Introduction). As shown in Fig. 24 (A and B, total eNOS) the data obtained corresponded to the measurements of NO production. In particular, in wild-type endothelial cells the total eNOS protein level was partially increased upon activation by PMA (Fig. 24, A and B; total eNOS; +/+). In contrast, in both untreated and treated plectin-deficient cells hardly any eNOS signal was detected (Fig. 24, A and B; total eNOS). Antibodies to the phosphoepitopes threonine 495 and serine 1177 showed patterns similar to that of total eNOS (Fig. 24, A and B; eNOS Thr495, eNOS Ser1177).

Protein kinase B/Akt is one of the kinases shown to phosphorylate and activate serine 1177 of eNOS. To find out whether the protein level or activation of this upstream activator kinase was similarly influenced by plectin deficiency, immunoblottings were performed using antibodies to total Akt kinase and alternatively to its phosphoepitope serine 473, that is responsible for its activation. Unlike eNOS, the protein level of total Akt kinase as well as the phosphoepitope serine 473 signal were very similar in wild-type and plectin-deficient cells, independent of whether they were PMA-treated or not (Fig. 24, A and B; total Akt, Akt Ser473).

Thus, the loss of NO production seemed to be a result of very low protein levels of eNOS, which would speak for an involvement of plectin in the regulation of eNOS expression and/or eNOS degradation. As these experiments were performed with immortalized cell cultures, which may have changed properties compared to genuine (non-immortalized) primary cells, in future studies, they should be confirmed using non-immortalized primary cell cultures.

Distribution of eNOS in endothelial cells

The observed decreased NO production and protein levels of eNOS in the absence of plectin prompted me to study the cellular localization of eNOS in endothelial cells. This was of

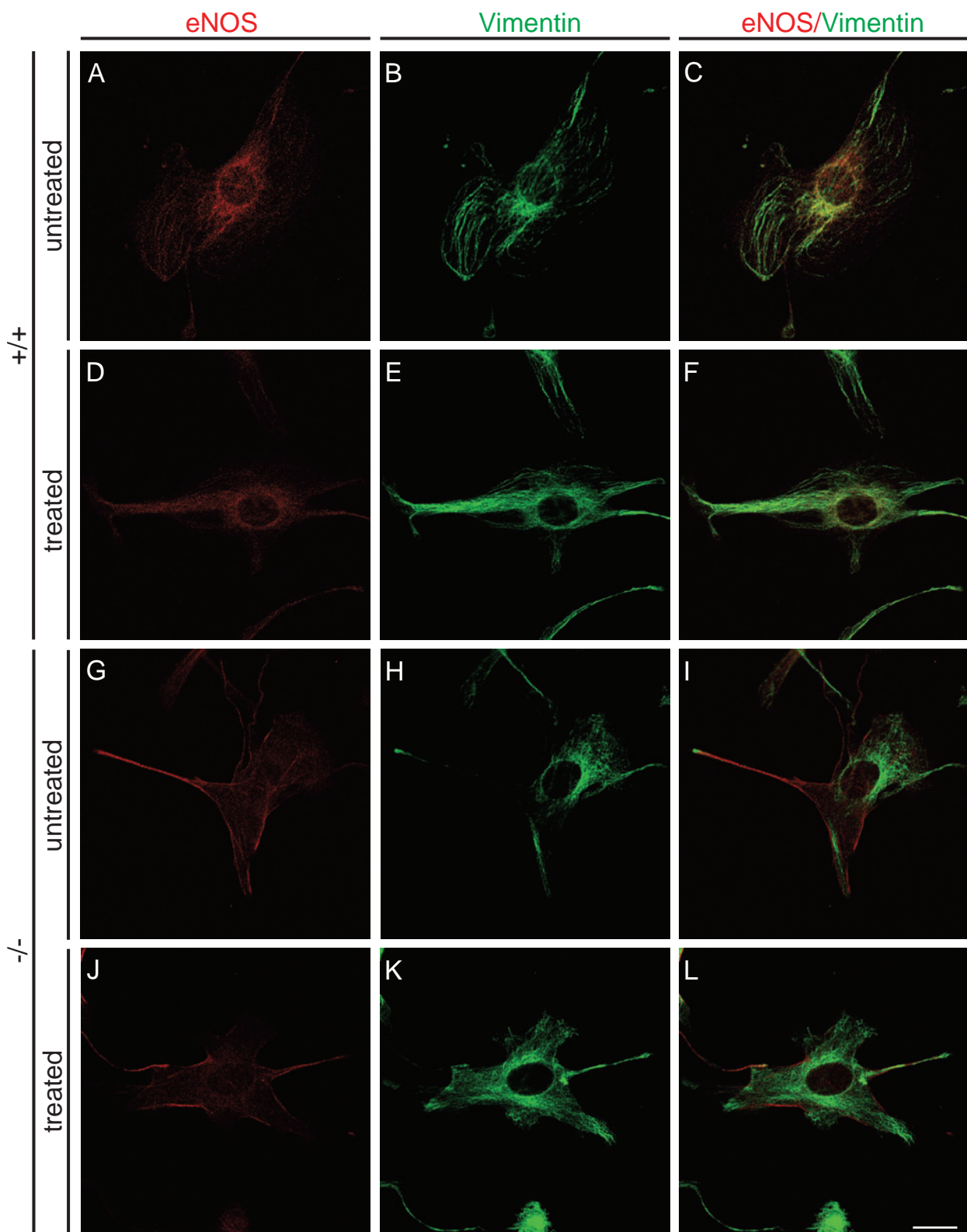


Figure 25. Immunofluorescence microscopy of wild-type and plectin-deficient endothelial cells after activation of eNOS. Cells were untreated, or treated with PMA, prior to immunostaining for eNOS, and vimentin. Bar, 20 μ m.

importance considering that membrane-bound eNOS associated with caveolin-1 in caveolae was found to be silenced and dependent on the activating mechanisms that disrupt its interaction with caveolin-1. Translocation of eNOS from caveolae to intracellular sites was found to result in the attenuation of NO production (Wu, 2002). Monitoring eNOS by immunofluorescence microscopy in wild-type endothelial cells upon eNOS induction, I found the enzyme to be diffusely distributed over the whole cytoplasm, which would correspond to the active form of eNOS (Fig. 25A). I did not observe any differences in the distribution of eNOS between untreated and PMA-treated cells (compare Fig. 25, A and D). In plectin knockout cells the eNOS signal was mainly observed at the periphery of cells, which would correspond to the inactive form of the enzyme (Fig. 25, G and J). These findings together with the results from expression/activation levels of eNOS, suggest a regulatory effect of plectin on eNOS activity.

8.3. PHOSPHORYLATION OF PLECTIN AND ITS EFFECT ON THE FORMATION OF VIMENTIN NETWORKS AND IF INTERMEDIATES

8.3.1. Plectin and vimentin form globular complexes upon phosphorylation by Cdk1 in vitro

As a cytoplasmic crosslinking element plectin could play an important role during mitosis when the cytoskeleton, including IF networks, is dramatically reorganized. It has previously been reported, that phosphorylation of plectin by serine/threonine kinases, including mitotic Cdk1, affects its binding affinity to vimentin (Foisner et al., 1991; Foisner et al., 1996; Malecz et al., 1996), suggesting that mitosis-specific phosphorylation regulates plectin's cross-linking activities and association with IFs. Both, plectin and vimentin have been shown to possess unique target sites for Cdk1 (Chou et al., 1990; Chou et al., 1991; Malecz et al., 1996), with plectin's phosphorylation site residing in the repeat 6 domain, not far from the IF-binding site. Phosphorylation of vimentin by mitotic Cdk1 has been shown to correlate with the disassembly of vimentin IF networks (Chou et al., 1990; Tsujimura et al., 1994).

To assess the effects of protein phosphorylation on the formation and binding affinity of plectin-vimentin protein complexes in vitro, recombinant versions of mouse vimentin and

of plectin domain R5-6, a C-terminal fragment of plectin containing its major IF-binding site flanked by two of its six repeat domains, were incubated with Cdk1 in various combinations under filament assembly conditions. Filaments assembled from vimentin alone, without prior incubation with Cdk1, were observed by negative staining electron microscopy predominantly in the form of loose filamentous networks (Fig. 26A). When preassembled filaments were incubated with roughly equimolar amounts of plectin R5-6 the networks formed were non-uniformly decorated with globular structures, presumably consisting of clustered plectin R5-6 molecules or complexes of R5-6 and vimentin (Fig. 26C). Plectin R5-6 incubated alone (without vimentin) under similar conditions formed aggregates of variable sizes and shapes (Fig. 26B), which were seen also in samples of R5-6-vimentin mixtures, without however showing association with filaments (Fig. 26C).

Upon phosphorylation of *in vitro* assembled vimentin filaments by Cdk1 (recombinant Cdk1/cyclinB complex; Chou et al., 1991), disassembly of filaments was observed, with the concurrent appearance of short fibrils and small aggregates (Fig. 26D). The appearance of plectin R5-6 was unaltered after Cdk1 phosphorylation (Fig. 26E). However,

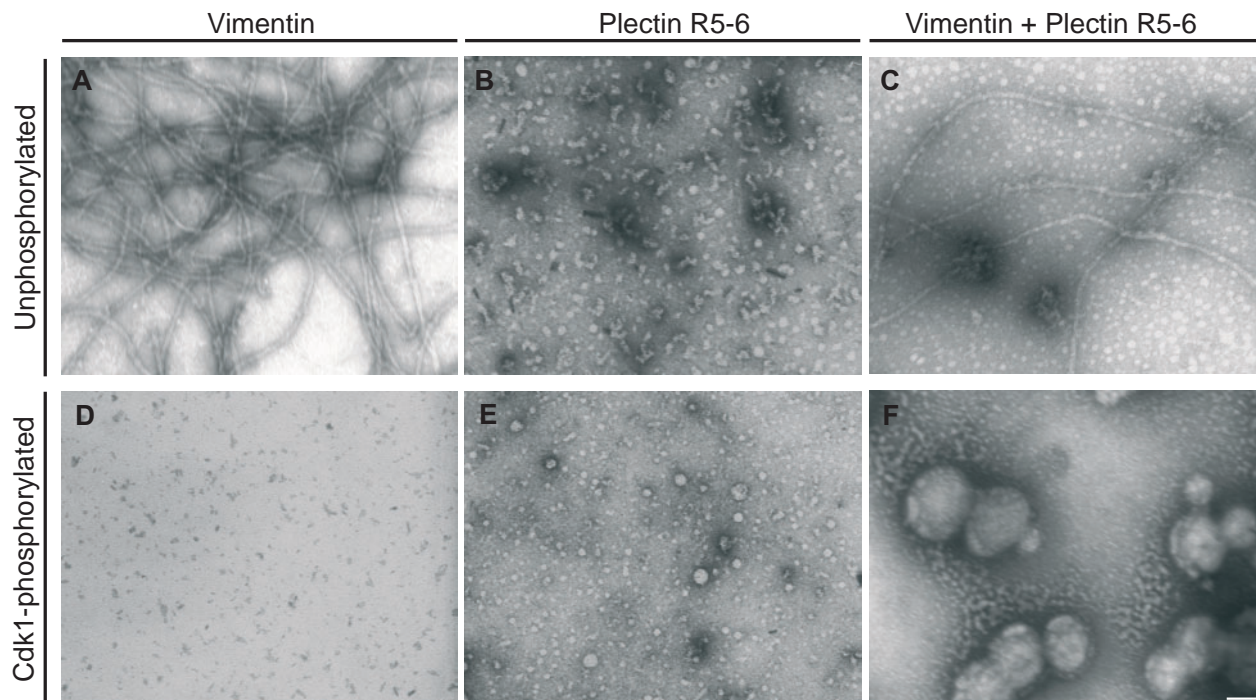


Figure 26. Formation of globular complexes from vimentin and a C-terminal plectin fragment upon Cdk1 phosphorylation *in vitro*. Electron microscopy of uranyl acetate-stained oligomeric structures formed from recombinant vimentin alone (A and D), plectin domain R5-6 alone (B and E), or equimolar mixtures of both (C and F). Specimens shown in A-C were unphosphorylated, those in D-F were phosphorylated by Cdk1 prior to incubation under assembly conditions and processing for electron microscopy (for details see text). Bar = 50 nm.

when Cdk1-phosphorylated vimentin was subjected to assembly conditions in the presence of phosphorylated plectin R5-6, globule-like structures with diameters of ~150 nm were visualized (Fig. 26F).

To gain more insight into the mechanism of globular particle formation, I examined whether Cdk1 or PKC phosphorylation of plectin and vimentin affected their binding affinities. To assess binding, unphosphorylated or *in vitro* phosphorylated samples of plectin fragments R5-6 or R5-6tail were coated onto microtiter plates, and overlaid with Eu³⁺-labeled (either unphosphorylated or phosphorylated) vimentin. Vimentin bound was then quantitatively determined after release of complexed Eu³⁺ and detection by time-resolved fluorometry (Soini and Kojola, 1983; Nikolic et al., 1996). As shown in Fig. 27A, Cdk1-phosphorylation of both proteins, plectin domain R5-6/R5-6tail and vimentin, led to an affinity comparable to that of the unphosphorylated forms (Fig. 27A, P*+V* versus P+V). Cdk1-phosphorylated plectin R5-6 showed lower (60%), albeit still significant, binding to vimentin compared to the unphosphorylated form (Fig. 27A, P*+V). In the reverse case, where vimentin but not plectin was phosphorylated, binding was considerably increased (Fig. 27A, P+V*). This elevation might be explained by an increased number of binding sites being accessible on phosphorylated (non-filamentous) vimentin which is known to exist as tetrameric molecules. Very similar results were obtained when I used plectin fragment R5-6tail. A general reduction in binding (~25% compared to the tail-less R5-6 domain) observed in this case pointed towards an influence of the tail domain on binding (Fig. 27A). The relatively small differences in binding affinities of Cdk1-phosphorylated, compared to non-phosphorylated forms of both proteins (see Fig. 27A) indicated that plectin and vimentin can bind to each other regardless of their Cdk1-phosphorylation status. This explains that, albeit Cdk1 phosphorylation causes the release of plectin from filamentous vimentin at the onset of mitosis in certain cell types, such as CHO cells (Foisner et al., 1996), a fraction of both proteins could also stay associated throughout mitosis. The association of both proteins during mitosis has also been reported by BHK-21 cells (Skalli et al., 1992). As the behavior of IF networks during mitosis considerably varies between cell types (Chou et al., 2007), so will probably also the fractions of both proteins forming a complex during mitosis.

Phosphorylation of plectin R5-6 and R5-6tail using protein kinase C β II (PKC) instead of Cdk1 decreased its affinity to vimentin to a similar level (~60%) as Cdk1 (Fig. 27B, P*+V, +DAG/PS). When a similar experiment was performed in the absence of DAG/PS

(diacylglycerol/phosphatidylserine) the activity decreased to 40% (Fig. 27B, P*+V, -DAG/PS). Plectin fragment R5-6tail showed similar tendencies although binding affinities in general were lower than that of fragment R5-6.

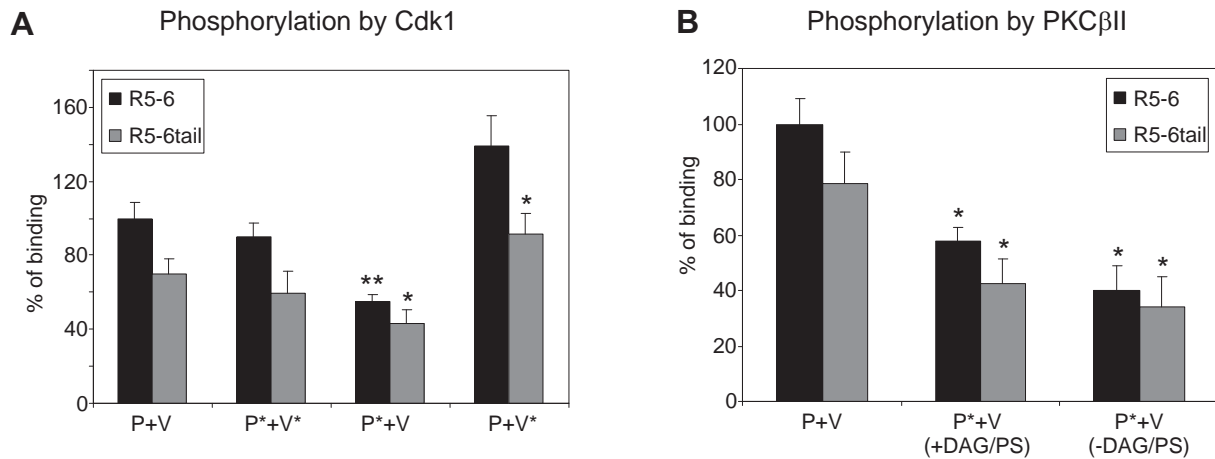


Figure 27. Binding of recombinant plectin domain R5-6 or R5-6tail to vimentin with and without Cdk1 (A) or PKCβII (B) phosphorylation. Phosphorylated or unphosphorylated samples of R5-6/R5-6tail were coated onto microtiter plates at concentrations of 100 nM, and overlaid with Eu^{3+} -labeled, phosphorylated/unphosphorylated recombinant vimentin at concentrations of 500 nM. P, plectin; V, vimentin; P*, V*, phosphorylated plectin and vimentin, respectively; DAG/PS, diacylglycerol/ phosphatidylserine. Data represent the mean \pm SEM of three independent experiments. * and **, $P < 0.05$ and $P < 0.01$, respectively.

8.3.2. Plectin deficiency affects vimentin network dynamics during cell division and leads to multipolar spindles

In interphase cells, cytoplasmic IF proteins typically form a network that extends from the nuclear surface towards the cell periphery, but as cells enter into mitosis, IFs are dramatically reorganized. Vimentin remains in partially filamentous form in some cells, or disassembles into non-filamentous granules in other cells upon phosphorylation by mitotic Cdk1 (Aubin et al., 1980; Franke et al., 1982; Rosevear et al., 1990; Chou et al., 2007).

In view of globule-like structure formation of mitotic Cdk1-phosphorylated vimentin in the presence of phosphorylated plectin R5-6, it was of interest to assess whether similar structures were present in dividing cells and whether plectin was associated with such structures. To address these questions, plectin^{+/+} and plectin^{-/-} fibroblast cell cultures were synchronized by double thymidine block followed by nocodazole-induced mitotic arrest. Detached premitotic cells were plated onto polylysine-coated coverslips and vimentin remodeling during various mitotic stages and new network formation during cytokinesis

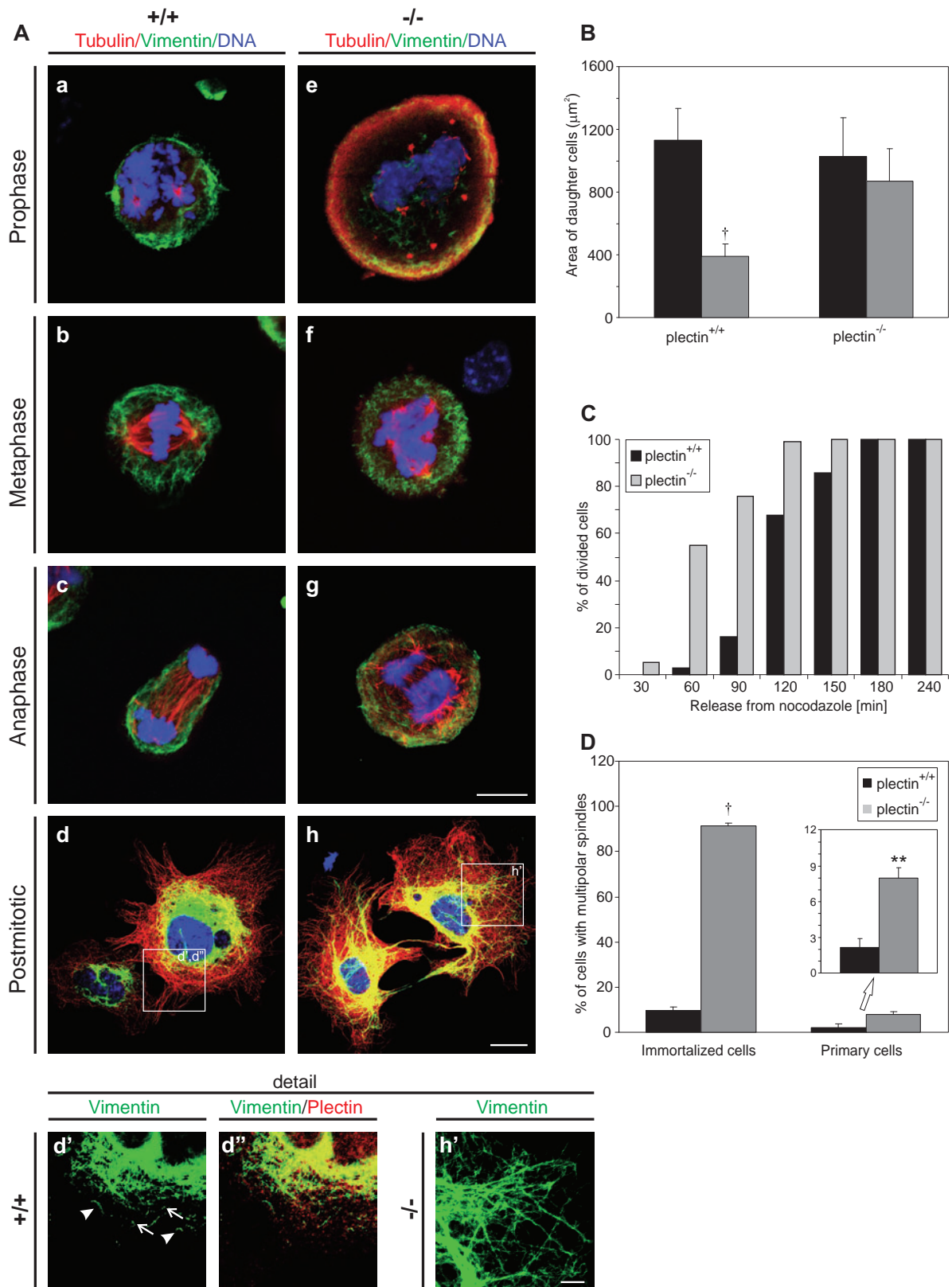


Figure 28. Immunofluorescence microscopy of wild-type and plectin-deficient fibroblasts during mitosis. A, Cells were synchronized by double thymidine block and fixed during prophase (a, e), metaphase (b, f), anaphase (c, g), and telophase/cytokinesis phase (d, h). For immunostaining, antibodies to vimentin, tubulin, and plectin were used, as indicated. DNA was visualized with Hoechst dye. Boxed areas in d and h are shown as magnified images in d', d'', and h'. Bar (g) = 20 µm (representative for rows prophase, metaphase and anaphase); bar (h) = 20 µm (representative for row postmitotic); bar (h') = 5 µm (representative for bottom row). B, Areas of daughter cell pairs. Black and grey columns represent larger and smaller cells, respectively. Values are based on the analysis of 20 pairs of daughter cells. C, Statistical evaluation of the length of mitosis. For each time point, the percentage of cells that had reached cytokinesis after nocodazole release and were connected by an intercellular bridge was calculated. D, Incidence of cells with multipolar spindles in immortalized or primary cells. Percentage was calculated by scoring 200 mitotic cells. Error bars represent SEM based on three independent experiments. †, $P < 0.001$.

were analyzed by immunofluorescence microscopy. In prophase, characterized by the appearance of two centrioles, vimentin networks in wild-type cells were found to have disassembled only partially, as filamentous structures were clearly visible, particularly in peripheral regions of the cell (Fig. 28A, a). These structures were maintained in metaphase, where they formed a cage-like network around the bipolar spindle (Fig. 28A, b). Upon chromosome separation, starting in anaphase and extending into telophase, these persisting filamentous vimentin structures became partitioned between the two newly forming cells (Fig. 28A, c). The majority of wild-type cells undergoing cytokinesis showed an uneven distribution of the vimentin network to the daughter cells (Fig. 28A, d), as confirmed by taking Z-stacks of the vimentin staining. Not unexpected, postmitotic cells displayed less vimentin structures in the smaller one of two daughter cells (Fig. 29, +/+). In newly spreading postmitotic cells, vimentin filament intermediates in the form of granules and squiggles were clearly visualized in peripheral region of wild-type cells (Fig. 28A, d'), and these structures were associated with plectin (Fig. 28A, d''). The shape and size of these vimentin granules in the postmitotic fibroblasts resembled that of globule-like structures formed when Cdk1-phosphorylated vimentin was assembled in the presence of phosphorylated plectin R5-6 (Fig. 26F), supporting the notion that the interaction of plectin with vimentin was important for their formation *in vivo*.

In mitotic plectin-deficient fibroblasts, I noticed several differences. During prophase and all the following stages of mitosis, vimentin-positive structures appeared less filamentous than those of wild-type cells (Fig. 28A, e-g; compare with a-c), suggesting that mitotic vimentin structures became more soluble in the absence of plectin. In addition, the majority of plectin-deficient prophase cells appeared to be larger than their wild-type counterparts and they showed prominent tubulin-specific staining associated with subplasma membrane structures partially overlapping with vimentin-positive structures (Fig. 28A, e). The hallmark feature of plectin^{-/-} cells, however, was the display of multiple centrioles during prophase and of multipolar spindles in meta- and anaphase, as revealed using anti- α -tubulin antibodies (Fig. 28A, f and g). Interestingly, there was also a much more even distribution of vimentin structures to separating daughter cells (Figs. 28A, h and 29, -/-), and finally, unlike wild-type cells, vimentin network assembly in postmitotic plectin-deficient cells occurred without the formation of granules and squiggles as intermediates (Fig. 28A, h and h').

A statistical analysis of the areas occupied by postmitotic daughter cells in wild-type

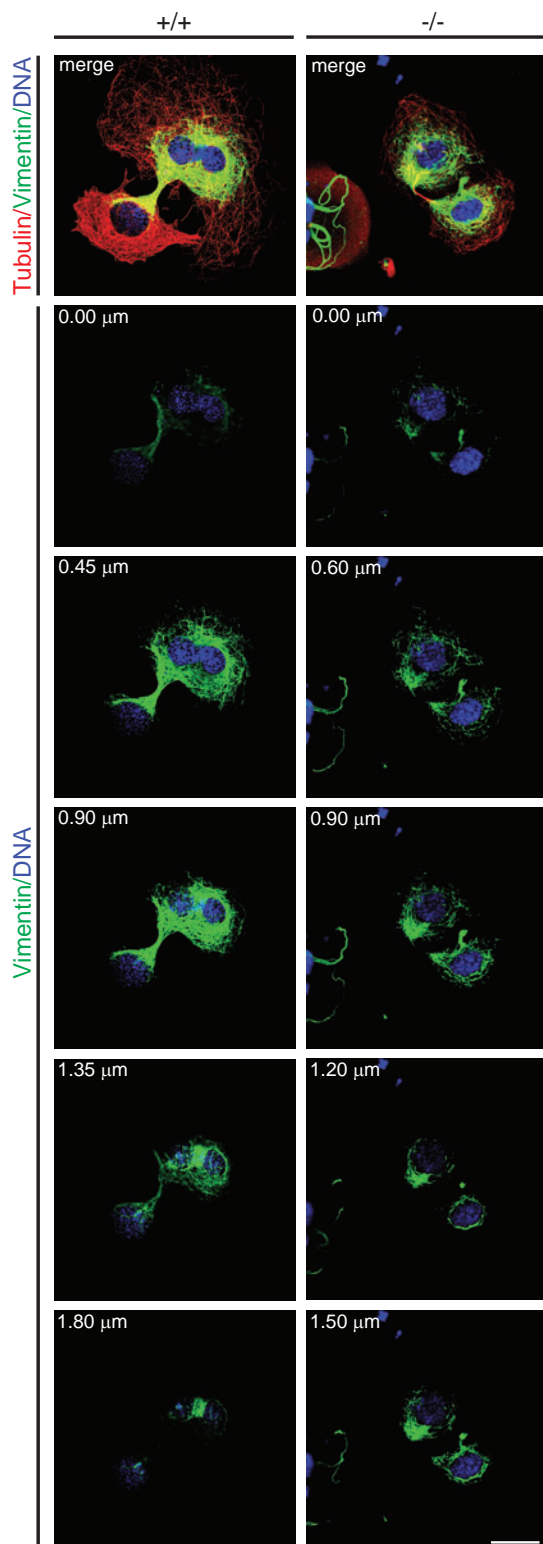


Figure 29. Immunofluorescence microscopy (Z-stacks) of postmitotic cells showing differences in the distribution of vimentin structures in wild-type and plectin-deficient fibroblasts. Z-stacks were taken at intervals indicated in panels. Combined Z-stack images of vimentin, tubulin, and DNA are shown in top panels (merge); individual Z-stack images show only vimentin and DNA signals. Note unequal versus equal distribution of vimentin signals in plectin^{+/+} and plectin^{-/-} cells, respectively. Bar = 20 μm .

and plectin^{-/-} cultures clearly showed that the partitioning of vimentin structures between daughter cells correlated with their size. As shown in Fig. 28B, wild-type daughter cells showed an almost 3-fold difference in occupied areas (~ 388 versus $\sim 1132 \mu\text{m}^2$), whereas corresponding areas measured for plectin^{-/-} cells varied insignificantly, ranging from 869–1028 μm^2 . Next, I examined whether the differences in IF assembly/disassembly patterns

observed in wild-type and plectin-deficient fibroblasts correlated with differences in their progression through mitosis. For this, I carried out a statistical analysis of synchronized cells that had passed through mitosis and started to undergo cytokinesis. As shown in Fig. 28C, already 55% of plectin^{-/-} cells had reached this stage within 60 min after nocodazole release, compared to only 3% of wild-type cells. Nearly all, namely 99%, of plectin^{-/-} fibroblasts had passed through mitosis within 120 min, whereas this applied to only 68% of wild-type cells; plectin^{+/+} fibroblasts had not finished cell division before 180 min (Fig. 28C). I attributed this difference to the fact that cells containing more loosely networked vimentin (due to the lack of plectin crossbridges) more readily undergo the structural reorganization that takes place during mitosis and cytokinesis. For a similar reason, vimentin is likely to get segregated more evenly to the two daughter cells. The uneven distribution of IFs becomes evident upon examination of pictures published as far back as 1980 (Aubin et al., 1980), although this phenomenon has not been discussed much. In all, these data revealed an interesting correlation between plectin-regulated IF dynamics and the duration and rate of mitosis.

The hallmark of plectin-deficient mitotic cells, centrosome amplification and multipolar spindles, was observed in ~90% of synchronized cells, compared to only 10% of similar wild-type cells (Fig. 28D). Inactivation of p53, which was used to obtain immortalized cell cultures, is known to result in centrosome amplification due to deregulation of the centrosome duplication cycle and failure to undergo cytokinesis (Fukasawa et al., 1996; Meraldi and Nigg, 2002; Tarapore and Fukasawa, 2002; Shinmura et al., 2007). As plectin^{+/+} and plectin^{-/-} fibroblasts were both lacking functional p53, the absence of p53 is unlikely to have accounted for the dramatic increase in multipolar spindle formation in plectin-deficient cells ($P < 0.001$). Nevertheless, to confirm that it must have been the loss of the plectin allele that greatly boosted multipolar spindle formation, I collected mitotic cells from primary cell cultures derived from p53 wild-type mice (p53^{+/+}) by mitotic shake-off (isolation of cells in sufficient amounts for synchronization was not possible), plated them and counted the cells carrying bipolar or multipolar spindles. The ratio of cells with bipolar spindles to those with multipolar spindles was 12:1 ($n = 200$) in the case of plectin-null cells compared to 49:1 ($n = 200$) for wild-type cells (plectin^{+/+} versus plectin^{-/-}; $P < 0.05$; Fig. 28D). Together these data clearly suggested a role for plectin in centromere duplication and/or spindle assembly.

8.3.3. Plectin-dependent formation of vimentin filament intermediates delays IF network assembly

IF networks assemble sequentially in several steps, from non-filamentous granules, short fibrous squiggles, to long fibrils, as shown by *in vivo* studies (Prahlad et al., 1998; Chou and Goldman, 2000). Although the binding of plectin to IFs, in particular to vimentin, has long been established using different methodologies (for review see Rezniczek et al., 2004), the issue of whether plectin-binding affects dynamic properties of IFs has not been addressed yet. Plectin as a major organizing element of IF network cytoarchitecture, may well have a function in IF network assembly and dynamics. Therefore the following questions were addressed: Is plectin-vimentin binding involved in the formation of IF intermediates, particularly of granules and squiggles, and if plectin influences the formation of IF intermediates, is it part of such structures?

To assess whether plectin has any influence on IF assembly, trypsinized cultures of immortalized plectin^{+/+} and plectin^{-/-} mouse fibroblasts were replated, and polymeric vimentin structures forming during cell spreading were monitored by immunofluorescence microscopy. As described by Goldman and Follett (Goldman and Follett, 1970), in wild-type cells IFs lost their extended network organization during trypsinization and collapsed into juxtannuclear aggregates that persisted up to 30 min after replating (Fig. 30A, a). Globular vimentin structures were observed in peripheral regions of such cells within 45 min after replating (Fig. 30A, b, b', b''). 120 min after replating, short filamentous vimentin structures resembling squiggles (Prahlad et al., 1998) became dominant over globular structures in these regions (Fig. 30A, c, c', c''). After 240 min, short squiggles were replaced by longer filamentous structures, and finally after 360 min, granules, squiggles, or filamentous structures with two free ends were hardly observed anymore (Fig. 30A, d). At that stage, IFs formed a delicate fibrous network concentrated around the nucleus with only a few filaments extending all the way to the cell periphery. As in postmitotic cells, all vimentin filament intermediates in the form of granules and squiggles have found to be associated with plectin (Fig. 30A, b'', c''). The microtubule network, showing a considerably faster assembly rate throughout cell spreading, had already reached its fully extended state at this time (Fig. 30A, e-h; note that single channel images of the same cells double-labeled

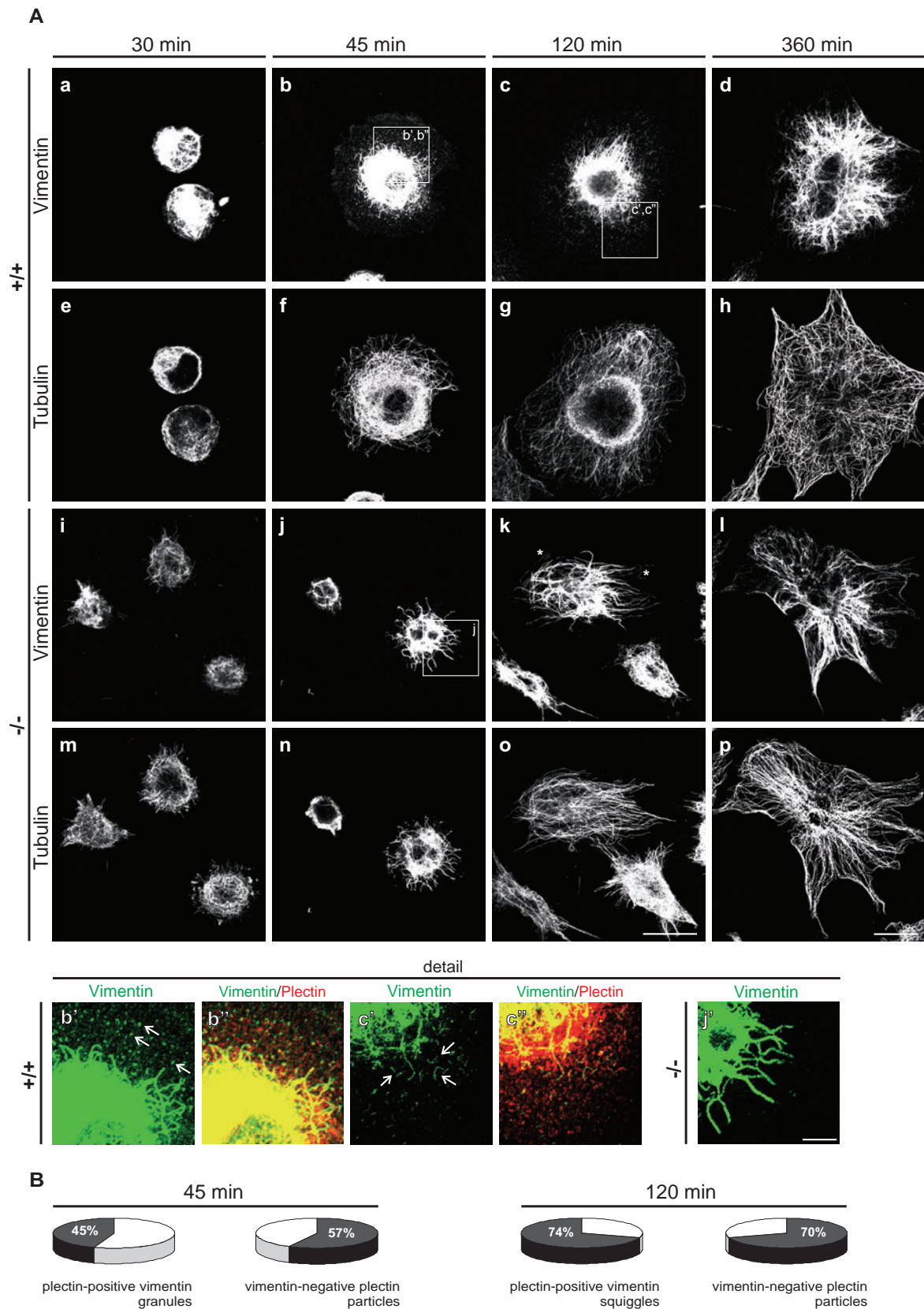


Figure 30. Immunofluorescence microscopy of wild-type (+/+) and plectin-deficient (-/-) fibroblasts. A, Cells were fixed at the times indicated (30, 45, 120, or 360 min) after trypsinization and replating, and immunostained using antibodies to vimentin, tubulin, or plectin, as indicated. The boxed areas in b, c, and j (designated with corresponding primed letters) are shown as magnified images in the bottom row (detail). Bar (p) = 20 μ m (representative for column 360 min); bar (o) = 20 μ m (representative for columns 30, 45, and 120 min); bar (j') = 5 μ m (representative for bottom row). B, Circle diagrams showing statistical evaluation of granule and squiggle compositions. Counts were taken from randomly chosen cells (n = 9), at time-points 45 min (granules and particles) and 120 min (squiggles); more than 100 granules or squiggles were counted per cell. Results represent average values from three independent experiments.

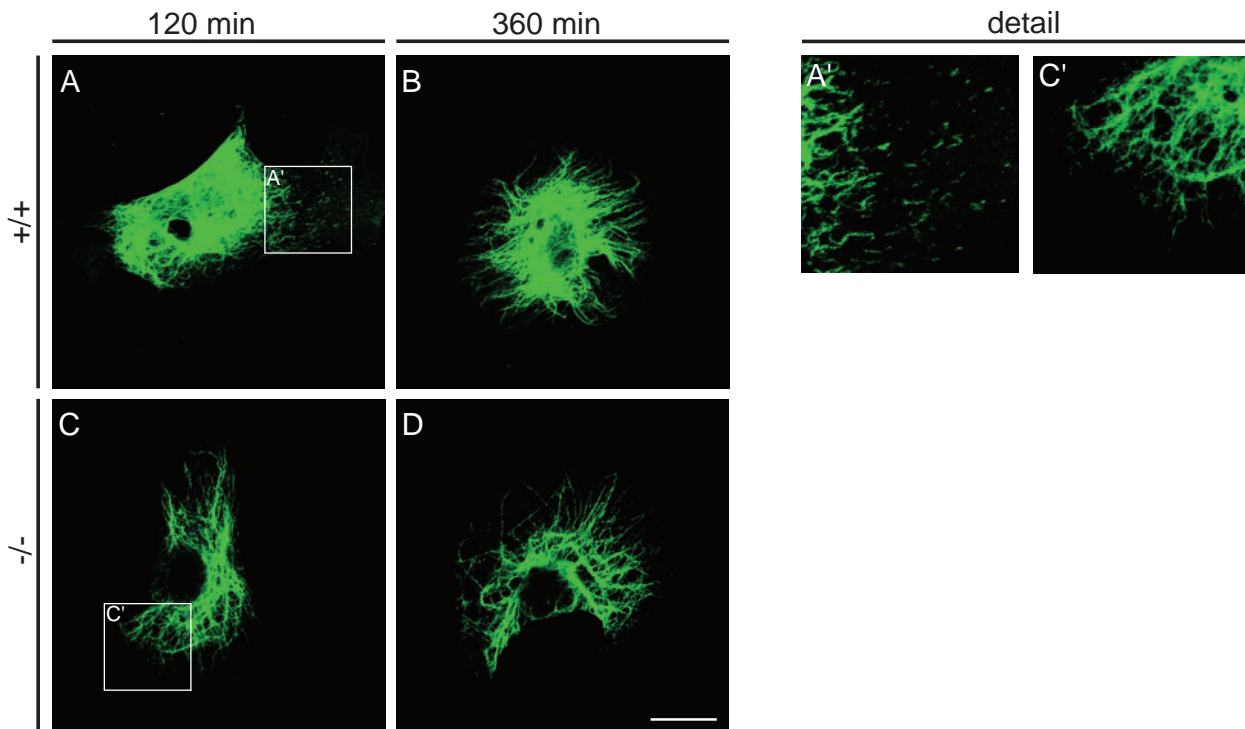


Figure 31. Immunofluorescence microscopy of primary wild-type (+/+) and plectin-deficient (-/-) fibroblasts. Cells were fixed at the times indicated (120 or 360 min) after trypsinization and replating, and immunostained using antibodies to vimentin, as indicated. The boxed areas in A and C (designated with corresponding primed letters) are shown as magnified images (detail). Bar = 20 μ m.

for vimentin and tubulin are shown in series a-d and e-h, respectively). Consistent with reports showing transport of squiggles along microtubules (Prahlad et al., 1998; Yabe et al., 1999a; Helfand et al., 2002), the majority of vimentin granules and squiggles forming during cell spreading co-aligned with microtubules.

In plectin-deficient fibroblasts, the formation of vimentin-positive granules or squiggles was not observed at any stage of cell spreading (Fig. 30A, i-l). However, a few quite long (up to $\sim 12 \mu$ m) filamentous structures with two free ends, presumably representing fragmented filaments, could occasionally be visualized in some of the cells, albeit not before the 120-min time point (Fig. 30A, k, asterisks). Interestingly, the formation of vimentin networks proceeded noticeably faster in the absence of plectin. Fully-spread vimentin networks had already formed within 120 min, compared to 360 min and more in wild-type cells (compare Figs. 30A, k and d). Both phenotypes, absence of filament intermediates and faster IF network formation, could be confirmed using primary cultures of plectin^{-/-} fibroblasts (Fig. 31). Thus, IF network formation in cells that were spreading after

trypsinization/replating in both wild-type and mutant cells followed patterns very similar to those of postmitotic cells.

A detailed examination of double-immunostained plectin^{+/+} fibroblasts during the time window when vimentin filament intermediates were formed (45-120 min), revealed that vimentin and plectin could form three different populations of globular structures, consisting of either both proteins, or each one alone. A statistical analysis showed that 45 min after replating only 45% of vimentin-positive granules observed were also plectin-positive (Fig. 30B, 45 min). Interestingly, 120 min after replating, when vimentin intermediates had already reached the stage of squiggles, most of them (74%) turned out to be plectin-positive (Fig. 30B, 120 min). A similar analysis of plectin-positive particles revealed that more than half (57%) were vimentin-negative (Fig. 30B, 45 min) and this percentage increased to 70% at the later stage (Fig. 30B, 120 min). These results suggested that while most of the vimentin was associated with plectin as filaments formed, plenty of plectin remained in a vimentin-unassociated state. Furthermore, the absence of vimentin intermediates in plectin-null fibroblasts pointed to a requirement for plectin in promoting their assembly.

8.3.4. Plectin-containing vimentin squiggles exhibit directional movement towards the cell periphery

Recent studies have revealed, that IFs are highly dynamic polymers, with three types of intermediate structures - granules, squiggles, and longer filaments. Furthermore, the smaller subunits were found to be motile, assembling into polymerized IFs in a stepwise process (Chou and Goldman, 2000; Chou et al., 2007). As the monitoring of vimentin and plectin during cell spreading showed, that plectin was associated with vimentin from the early stages of assembly and that the formation of vimentin intermediates was plectin dependent, the question arose whether plectin influences the transport and kinetics of vimentin intermediates and/or the stepwise formation of stable IFs.

To monitor vimentin granule and squiggle formation during fibroblast cell spreading *in vivo*, cells were transiently transfected with a cDNA expression vector encoding a GFP–vimentin fusion protein. Twenty four hours after transfection, cells were trypsinized and replated, and the behavior of the fusion protein was monitored by time-lapse microscopy of

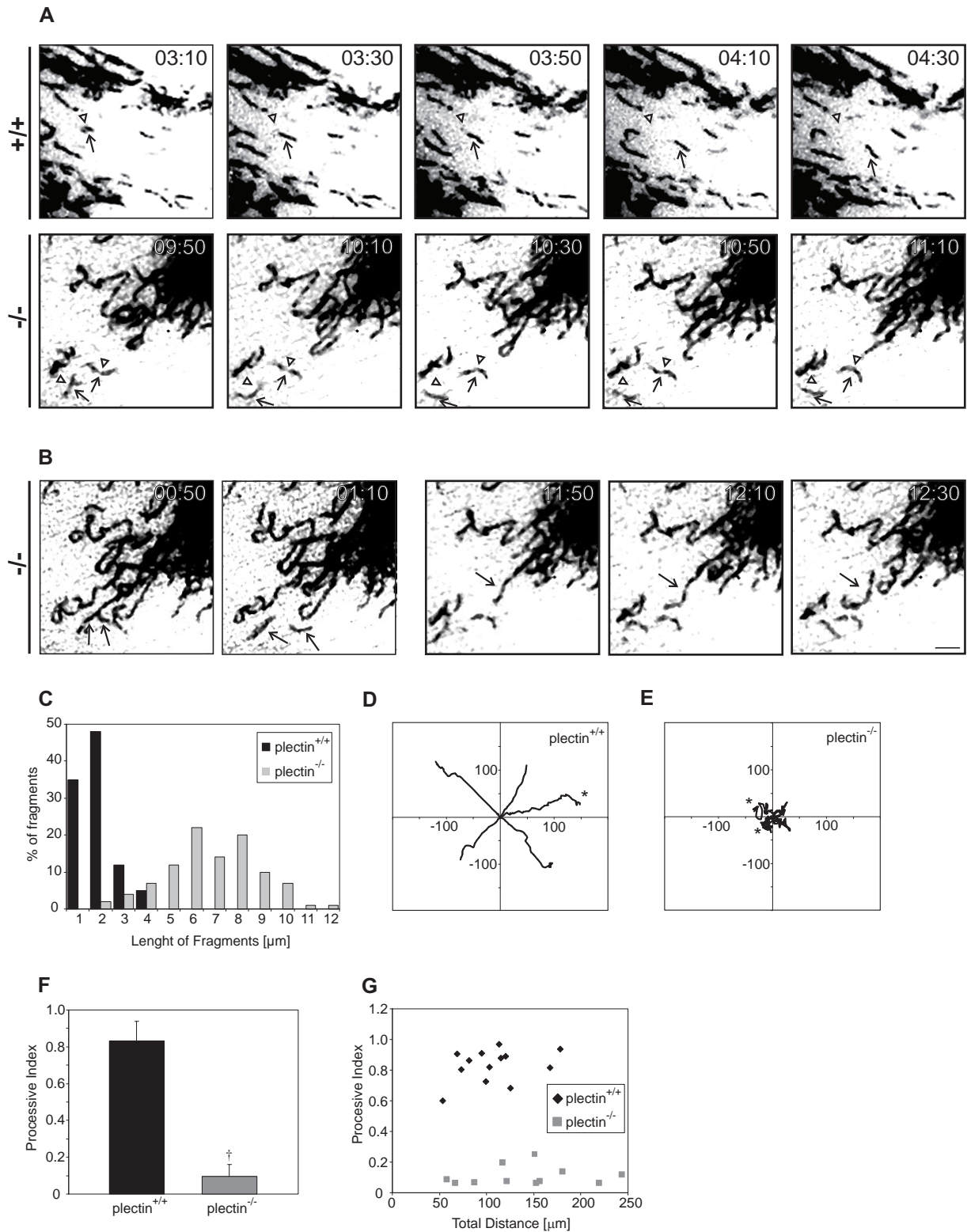


Figure 32. Time-lapse observations of vimentin intermediates in a spreading (live) fibroblast cell transfected with GFP-vimentin. A, Images of vimentin squiggle movement in wild-type, and of vimentin fragments in plectin knock-out (-/-) cells. Arrowheads, starting positions; arrows, actual positions. B, Process of fragmentation visualized in a plectin knockout cell. Formed fragments are indicated with arrows. Bar = 10 μm. C, Statistical evaluation of squiggle and fragment sizes in wild-type versus plectin-deficient cells. D and E, Diagrams representing directionality of processive migration of squiggles and fragments in wild-type (+/+) and plectin-deficient (-/-) cells. Five migration tracks of squiggles/fragments are shown in each case. Asterisks correspond to squiggle/fragment tracked in A. F, Statistical evaluation of processive indexes. G, Scatter diagram showing processive indexes as a function of total distances. Data shown represent mean values (± SEM) of five independent experiments (13 trajectories were measured). †, $P < 0.001$.

spreading cells. Granules and squiggles observed in lamellipodial regions of live cells (Fig. 32A, upper row) were indistinguishable regarding shape and dimensions from those visualized in fixed (untransfected) spreading cells using immunofluorescence microscopy. Granules and squiggles containing GFP-tagged vimentin were motile, showing movement preferentially towards peripheral regions of the cells (Fig. 32A, +/+). Squiggle movement was linear and continuous as is evident from the positions of the arrow in Fig. 32A, +/+, which marks the actual positions of a squiggle relative to that of its starting position (arrowhead).

When similar experiments were carried out with plectin-deficient fibroblasts, GFP-tagged vimentin was found incorporated mostly into filamentous networks and what appeared to be fragmented filaments, but granules and squiggles typical for wild-type cells were not visualized (Fig. 32A, -/-). The discontinuous filamentous structures observed in plectin^{-/-} cells in general were significantly longer than typical squiggles and they were lacking any directional movement; instead they were bending rather stochastically, remaining at one and the same place (Fig. 32A, -/-). In fact, fragment formation from preexisting vimentin networks, could occasionally be observed, as shown for two examples in Fig. 32B, where fragmentations were captured at two different time points of one movie series. Similar fragments were observed in fixed, untransfected spreading cells (Fig. 30A, k).

To quantitatively analyze differences between squiggles typical for wild-type cells and filament fragments observed in plectin^{-/-} cells, I performed statistical analyses of the size and directionality of the movement of both structures (Fig. 32C-G). The average size of vimentin fragments in knockout cells was 6-8 μm , while that of squiggles $\sim 2 \mu\text{m}$ (Fig. 32C). Quantization of the directionality of processive squiggle movement along five migration tracks revealed relatively straight migration paths in wild-type cells (Fig. 32D; migration path marked by asterisk represents squiggle shown in Fig. 32A, +/+). In contrast, a similar analysis of representative fragments in plectin^{-/-} fibroblasts revealed that they traveled along chaotic and nonlinear paths (Fig. 32E; non-migrating fragments shown in Fig. 32A, -/-, are indicated by asterisks). Calculating the processive index (PI) of movement, where PI is defined as the linear distance between the start and end points divided by the total distance traversed by the fragment, squiggles of plectin^{+/+} fibroblasts had an average PI of 0.77, approaching the ideal PI of 1.0 for linear migration, while fragments in plectin^{-/-} fibroblasts reached an average PI of 0.088 (Fig. 32F and G).

In all, these time lapse experiments not only confirmed that IF squiggle formation in fibroblasts was plectin-dependent, but more importantly, they also suggested that plectin was important for the directional transport of squiggles towards the cell periphery, as short filaments, generated by the partial fragmentation of the IF network in plectin^{-/-} cells, were found to lack such oriented movement.

9. DISCUSSION

Plectin is a cytoskeletal protein that forms dumbbell-shaped homodimers comprising a central parallel α -helical coiled coil rod domain flanked by two globular domains. Its molecular backbone seems ideally suited to mediate the protein's interactions with an array of other cytoskeletal elements. Plectin self-associates, interacts with actin and IF cytoskeleton networks, and binds to the hemidesmosomal transmembrane protein integrin β 4 as well as other junctional proteins (reviewed in Reznicek et al., 2004). Consisting of six structural repeats and harboring binding sites for different IF proteins and proteins involved in signaling, plectin's C-terminal domain is of strategic functional importance. Plectin is also a target of Cdk1 kinase and during mitosis it becomes phosphorylated at a unique site (threonine 4542) in plectin's C-terminal repeat 6 domain (Malecz et al., 1996), not far from the IF-binding site residing in the linker region between repeat domains 5 and 6.

In view of plectin's enormous size (>500 kDa) and exposure to mechanical stress forces, the question arises how the molecule maintains its structural integrity. Four highly conserved residues of at least 13 cysteines in the C-terminal part of plectin are clustered in its repeat 5 domain (Wiche et al., 1993; Liu et al., 1996; Elliott et al., 1997; Fuchs et al., 1999). Forming intra- and inter-repeat disulfide bridges, these cysteines could serve a functional purpose, providing structural rigidity to the protein. Furthermore, the formation of reversible intracellular disulfide bridges could modulate the response to mechanical, oxidative, or other types of stress. My studies provided evidence that at least one of the cysteines was reactive as reflected by its ability to form disulfide bridges and to serve as a target for nitrosylation.

Previous studies have demonstrated that vimentin networks are highly dynamic structures whose assembly and disassembly is accomplished stepwise via several intermediates (Prahlad et al., 1998). The intermediate forms as well as filamentous vimentin are found in cells in a dynamic equilibrium characterized by the turnover of the subunits within the polymer and the movement of the precursor intermediates. I found that plectin is associated with vimentin from the early stages of assembly and is required for vimentin motility as well as for the stepwise formation of stable filaments.

9.1. Cysteines proximal to the IF-binding site of plectin

Structural implications of repeat 5 domain cysteines

The building block of plectin's C-terminal domain is a repeat domain known as the plakin or plectin repeat domain (Janda et al., 2001; Leung et al., 2002). Repeat domains consist of a conserved core domain or module, separated from each other by linker sequences of variable lengths. The three repeat domains in desmoplakin were proposed to have an independent structure arranged into "beads-on-a-string" (Choi et al., 2002). In contrast, Janda et al. (2001) proposed a model where the six repeat domains of plectin are packed against each other, with repeats 1-5 arranged around the central repeat 6 domain, forming a compact C-terminal globular domain. Cysteine disulfide bridges could contribute to stabilizing this structure in addition to the reciprocal hydrogen bond interactions mediated by hydrophobic residues (Janda et al., 2001). The conception of compact plectin repeat packing is supported by electron microscopy, visualizing the C-terminal domain as a globule of 9 nm diameter (Foisner and Wiche, 1987). Homology modelling of each of the six plectin repeats based on the known structure of the corresponding desmoplakin repeats (50-73% sequence identity) yielded a cylinder-like configuration with an average size of 45x25 Å. Therefore, accommodation of six repeats within a 9 nm globule would indeed require tight packing of the repeats rather than a loose beads-on-a-string arrangement.

Cross-linking experiments revealed that two of the four cysteines in the repeat 5 domain, Cys1 and Cys4, could form intramolecular disulfide bridges, and that the oxidized form of repeat 5 domain migrated faster in SDS-PAGE than the reduced form, suggesting conformational changes of the repeat 5 domain upon oxidation. As the modelling of the repeat 5 domain revealed Cys1 to be partially buried in the core of the protein, the presence of the linker in the cross-linked repeat 5 domain species probably caused a change in its local conformation, exposing the vicinity of Cys1 on the surface and promoting the formation of a disulfide bridge.

Repeat 4 has a single cysteine in a position equivalent to Cys2 of the repeat 5 domain; this cysteine can form disulfide bridges with cysteines of the repeat 5 domain linking these repeats together. It can be assumed that corresponding cysteines in the other repeats behave similarly. These findings support the model suggested by Janda et al. (2001).

Functional implications of repeat 5 domain cysteines as a target for nitrosylation

Plectin-binding to IFs is essential not only for the mechanical stabilization of the cytoskeleton due to plectin's role as a cytolinker, where it interlinks different cytoskeletal proteins and anchors them to the plasma membrane, but also for the proper IF cyto-architecture with important consequences for signaling cascades controlling basic cellular functions (Osmanagic-Myers and Wiche, 2004; Gregor et al., 2006; Osmanagic-Myers et al., 2006).

Data obtained in my thesis showed that the reduced form of plectin's repeat 5 domain binds more efficiently to vimentin than its oxidized form. The dissociation constant of the R5 Cys-free mutant (0.96×10^{-7} M) was 2x and 3x lower than that of the reduced and oxidized forms of the repeat 5 domain, respectively. The substitution of a cysteine with a serine being limited to the exchange of an –SH group with an –OH group is a quite conservative mutation, which is not expected to cause a conformational change by itself. This could be the case, however, if the substitution disrupts the formation of one or more disulfide bridges. Because I have shown that Cys1 and Cys4 easily form a disulfide bridge that could alter the conformational parameters of the repeat, the finding that the cysteine-free mutant and the reduced form of repeat 5 domain bind better to vimentin could be interpreted as a signal that, when the repeat 5 domain is in a reduced, i.e. more open conformation, the vimentin-binding site might be more exposed, facilitating its interaction. Not only cysteines inside the repeat 5 domain could influence plectin-vimentin affinity, but also neighboring repeats 4 and 6 and/or their cysteines, as well as the tail region. While the presence of repeat 4 and 6 domains led to an increased affinity comparable to the reduced form of the repeat 5 domain alone, the presence of the tail region had a negative effect on the binding of plectin R5-6tail to vimentin. These findings suggest that cysteines affect the conformation of repeat domains, which in turn modulates the binding to vimentin.

In contrast to its reduced form, the oxidized form of the repeat 5 domain appears to adopt a conformation where the vimentin-binding site is inaccessible. A plectin molecule unable to bind to vimentin could severely affect cellular functions known to be IF-dependent, including structural reinforcement of the cytoplasm and control of signaling cascades, similar to the plectin-null situation (Osmanagic-Myers and Wiche, 2004; Gregor et al., 2006; Osmanagic-Myers et al., 2006). In the cellular context, reversible *in vivo* modifications of Cys4 by local redox changes could lead to either cysteine oxidation through reactive oxygen

species (ROS), or to S-nitrosylation through reactive NO. In addition, ROS could convert NO into higher oxides of nitrogen and radicals, such as peroxynitrite, which efficiently oxidizes thiol groups (Lane et al., 2001).

This study showed that Cys4 in repeat 5 domain is highly reactive and that plectin is a target for nitrosylation *in vitro* and *in vivo*. S-nitrosylation of cysteines leading to nitrosothiols is a biochemical posttranslational modification of proteins that allows cells to respond to environmental changes in specific subcellular compartments, and can modulate protein activity in a fashion analogous to phosphorylation (Lane et al., 2001). Despite the existence of cysteine residues in virtually all proteins, proteomic analysis of S-nitrosylated proteins in extracts from brain (Jaffrey et al., 2001), mesangial cells (Kuncewicz et al., 2003), and intact endothelial cells (Martinez-Ruiz and Lamas, 2004) revealed that S-nitrosylation is restricted to a small number of proteins. Furthermore, S-nitrosylation is not a function of total cysteine content, since generally, only one single cysteine thiol in the protein is modified. The specificity is determined by structural motifs around the cysteine and the intracellular proximity to a NO generator, such as the enzyme nitric oxide synthase (NOS), which produces NO through the conversion of L-arginine into L-citrulline. Both requirements seem to be fulfilled by Cys4 in plectin's repeat 5 domain. The residues upstream (QE) and downstream (E) of Cys4 perfectly match the consensus motif for S-nitrosylation.

The results obtained in studies on endothelial cells suggested that plectin may play an important role in the distribution of eNOS, one of three isoenzymes of NOS differentially expressed in different cell types. In wild-type cells I found activated eNOS to be distributed over the whole cytoplasm, and this distribution stayed unchanged upon treatment of cells with eNOS activator. In contrast, in plectin-deficient cells eNOS was localized mainly at the plasma membrane, representing its inactive form. These findings were in accordance with NO production measurements, which revealed decreased NO production in plectin-deficient cells. Thus, plectin could be responsible for the observed alterations in eNOS activity due to the altered distribution of eNOS over the cytoplasm.

Although the association of endogenous NOSs with plectin and their colocalization in different cell types and tissues has not yet been studied comprehensively, there is solid evidence for the intracellular proximity of nNOS and plectin in skeletal muscle. nNOS was found to be targeted to the dystrophin-associated protein α 1-syntrophin at specialized structures on the surface membrane of muscle fibers, such as neuromuscular junctions

(NMJs), myotendinous junctions (MTJs), and costamers (Stamler and Meissner, 2001). Plectin, as a prominent component of NMJs, MTJs, and costamers, is also associated with the sarcolemma and has been found to colocalize with dystrophin (Schröder et al., 2002; Hijikata et al., 2003; Konieczny et al., 2008).

Role of plectin in NO-induced IF collapse

Assessing whether S-nitrosylation of plectin effected by exposing endothelial cells to NO donors had any effects on cellular cytoarchitecture, I found an interesting link between plectin deficiency and the dynamics of IF network formation. While in wild-type cells, well spread cellular vimentin networks largely persisted (for up to 6 h) after treating cells with the NO donor SNAP, in plectin-deficient cells, I observed a progressive collapse of vimentin filament networks into perinuclear bundles. One explanation for this phenomenon could be, that plectin protects vimentin against oxidation. Vimentin, like all other members of type III IFs, contains a single cysteine residue at a highly conserved position (328 in the human protein). The corresponding residue in desmin has been shown to form disulfide bridges leading to crosslinked dimers within filaments (Quinlan and Franke, 1982), and in cytoskeletal preparations from baby hamster kidney and human glioma (astrocytoma) cells a certain proportion of disulfide-crosslinked heterodimers, consisting of vimentin and desmin, or GFAP, respectively, has been reported (Quinlan and Franke, 1982, 1983). In fact, vimentin's thiol is oxidized in preference to other cytoskeleton proteins in fibroblast-like synoviocytes upon exposure to H₂O₂ (Rogers et al., 1991). Furthermore, these cells showed increased susceptibility to vimentin collapse around the nucleus on exposure to oxidative stress, and vimentin IFs in rheumatoid synoviocytes are more susceptible than in normal synoviocytes, bearing a possible pathological significance (Rogers et al., 1989). The proposal that synoviocyte vimentin becomes glutathionylated (Rogers et al., 1991) has recently been confirmed by proteomic approaches showing that vimentin is glutathionylated in human T lymphocytes and rat aortic smooth muscle cells (Fratelli et al., 2002; West et al., 2006). Finally, prostanylation of the vimentin thiol has been found in mesangial cells (Stamatakis et al., 2006) and its nitrosylation in endothelial cells (Yang and Loscalzo, 2005).

By binding to vimentin, plectin may either sterically hinder the access of oxidants and thus prevent or impede IF collapse or prevent vimentin molecules from assuming a conformation enabling vimentin-vimentin disulfide bridge formation. There is evidence, at

least from *in vitro* experiments, that disulfide crosslinked vimentin homodimers or desmin-vimentin heterodimers were filament assembly-incompetent under nonreducing conditions (Fraser and MacRae, 1985; Traub et al., 1993). The proposed shielding effect of plectin on vimentin's thiol group may be further enhanced by the multitude of proteins bound to its surface as a consequence of its scaffolding function (Osmanagic-Myers and Wiche, 2004). Alternatively, transient nitrosylation of Cys4 in plectin's repeat 5 domain may promote its subsequent disulfide bond formation with the unique cysteine of vimentin, thereby preventing its bond formation with another vimentin molecule, eventually leading to filament collapse. In fact, the results of my studies indicate that repeat 5 domain Cys4 of plectin can form disulfide bridges with the unique cysteine of vimentin *in vitro*.

Another conceivable way how plectin might affect NO-induced IF network collapse involves protein phosphorylation. The reversible process of phosphorylation/dephosphorylation of IF subunit proteins has been well established as a cellular mechanism leading to the disassembly of IFs. Recently, it has been found that the collapse of keratin networks, induced by the protein phosphatase (PPase) inhibitor ocadaic acid (OA), in keratinocytes proceeds considerably faster in plectin-deficient compared to wild-type cells (Osmanagic-Myers et al., 2006). This finding also applies to the vimentin network of fibroblasts (unpublished data, M. Gregor). Several groups have reported an inhibition of PPases by endogenously produced ROS, and it has been shown that the exposure of purified PPases to NO donors leads to reversible enzyme inhibition (Caselli et al., 1995; Callsen et al., 1999; Xian et al., 2000). Furthermore, NO activates serine/threonine kinases, including cGMP-activated protein kinase (PKG), as well as various tyrosine kinases (Denninger and Marletta, 1999; Lincoln et al., 2001). Thus, the NO-triggered accelerated collapse of the vimentin network in plectin-deficient endothelial cells, similar to OA-treated cells, could be caused by protein hyperphosphorylation, affected by NO-activated phosphorylation. The mechanism how plectin counteracts/antagonizes hyperphosphorylation of vimentin networks in wild-type endothelial cells remains to be revealed. One can expect, however, that similar to other cell types, plectin influences the cytoarchitecture of the IF network and thereby regulates certain signaling cascades (Osmanagic-Myers and Wiche, 2004; Osmanagic-Myers et al., 2006).

Plectin deficiency affects NO production by eNOS

Assessing whether S-nitrosylation-induced IF collapse in the absence of plectin has any consequences on the correct function of eNOS, my studies revealed that NO production by eNOS was strongly affected in plectin-deficient cells. In contrast to wild-type endothelial cells, in the absence of plectin, NO production was dramatically decreased to hardly detectable values. These observations were confirmed by the analysis of protein levels of eNOS in plectin^{+/+} and plectin^{-/-} cells. Neither activated eNOS (specifically phosphorylated on threonine 495 or serine 1177) nor total eNOS expression were hardly detectable in plectin-deficient cells. The protein level and activation status of the upstream eNOS activator Akt kinase stayed unchanged, suggesting that eNOS activity affected by plectin deficiency was not an indirect effect on activators/inhibitors, but that plectin can directly regulate eNOS protein expression. To explain and mechanistically link NO donor-induced IF collapse, decreased NO production, and decreased eNOS protein levels, two possibilities should be considered. One is, that in the absence of plectin NO production and/or eNOS activity is abolished as a protection of cell against nitrosylation-induced IF collapse. Another conceivable explanation might be, that nitrosylation-induced vimentin network collapse alters the normal function of eNOS, i.e. NO production.

Collapse of the vimentin filament network and/or decreased NO production probably compromises the normal ability of endothelial cells to respond to an appropriate stimulus causing vasodilatation in smooth muscle. As such a dysfunction is thought to be a key event in the development of atherosclerosis and has also been shown to be of prognostic significance in predicting vascular pathological events, including stroke and heart attacks (Kojda and Harrison, 1999), it will be of interest to investigate whether plectin integrity plays a role in these diseases.

In conclusion, my studies have shown that cysteines residing proximal to the IF-binding site of plectin's repeat 5 domain have the ability to form disulfide bridges with consequences for conformational and biochemical properties of the repeat domain. The redox state of these cysteines was found to have an influence on vimentin-binding affinity, and one of the cysteines was identified as a specific target for nitrosylation. The observation that plectin-deficient endothelial cells were more sensitive towards NO donor-induced IF network collapse than wild-type cells, suggests an antagonistic role of plectin in oxidative stress-mediated alterations of the cytoskeleton and a possible role of a plectin-based cysteine as a

regulatory switch. Furthermore, my studies revealed that NO production, as well as expression levels of eNOS are plectin-dependent.

9.2. The role of plectin in the formation of vimentin filament intermediates

Vimentin network formation

Recent studies have revealed IFs as highly dynamic polymers, with three types of structures (granules, squiggles, and filaments) coexisting in the cell. Particularly IF intermediates in the form of granules and squiggles have an important role in the assembly of IF networks (Prahlad et al., 1998). The smaller subunits were found to be motile, assembling into polymerized IFs following a stepwise process (Prahlad et al., 1998; Chou and Goldman, 2000; Chou et al., 2007). Although the binding of plectin to IFs, in particular to vimentin, has long been established using different methodologies (for review see Rezniczek et al., 2004), it was only recently shown, that plectin affects the cytoarchitecture of IFs with important consequences for cellular signaling and response to different types of stress (Osmanagic-Myers et al., 2006). As the issue of whether plectin-binding affects dynamic properties of IFs has not been addressed before, in this study I set out to investigate the interaction of plectin with vimentin filament intermediates in situations where these intermediates have been best defined, namely during cell-spreading and mitotic cell division.

Using immortalized and primary fibroblasts derived from wild-type and plectin-null mice I found that plectin is already associated with small and medium-sized vimentin filament intermediates (granules and squiggles, respectively), that are characteristics of the cell spreading process. By contrast, these intermediates could not be detected in the absence of plectin, and long, scarcely networked filaments were observed instead. These filaments clearly assembled considerably faster than the more complex vimentin networks formed in the presence of plectin. This could be explained by assuming that in the absence of plectin, vimentin assembly proceeds without crossbridge stabilization, similar to the self-assembly of IFs *in vitro*. In fact, there is evidence that plectin^{-/-} fibroblasts contain higher levels of soluble vimentin than wild-type cells suggesting that filaments are less stable (unpublished data, M. Gregor). Furthermore, since the directional (anterograde) movement typical of vimentin intermediates (Prahlad et al., 1998) took place only in the presence of plectin, my

work suggests that plectin is required for both, the stepwise formation of a robust vimentin network from granules and squiggles and the transport of these intermediate structures to the cell periphery and other areas where they are required. Vimentin network fragmentation observed in plectin-null cells apparently was a result of network instability due to the absence of plectin. The collapse of keratin networks induced in keratinocytes by the protein phosphatase inhibitor okadaic acid proceeds considerably faster in the absence of the plectin (Osmanagic-Myers et al., 2006). Furthermore as revealed in this study, NO-donor induced IF collapse in endothelial cell proceeds dramatically faster in plectin-deficient cells compared to wild-type cells.

In general, the most widely proposed function of IFs would be to serve as mechanical integrators of the cytoplasm. The formation of IF intermediates and their transport could provide cells with an efficient mechanism for delivering IF building material to cytoplasmic regions where mechanical stability is required. A possible mechanism how plectin is involved in the formation and transport of intermediates could be, that plectin does so by crosslinking vimentin filaments among themselves and probably to other structures, such as microtubules, and by concomitantly scaffolding the additional proteins needed for the movement of vimentin granules and squiggles. While microtubules are known to be associated with plectin (Koszka et al., 1985; Svitkina et al., 1996), an association of plectin with kinesin has not yet been reported, although kinesin could be recruited to the plectin scaffold via vimentin (Helfand et al., 2002). Plectin could serve as a filament nucleation center by acting as a platform for all other molecules required for the formation of granules. In the absence of plectin, when these nucleation centers are not present, granules cannot be formed and the cell is presumably using an alternative method for IF network formation. Hypothetically, in this case the network is formed by simple self-assembly of IFs from the basic building components – vimentin tetramers – and this formation is not under precise control like in the presence of plectin.

Vimentin dynamics during mitosis and cytokinesis

Cytoplasmic IF proteins in interphase cells typically form a network that extends from the nuclear surface towards the cell periphery, but as cells enter into mitosis IFs undergo a intensive reorganization upon phosphorylation by Cdk1 (Franke et al., 1982; Chou et al., 1991). The fate of vimentin as it passes through the cell cycle seems to be dependent on the

cell type. In mitotic BHK-21 cells, the interphase IF network, composed of vimentin and desmin, is completely disassembled into non-filamentous granules (Rosevear et al., 1990). In PtK2 epithelial cells both vimentin and keratin IF networks remain intact during the mitotic process (Aubin et al., 1980). In HeLa cells, which also possess keratin and vimentin networks, the keratin IF network is disassembled into spheroid bodies, whereas vimentin remains filamentous (Franke et al., 1982; Jones et al., 1985).

Plectin is also phosphorylated by Cdk1, experiencing structural changes and dissociating from vimentin filaments. Foisner et al. (1996) documented that plectin changes from a mostly IF-associated form during interphase to a more soluble, IF-independent, and diffusely distributed form in mitosis. By reexamining this issue using new strategies and focusing on plectin's interaction with dynamic forms of vimentin, my present study revealed that a fraction of plectin remains associated with vimentin throughout mitosis. Furthermore, phosphorylation of vimentin by Cdk1 *in vitro* was found not to decrease plectin-vimentin binding affinity, indicating that plectin can interact with vimentin under conditions where vimentin filaments are disassembled. The residual plectin-associated vimentin filaments found in wild-type cells appeared dispersed over the whole cytoplasm, and the daughter cells rebuilt their vimentin networks via intermediate forms (granules and squiggles) in a similar fashion as during spreading after trypsinization and replating. In contrast, in cells lacking plectin, discontinuous forms of filamentous vimentin prevailed. No intermediate forms were observed in these cells as they rebuilt the vimentin network upon cytokinesis.

In many cell types filamentous vimentin forms cage-like structures surrounding the mitotic apparatus during all stages of mitosis (Aubin et al., 1980; Zieve et al., 1980). Plectin, serving as a structural cross-linker, regulates cell cytoarchitecture, connects microtubules to other filaments systems and recruits signaling molecules to its surface. In fact, plectin has been shown to be associated with microtubules assembled in a mammalian mitotic extract together with 15 other proteins with known functional roles in spindle assembly (Mack and Compton, 2001). It is thus conceivable that plectin promotes crosstalk between IFs and mitotic spindle components. Loss of such cross-linkages and/or altered vimentin network cytoarchitecture in plectin-deficient cells could consequently lead to a delay in progression through mitosis and completion of cytokinesis. Therefore, the observation that after nocodazole release plectin-null cells passed through mitosis faster than wild-type cells could be accounted for by the lack of supracytoplasmic organization brought about by plectin

networking, leading to a fully disassembled state of vimentin filaments in the absence of plectin. Furthermore, the unequal distribution of vimentin into daughter cells in wild-type as opposed to the more even distribution in plectin-null cells, may reflect the still partially assembled and squiggle-associated, versus the disassembled and more soluble states of vimentin.

Oddly, there is not yet any report about unequal distribution of IFs during mitosis. However, already in the early publication of Aubin et al. (1980) an obviously unequal distribution of vimentin during telophase and cytokinesis in PtK2 cells is clearly visible. To our knowledge, this very interesting phenomenon has not yet been noticed in other cell types. However, an unequal distribution of several proteins has been described during asymmetric cell division (Knoblich, 2001). My observations revealed, that unequal distribution of vimentin occurred in fibroblasts, when two daughter cells with different sizes were formed. So far, asymmetric cell division has been described only for the *C. elegans* zygote, neuroblasts, the precursors of the central nervous system and several types of stem cells (Knoblich, 2001; Wildner et al., 2006; Gonzalez, 2007). Asymmetric cell divisions provide a mechanism for placing specific cell types into defined positions in the developing organism (Horvitz and Herskowitz, 1992). Plectin could be partially responsible for this phenomenon, as the completely disassembled vimentin in plectin-null cells was found distributed equally to the newly formed daughter cells. In general, very little is known about how the distribution of the cytoskeleton is regulated during cell division. Cdk1-induced vimentin-Ser82 phosphorylation plays an important role in vimentin filament segregation, together with Rho-kinase and Aurora-B kinase (Yamaguchi et al., 2005).

Phosphorylation and formation of vimentin filament intermediates

IF granules, as transporting reservoirs, were described as possible basic building blocks for filamentous IF network assembly (Aubin et al., 1980; Franke et al., 1982; Rosevear et al., 1990; Prahlad et al., 1998; Chou and Goldman, 2000; Helfand et al., 2003). I show evidence that plectin plays an essential role in the formation of vimentin granules, which are formed upon phosphorylation and have plectin associated with them.

The first question arising is why such globular structures are formed and what advantage they pose for the cell. As described above, these structures were observed during early stages of cell spreading when IF formation started. The cell needs some mechanism

how to transport IF material effectively under appropriate control to the regions where it is needed. Formation of reservoir granules seems to be an ideal form how to effectively pack the IF material and quickly transport it to the required regions. To transport single molecules as well as some longer filamentous structures seem to be energetically ineffective. This is in accordance with the findings, that as granules get prolonged into longer filaments their speed is decreased with increasing length (Chou and Goldman, 2000; Helfand et al., 2002). On the other hand, local assembly of IFs from IF intermediates suggests that cells need to regulate the local amounts of vimentin in a precise manner, particularly in rapidly spreading regions. The functional significance of such an assembly mechanism may be related to the role of IFs as mechanical cell shape stabilizer and mediators of cytoskeletal interactions (Goldman et al., 1996; Fuchs and Cleveland, 1998).

Another question which arises is what molecular structure and composition these granules have. The factors that maintain vimentin in its non-filamentous intermediate state, or promote its polymerization into IF are unknown. Previous studies have shown that the formation of protofilamentous vimentin globules is correlated with the phosphorylation of vimentin by Cdk1 (Chou et al., 1990; Chou et al., 1996). Therefore, the state of phosphorylation may also regulate the conversion of non-filamentous vimentin granules to filamentous 10 nm filaments. The local control of phosphorylation may also disassemble selectively some of the filaments into smaller structures, such as granules, in one region of the cytoplasm for rapid transport to other regions. This regional control of IF phosphorylation could provide a mechanism for enhancing the dynamics of IF networks in regions where the cytoskeleton is to be rapidly reorganized.

As discussed above, plectin may serve as a nucleation center for the formation of granules, the basic building blocks of IFs, and phosphorylation keeps vimentin in non-filamentous form. Meeting these two criteria seems sufficient for the formation of IF granules, as confirmed by my *in vitro* data, showing that Cdk1-phosphorylates vimentin in the presence of similarly phosphorylated plectin was able to form globular structures resembling vimentin granules observed during spreading. IF granules have been reported in many cell types, like in fibroblasts (Prahlad et al., 1998) nerve cells (Yabe et al., 1999a), epithelial cells (Windoffer and Leube, 1999b), or in several types of mitotic cells (Rosevear et al., 1990). IF granules in spreading cells examined by electron microscopy appear to consist of nonmembrane-bound globular vimentin aggregates (Prahlad et al., 1998), or

aggregates of densely packed cytokeratin granular particles with a diameter of 0.2-1.5 μm (Franke et al., 1982). Until now little is known about the composition of these structures, but I can hypothesize that these granules are at least composed of disassembled vimentin and plectin (as nucleation factor) and probably kinesin or/and dynein (as molecular motors for their transport).

It has previously been reported, that phosphorylation of plectin by serine/threonine kinases, including mitotic Cdk1, decreases its binding affinity to vimentin (Foisner et al., 1996). In this study, using a recombinant version of plectin containing its major IF-binding domain, I confirmed these results by showing that the affinity of Cdk1-phosphorylated plectin for unphosphorylated vimentin is lower, than when both proteins are either phosphorylated or non-phosphorylated. Furthermore, my data revealed that the binding affinities of Cdk1-phosphorylated and of non-phosphorylated forms of both proteins are very similar, indicating that plectin and vimentin can bind to each other regardless of their Cdk1 phosphorylation status. This establishes that a fraction of both proteins could also stay associated throughout mitosis. Thus a partial association of plectin with vimentin throughout mitosis is likely to facilitate the rapid rebuilding of the IF network after cytokinesis. Previously, Skalli et al. (1992) reported that plectin and vimentin remain associated in BHK cells during mitosis and suggested that the binding of plectin to vimentin is not significantly altered when both proteins are phosphorylated by Cdk1. Finally, the observed high affinity of unphosphorylated plectin to phosphorylated vimentin would be consistent with a model where dephosphorylation of plectin after mitosis occurs prior to that of vimentin, promoting reassociation of the entire vimentin pool with plectin.

Taken together my studies show that plectin prevents vimentin networks from complete disassembly during mitosis, facilitating the rebuilding of the IF network in daughter cells. In this scenario, plectin may serve as a nucleation center for the formation of vimentin intermediates, enabling them to recruit molecular motors and anchoring proteins required for their transport and targeting to specific intracellular destinations. Furthermore, a better understanding of how the transport of IFs is regulated should shed new light on the molecular basis of numerous human diseases, such as amyotrophic lateral sclerosis and Parkinson's disease (Toyoshima et al., 1989; Galloway et al., 1992; Xu et al., 1993), whose pathological characteristics include abnormal aggregation of IFs in axons and skin fibroblasts combined with giant axonal neuropathy (Pena, 1982; Bousquet et al., 1996).

10. REFERENCES

- Abrahamsberg, C., Fuchs, P., Osmanagic-Myers, S., Fischer, I., Propst, F., Elbe-Bürger, A., and Wiche, G. (2005). Targeted ablation of plectin isoform 1 uncovers role of cytolinker proteins in leukocyte recruitment. *Proc Natl Acad Sci U S A* **102**, 18449-18454.
- Ackerl, R., Walko, G., Fuchs, P., Fischer, I., Schmuth, M., and Wiche, G. (2007). Conditional targeting of plectin in prenatal and adult mouse stratified epithelia causes keratinocyte fragility and lesional epidermal barrier defects. *J Cell Sci* **120**, 2435-2443.
- Alderton, W. K., Cooper, C. E., and Knowles, R. G. (2001). Nitric oxide synthases: structure, function and inhibition. *Biochem J* **357**, 593-615.
- Andrä, K., Kornacker, I., Jörgl, A., Zörer, M., Spazierer, D., Fuchs, P., Fischer, I., and Wiche, G. (2003). Plectin-isoform-specific rescue of hemidesmosomal defects in plectin (-/-) keratinocytes. *J Invest Dermatol* **120**, 189-197.
- Andrä, K., Lassmann, H., Bittner, R., Shorny, S., Fässler, R., Propst, F., and Wiche, G. (1997). Targeted inactivation of plectin reveals essential function in maintaining the integrity of skin, muscle, and heart cytoarchitecture. *Genes Dev* **11**, 3143-3156.
- Andrä, K., Nikolic, B., Stocher, M., Drenckhahn, D., and Wiche, G. (1998). Not just scaffolding: plectin regulates actin dynamics in cultured cells. *Genes Dev* **12**, 3442-3451.
- Armstrong, D. K., McKenna, K. E., Purkis, P. E., Green, K. J., Eady, R. A., Leigh, I. M., and Hughes, A. E. (1999). Haploinsufficiency of desmoplakin causes a striate subtype of palmo-plantar keratoderma. *Hum Mol Genet* **8**, 143-148.
- Aubin, J. E., Osborn, M., Franke, W. W., and Weber, K. (1980). Intermediate filaments of the vimentin-type and the cytokeratin-type are distributed differently during mitosis. *Exp Cell Res* **129**, 149-165.
- Berka, V., Yeh, H. C., Gao, D., Kiran, F., and Tsai, A. L. (2004). Redox function of tetrahydrobiopterin and effect of L-arginine on oxygen binding in endothelial nitric oxide synthase. *Biochemistry* **43**, 13137-13148.

- Bousquet, O., Basseville, M., Vila-Porcile, E., Billette de Villemeur, T., Hauw, J. J., Landrieu, P., and Portier, M. M. (1996). Aggregation of a subpopulation of vimentin filaments in cultured human skin fibroblasts derived from patients with giant axonal neuropathy. *Cell Motil Cytoskeleton* **33**, 115-129.
- Brown, A., Bernier, G., Mathieu, M., Rossant, J., and Kothary, R. (1995). The mouse dystonia musculorum gene is a neural isoform of bullous pemphigoid antigen 1. *Nat Genet* **10**, 301-306.
- Callsen, D., Sandau, K. B., and Brune, B. (1999). Nitric oxide and superoxide inhibit platelet-derived growth factor receptor phosphotyrosine phosphatases. *Free Radic Biol Med* **26**, 1544-1553.
- Caselli, A., Chiarugi, P., Camici, G., Manao, G., and Ramponi, G. (1995). In vivo inactivation of phosphotyrosine protein phosphatases by nitric oxide. *FEBS Lett* **374**, 249-252.
- Combet, C., Jambon, M., Deleage, G., and Geourjon, C. (2002). Geno3D: automatic comparative molecular modelling of protein. *Bioinformatics* **18**, 213-214.
- Creighton, T. E. (1986). Disulfide bonds as probes of protein folding pathways. *Methods Enzymol* **131**, 83-106.
- Dang, M., Pulkkinen, L., Smith, F. J., McLean, W. H., and Uitto, J. (1998). Novel compound heterozygous mutations in the plectin gene in epidermolysis bullosa with muscular dystrophy and the use of protein truncation test for detection of premature termination codon mutations. *Lab Invest* **78**, 195-204.
- Denninger, J. W., and Marletta, M. A. (1999). Guanylate cyclase and the .NO/cGMP signaling pathway. *Biochim Biophys Acta* **1411**, 334-350.
- DiColandrea, T., Karashima, T., Maatta, A., and Watt, F. M. (2000). Subcellular distribution of envoplakin and periplakin: insights into their role as precursors of the epidermal cornified envelope. *J Cell Biol* **151**, 573-586.
- Dowling, J., Yang, Y., Wollmann, R., Reichardt, L. F., and Fuchs, E. (1997). Developmental expression of BPAG1-n: insights into the spastic ataxia and gross neurologic degeneration in

- dystonia musculorum mice. *Dev Biol* **187**, 131-142.
- Duchen, L. W. (1976). Dystonia musculorum—an inherited disease of the nervous system in the mouse. *Adv Neurol* **14**, 353-365.
- Eger, A., Stockinger, A., Wiche, G., and Foisner, R. (1997). Polarisation-dependent association of plectin with desmoplakin and the lateral submembrane skeleton in MDCK cells. *J Cell Sci* **110**, 1307-1316.
- Elliott, C. E., Becker, B., Oehler, S., Castañón, M. J., Hauptmann, R., and Wiche, G. (1997). Plectin transcript diversity: identification and tissue distribution of variants with distinct first coding exons and rodless isoforms. *Genomics* **42**, 115-125.
- Errante, L. D., Wiche, G., and Shaw, G. (1994). Distribution of plectin, an intermediate filament-associated protein, in the adult rat central nervous system. *J Neurosci Res* **37**, 515-528.
- Finkel, T. (1998). Oxygen radicals and signaling. *Curr Opin Cell Biol* **10**, 248-253.
- Fleming, I., and Busse, R. (2003). Molecular mechanisms involved in the regulation of the endothelial nitric oxide synthase. *Am J Physiol Regul Integr Comp Physiol* **284**, R1-12.
- Foisner, R., Feldman, B., Sander, L., Seifert, G., Artlieb, U., and Wiche, G. (1994). A panel of monoclonal antibodies to rat plectin: distinction by epitope mapping and immunoreactivity with different tissues and cell lines. *Acta Histochem* **96**, 421-438.
- Foisner, R., Leichtfried, F. E., Herrmann, H., Small, J. V., Lawson, D., and Wiche, G. (1988). Cytoskeleton-associated plectin: in situ localization, in vitro reconstitution, and binding to immobilized intermediate filament proteins. *J Cell Biol* **106**, 723-733.
- Foisner, R., Malecz, N., Dressel, N., Stadler, C., and Wiche, G. (1996). M-phase-specific phosphorylation and structural rearrangement of the cytoplasmic cross-linking protein plectin involve p34cdc2 kinase. *Mol Biol Cell* **7**, 273-288.
- Foisner, R., Traub, P., and Wiche, G. (1991). Protein kinase A- and protein kinase C-regulated interaction of plectin with lamin B and vimentin. *Proc Natl Acad Sci U S A* **88**, 3812-3816.

- Foisner, R., and Wiche, G. (1987). Structure and hydrodynamic properties of plectin molecules. *J Mol Biol* **198**, 515-531.
- Foisner, R., and Wiche, G. (1991). Intermediate filament-associated proteins. *Curr Opin Cell Biol* **3**, 75-81.
- Franke, W. W., Kapprell, H. P., and Cowin, P. (1987). Immunolocalization of plakoglobin in endothelial junctions: identification as a special type of Zonulae adhaerentes. *Biol Cell* **59**, 205-218.
- Franke, W. W., Schmid, E., Grund, C., and Geiger, B. (1982). Intermediate filament proteins in nonfilamentous structures: transient disintegration and inclusion of subunit proteins in granular aggregates. *Cell* **30**, 103-113.
- Fraser, R. D., and MacRae, T. P. (1985). Intermediate filament structure. *Biosci Rep* **5**, 573-579.
- Fratelli, M., Demol, H., Puype, M., Casagrande, S., Eberini, I., Salmona, M., Bonetto, V., Mengozzi, M., Duffieux, F., Miclet, E., Bachi, A., Vandekerckhove, J., Gianazza, E., and Ghezzi, P. (2002). Identification by redox proteomics of glutathionylated proteins in oxidatively stressed human T lymphocytes. *Proc Natl Acad Sci U S A* **99**, 3505-3510.
- Fuchs, E., and Cleveland, D. W. (1998). A structural scaffolding of intermediate filaments in health and disease. *Science* **279**, 514-519.
- Fuchs, P., Zörer, M., Rezniczek, G. A., Spazierer, D., Oehler, S., Castañón, M. J., Hauptmann, R., and Wiche, G. (1999). Unusual 5' transcript complexity of plectin isoforms: novel tissue-specific exons modulate actin binding activity. *Hum Mol Genet* **8**, 2461-2472.
- Fujiwara, S., Kohno, K., Iwamatsu, A., Naito, I., and Shinkai, H. (1996). Identification of a 450-kDa human epidermal autoantigen as a new member of the plectin family. *J Invest Dermatol* **106**, 1125-1130.
- Fukasawa, K., Choi, T., Kuriyama, R., Rulong, S., and Vande Woude, G. F. (1996). Abnormal centrosome amplification in the absence of p53. *Science* **271**, 1744-1747.

- Fulton, D., Babbitt, R., Zoellner, S., Fontana, J., Acevedo, L., McCabe, T. J., Iwakiri, Y., and Sessa, W. C. (2004). Targeting of endothelial nitric-oxide synthase to the cytoplasmic face of the Golgi complex or plasma membrane regulates Akt- versus calcium-dependent mechanisms for nitric oxide release. *J Biol Chem* **279**, 30349-30357.
- Fulton, D., Fontana, J., Sowa, G., Gratton, J. P., Lin, M., Li, K. X., Michell, B., Kemp, B. E., Rodman, D., and Sessa, W. C. (2002). Localization of endothelial nitric-oxide synthase phosphorylated on serine 1179 and nitric oxide in Golgi and plasma membrane defines the existence of two pools of active enzyme. *J Biol Chem* **277**, 4277-4284.
- Gache, Y., Chavanas, S., Lacour, J. P., Wiche, G., Owaribe, K., Meneguzzi, G., and Ortonne, J. P. (1996). Defective expression of plectin/HD1 in epidermolysis bullosa simplex with muscular dystrophy. *J Clin Invest* **97**, 2289-2298.
- Gallicano, G. I., Kouklis, P., Bauer, C., Yin, M., Vasioukhin, V., Degenstein, L., and Fuchs, E. (1998). Desmoplakin is required early in development for assembly of desmosomes and cytoskeletal linkage. *J Cell Biol* **143**, 2009-2022.
- Galloway, P. G., Mulvihill, P., and Perry, G. (1992). Filaments of Lewy bodies contain insoluble cytoskeletal elements. *Am J Pathol* **140**, 809-822.
- Geisler, N., and Weber, K. (1982). The amino acid sequence of chicken muscle desmin provides a common structural model for intermediate filament proteins. *Embo J* **1**, 1649-1656.
- Giese, G., and Traub, P. (1986). Induction of vimentin synthesis in mouse myeloma cells MPC-11 by 12-0-tetradecanoylphorbol-13-acetate. *Eur J Cell Biol* **40**, 266-274.
- Goldman, R. D., and Follett, E. A. (1970). Birefringent filamentous organelle in BHK-21 cells and its possible role in cell spreading and motility. *Science* **169**, 286-288.
- Goldman, R. D., Khuon, S., Chou, Y. H., Opal, P., and Steinert, P. M. (1996). The function of intermediate filaments in cell shape and cytoskeletal integrity. *J Cell Biol* **134**, 971-983.
- Golenhofen, N., Ness, W., Wawrousek, E. F., and Drenckhahn, D. (2002). Expression and induction of the stress protein alpha-B-crystallin in vascular endothelial cells. *Histochem Cell Biol* **117**, 203-209.

- Gonzalez, C. (2007). Spindle orientation, asymmetric division and tumour suppression in *Drosophila* stem cells. *Nat Rev Genet* **8**, 462-472.
- Green, K. J., Parry, D. A., Steinert, P. M., Virata, M. L., Wagner, R. M., Angst, B. D., and Nilles, L. A. (1990). Structure of the human desmoplakins. Implications for function in the desmosomal plaque. *J Biol Chem* **265**, 11406-11407.
- Green, K. J., Stappenbeck, T. S., Parry, D. A., and Virata, M. L. (1992). Structure of desmoplakin and its association with intermediate filaments. *J Dermatol* **19**, 765-769.
- Gregor, M., Zeöld, A., Oehler, S., Marobela, K. A., Fuchs, P., Weigel, G., Hardie, D. G., and Wiche, G. (2006). Plectin scaffolds recruit energy-controlling AMP-activated protein kinase (AMPK) in differentiated myofibres. *J Cell Sci* **119**, 1864-1875.
- Gregory, S. L., and Brown, N. H. (1998). kakapo, a gene required for adhesion between and within cell layers in *Drosophila*, encodes a large cytoskeletal linker protein related to plectin and dystrophin. *J Cell Biol* **143**, 1271-1282.
- Helfand, B. T., Chang, L., and Goldman, R. D. (2003). The dynamic and motile properties of intermediate filaments. *Annu Rev Cell Dev Biol* **19**, 445-467.
- Helfand, B. T., Mikami, A., Vallee, R. B., and Goldman, R. D. (2002). A requirement for cytoplasmic dynein and dynactin in intermediate filament network assembly and organization. *J Cell Biol* **157**, 795-806.
- Heller, R., Werner-Felmayer, G., and Werner, E. R. (2006). Antioxidants and endothelial nitric oxide synthesis. *Eur J Clin Pharmacol* **62 Suppl 1**, 21-28.
- Herrmann, H., and Aebi, U. (1999). Intermediate filament assembly: temperature sensitivity and polymorphism. *Cell Mol Life Sci* **55**, 1416-1431.
- Herrmann, H., Haner, M., Brettel, M., Muller, S. A., Goldie, K. N., Fedtke, B., Lustig, A., Franke, W. W., and Aebi, U. (1996). Structure and assembly properties of the intermediate filament protein vimentin: the role of its head, rod and tail domains. *J Mol Biol* **264**, 933-953.

- Herrmann, H., Hesse, M., Reichenzeller, M., Aebi, U., and Magin, T. M. (2003). Functional complexity of intermediate filament cytoskeletons: from structure to assembly to gene ablation. *Int Rev Cytol* **223**, 83-175.
- Hess, D. T., Matsumoto, A., Kim, S. O., Marshall, H. E., and Stamler, J. S. (2005). Protein S-nitrosylation: purview and parameters. *Nat Rev Mol Cell Biol* **6**, 150-166.
- Hijikata, T., Murakami, T., Ishikawa, H., and Yorifuji, H. (2003). Plectin tethers desmin intermediate filaments onto subsarcolemmal dense plaques containing dystrophin and vinculin. *Histochem Cell Biol* **119**, 109-123.
- Horvitz, H. R., and Herskowitz, I. (1992). Mechanisms of asymmetric cell division: two Bs or not two Bs, that is the question. *Cell* **68**, 237-255.
- House, C. M., Frew, I. J., Huang, H. L., Wiche, G., Traficante, N., Nice, E., Catimel, B., and Bowtell, D. D. (2003). A binding motif for Siah ubiquitin ligase. *Proc Natl Acad Sci U S A* **100**, 3101-3106.
- Chavanas, S., Pulkkinen, L., Gache, Y., Smith, F. J., McLean, W. H., Uitto, J., Ortonne, J. P., and Meneguzzi, G. (1996). A homozygous nonsense mutation in the PLEC1 gene in patients with epidermolysis bullosa simplex with muscular dystrophy. *J Clin Invest* **98**, 2196-2200.
- Choi, H. J., Park-Snyder, S., Pascoe, L. T., Green, K. J., and Weis, W. I. (2002). Structures of two intermediate filament-binding fragments of desmoplakin reveal a unique repeat motif structure. *Nat Struct Biol* **9**, 612-620.
- Chou, Y. H., Bischoff, J. R., Beach, D., and Goldman, R. D. (1990). Intermediate filament reorganization during mitosis is mediated by p34cdc2 phosphorylation of vimentin. *Cell* **62**, 1063-1071.
- Chou, Y. H., Flitney, F. W., Chang, L., Mendez, M., Grin, B., and Goldman, R. D. (2007). The motility and dynamic properties of intermediate filaments and their constituent proteins. *Exp Cell Res* **313**, 2236-2243.
- Chou, Y. H., and Goldman, R. D. (2000). Intermediate filaments on the move. *J Cell Biol* **150**, F101-106.

- Chou, Y. H., Ngai, K. L., and Goldman, R. (1991). The regulation of intermediate filament reorganization in mitosis. p34cdc2 phosphorylates vimentin at a unique N-terminal site. *J Biol Chem* **266**, 7325-7328.
- Chou, Y. H., Opal, P., Quinlan, R. A., and Goldman, R. D. (1996). The relative roles of specific N- and C-terminal phosphorylation sites in the disassembly of intermediate filament in mitotic BHK-21 cells. *J Cell Sci* **109** (Pt 4), 817-826.
- Jaffrey, S. R., Erdjument-Bromage, H., Ferris, C. D., Tempst, P., and Snyder, S. H. (2001). Protein S-nitrosylation: a physiological signal for neuronal nitric oxide. *Nat Cell Biol* **3**, 193-197.
- Jaffrey, S. R., and Snyder, S. H. (2001). The biotin switch method for the detection of S-nitrosylated proteins. *Sci STKE* **2001**, PL1.
- Jagnandan, D., Sessa, W. C., and Fulton, D. (2005). Intracellular location regulates calcium-calmodulin-dependent activation of organelle-restricted eNOS. *Am J Physiol Cell Physiol* **289**, C1024-1033.
- Janda, L., Damborsky, J., Rezniczek, G. A., and Wiche, G. (2001). Plectin repeats and modules: strategic cysteines and their presumed impact on cytolinker functions. *Bioessays* **23**, 1064-1069.
- Jones, J. C., Goldman, A. E., Yang, H. Y., and Goldman, R. D. (1985). The organizational fate of intermediate filament networks in two epithelial cell types during mitosis. *J Cell Biol* **100**, 93-102.
- Kim, S. O., Merchant, K., Nudelman, R., Beyer, W. F., Jr., Keng, T., DeAngelo, J., Hausladen, A., and Stamler, J. S. (2002). OxyR: a molecular code for redox-related signaling. *Cell* **109**, 383-396.
- Kirschner, M., and Mitchison, T. (1986). Beyond self-assembly: from microtubules to morphogenesis. *Cell* **45**, 329-342.
- Knoblich, J. A. (2001). Asymmetric cell division during animal development. *Nat Rev Mol Cell Biol* **2**, 11-20.

- Kobe, B., and Kajava, A. V. (2000). When protein folding is simplified to protein coiling: the continuum of solenoid protein structures. *Trends Biochem Sci* **25**, 509-515.
- Kojda, G., and Harrison, D. (1999). Interactions between NO and reactive oxygen species: pathophysiological importance in atherosclerosis, hypertension, diabetes and heart failure. *Cardiovasc Res* **43**, 562-571.
- Konieczny, P., Fuchs, P., Reipert, S., Kunz, W. S., Zeöld, A., Fischer, I., Paulin, D., Schroder, R., and Wiche, G. (2008). Myofiber integrity depends on desmin network targeting to Z-disks and costameres via distinct plectin isoforms. *J Cell Biol* **181**, 667-681.
- Koss-Harnes, D., Hoyheim, B., Anton-Lamprecht, I., Gjesti, A., Jorgensen, R. S., Jahnsen, F. L., Olaisen, B., Wiche, G., and Gedde-Dahl, T., Jr. (2002). A site-specific plectin mutation causes dominant epidermolysis bullosa simplex Ogna: two identical de novo mutations. *J Invest Dermatol* **118**, 87-93.
- Koss-Harnes, D., Jahnsen, F. L., Wiche, G., Soyland, E., Brandtzaeg, P., and Gedde-Dahl, T., Jr. (1997). Plectin abnormality in epidermolysis bullosa simplex Ogna: non-responsiveness of basal keratinocytes to some anti-rat plectin antibodies. *Exp Dermatol* **6**, 41-48.
- Koszka, C., Leichtfried, F. E., and Wiche, G. (1985). Identification and spatial arrangement of high molecular weight proteins (Mr 300 000-330 000) co-assembling with microtubules from a cultured cell line (rat glioma C6). *Eur J Cell Biol* **38**, 149-156.
- Kouklis, P. D., Hutton, E., and Fuchs, E. (1994). Making a connection: direct binding between keratin intermediate filaments and desmosomal proteins. *J Cell Biol* **127**, 1049-1060.
- Kumar, S., Yin, X., Trapp, B. D., Hoh, J. H., and Paulaitis, M. E. (2002). Relating interactions between neurofilaments to the structure of axonal neurofilament distributions through polymer brush models. *Biophys J* **82**, 2360-2372.
- Kuncewicz, T., Sheta, E. A., Goldknopf, I. L., and Kone, B. C. (2003). Proteomic analysis of S-nitrosylated proteins in mesangial cells. *Mol Cell Proteomics* **2**, 156-163.
- Lane, P., Hao, G., and Gross, S. S. (2001). S-nitrosylation is emerging as a specific and fun-

damental posttranslational protein modification: head-to-head comparison with O-phosphorylation. *Sci STKE* **2001**, RE1.

Leikert, J. F., Rathel, T. R., Muller, C., Vollmar, A. M., and Dirsch, V. M. (2001). Reliable in vitro measurement of nitric oxide released from endothelial cells using low concentrations of the fluorescent probe 4,5-diaminofluorescein. *FEBS Lett* **506**, 131-134.

Leung, C. L., Green, K. J., and Liem, R. K. (2002). Plakins: a family of versatile cytolinker proteins. *Trends Cell Biol* **12**, 37-45.

Leung, C. L., Liem, R. K., Parry, D. A., and Green, K. J. (2001). The plakin family. *J Cell Sci* **114**, 3409-3410.

Leung, C. L., Sun, D., and Liem, R. K. (1999). The intermediate filament protein peripherin is the specific interaction partner of mouse BPAG1-n (dystonin) in neurons. *J Cell Biol* **144**, 435-446.

Li, H., Ohrlein, S. A., Wallerath, T., Ihrig-Biedert, I., Wohlfart, P., Ulshofer, T., Jessen, T., Herget, T., Forstermann, U., and Kleinert, H. (1998). Activation of protein kinase C alpha and/or epsilon enhances transcription of the human endothelial nitric oxide synthase gene. *Mol Pharmacol* **53**, 630-637.

Lincoln, T. M., Dey, N., and Sellak, H. (2001). Invited review: cGMP-dependent protein kinase signaling mechanisms in smooth muscle: from the regulation of tone to gene expression. *J Appl Physiol* **91**, 1421-1430.

Liu, C. G., Maercker, C., Castañón, M. J., Hauptmann, R., and Wiche, G. (1996). Human plectin: organization of the gene, sequence analysis, and chromosome localization (8q24). *Proc Natl Acad Sci U S A* **93**, 4278-4283.

Liu, L., Yan, Y., Zeng, M., Zhang, J., Hanes, M. A., Ahearn, G., McMahon, T. J., Dickfeld, T., Marshall, H. E., Que, L. G., and Stamler, J. S. (2004). Essential roles of S-nitrosothiols in vascular homeostasis and endotoxic shock. *Cell* **116**, 617-628.

Locker, J. K., and Griffiths, G. (1999). An unconventional role for cytoplasmic disulfide bonds in vaccinia virus proteins. *J Cell Biol* **144**, 267-279.

- Lunter, P. C., and Wiche, G. (2002). Direct binding of plectin to Fer kinase and negative regulation of its catalytic activity. *Biochem Biophys Res Commun* **296**, 904-910.
- Mack, G. J., and Compton, D. A. (2001). Analysis of mitotic microtubule-associated proteins using mass spectrometry identifies astrin, a spindle-associated protein. *Proc Natl Acad Sci U S A* **98**, 14434-14439.
- Malecz, N., Foisner, R., Stadler, C., and Wiche, G. (1996). Identification of plectin as a substrate of p34cdc2 kinase and mapping of a single phosphorylation site. *J Biol Chem* **271**, 8203-8208.
- Martinez-Ruiz, A., and Lamas, S. (2004). Detection and proteomic identification of S-nitrosylated proteins in endothelial cells. *Arch Biochem Biophys* **423**, 192-199.
- Määttä, A., DiColandrea, T., Groot, K., and Watt, F. M. (2001). Gene targeting of envoplakin, a cytoskeletal linker protein and precursor of the epidermal cornified envelope. *Mol Cell Biol* **21**, 7047-7053.
- Määttä, A., Ruhrberg, C., and Watt, F. M. (2000). Structure and regulation of the envoplakin gene. *J Biol Chem* **275**, 19857-19865.
- McLean, W. H., Pulkkinen, L., Smith, F. J., Rugg, E. L., Lane, E. B., Bullrich, F., Burgeson, R. E., Amano, S., Hudson, D. L., Owaribe, K., McGrath, J. A., McMillan, J. R., Eady, R. A., Leigh, I. M., Christiano, A. M., and Uitto, J. (1996). Loss of plectin causes epidermolysis bullosa with muscular dystrophy: cDNA cloning and genomic organization. *Genes Dev* **10**, 1724-1735.
- McPherson, A. (1982). *Preparation and Analysis of Protein Crystals* (New York: John Wiley & Sons.).
- Mellerio, J. E., Smith, F. J., McMillan, J. R., McLean, W. H., McGrath, J. A., Morrison, G. A., Tierney, P., Albert, D. M., Wiche, G., Leigh, I. M., Geddes, J. F., Lane, E. B., Uitto, J., and Eady, R. A. (1997). Recessive epidermolysis bullosa simplex associated with plectin mutations: infantile respiratory complications in two unrelated cases. *Br J Dermatol* **137**, 898-906.

- Meraldi, P., and Nigg, E. A. (2002). The centrosome cycle. *FEBS Lett* **521**, 9-13.
- Merrill, G. F. (1998). Cell synchronization. *Methods Cell Biol* **57**, 229-249.
- Moncada, S., and Erusalimsky, J. D. (2002). Does nitric oxide modulate mitochondrial energy generation and apoptosis? *Nat Rev Mol Cell Biol* **3**, 214-220.
- Nagai, K., and Thogersen, H. C. (1987). Synthesis and sequence-specific proteolysis of hybrid proteins produced in *Escherichia coli*. *Methods Enzymol* **153**, 461-481.
- Nathan, C. (2003). Specificity of a third kind: reactive oxygen and nitrogen intermediates in cell signaling. *J Clin Invest* **111**, 769-778.
- Nikolic, B., Mac Nulty, E., Mir, B., and Wiche, G. (1996). Basic amino acid residue cluster within nuclear targeting sequence motif is essential for cytoplasmic plectin-vimentin network junctions. *J Cell Biol* **134**, 1455-1467.
- O'Brien, A. J., Young, H. M., Povey, J. M., and Furness, J. B. (1995). Nitric oxide synthase is localized predominantly in the Golgi apparatus and cytoplasmic vesicles of vascular endothelial cells. *Histochem Cell Biol* **103**, 221-225.
- O'Keefe, E. J., Erickson, H. P., and Bennett, V. (1989). Desmoplakin I and desmoplakin II. Purification and characterization. *J Biol Chem* **264**, 8310-8318.
- Osmanagic-Myers, S., Gregor, M., Walko, G., Burgstaller, G., Reipert, S., and Wiche, G. (2006). Plectin-controlled keratin cytoarchitecture affects MAP kinases involved in cellular stress response and migration. *J Cell Biol* **174**, 557-568.
- Osmanagic-Myers, S., and Wiche, G. (2004). Plectin-RACK1 (receptor for activated C kinase 1) scaffolding: a novel mechanism to regulate protein kinase C activity. *J Biol Chem* **279**, 18701-18710.
- Parry, D. A., and Steinert, P. M. (1999). Intermediate filaments: molecular architecture, assembly, dynamics and polymorphism. *Q Rev Biophys* **32**, 99-187.

- Peitsch, W. K., Hofmann, I., Pratzel, S., Grund, C., Kuhn, C., Moll, I., Langbein, L., and Franke, W. W. (2001). Drebrin particles: components in the ensemble of proteins regulating actin dynamics of lamellipodia and filopodia. *Eur J Cell Biol* **80**, 567-579.
- Pena, S. D. (1982). Giant axonal neuropathy: an inborn error of organization of intermediate filaments. *Muscle Nerve* **5**, 166-172.
- Pollard, T. D., and Cooper, J. A. (1986). Actin and actin-binding proteins. A critical evaluation of mechanisms and functions. *Annu Rev Biochem* **55**, 987-1035.
- Prahlad, V., Yoon, M., Moir, R. D., Vale, R. D., and Goldman, R. D. (1998). Rapid movements of vimentin on microtubule tracks: kinesin-dependent assembly of intermediate filament networks. *J Cell Biol* **143**, 159-170.
- Pulkkinen, L., Smith, F. J., Shimizu, H., Murata, S., Yaoita, H., Hachisuka, H., Nishikawa, T., McLean, W. H., and Uitto, J. (1996). Homozygous deletion mutations in the plectin gene (PLEC1) in patients with epidermolysis bullosa simplex associated with late-onset muscular dystrophy. *Hum Mol Genet* **5**, 1539-1546.
- Pytela, R., and Wiche, G. (1980). High molecular weight polypeptides (270,000-340,000) from cultured cells are related to hog brain microtubule-associated proteins but copurify with intermediate filaments. *Proc Natl Acad Sci U S A* **77**, 4808-4812.
- Quinlan, R. A., and Franke, W. W. (1982). Heteropolymer filaments of vimentin and desmin in vascular smooth muscle tissue and cultured baby hamster kidney cells demonstrated by chemical crosslinking. *Proc Natl Acad Sci U S A* **79**, 3452-3456.
- Quinlan, R. A., and Franke, W. W. (1983). Molecular interactions in intermediate-sized filaments revealed by chemical cross-linking. Heteropolymers of vimentin and glial filament protein in cultured human glioma cells. *Eur J Biochem* **132**, 477-484.
- Rathel, T. R., Leikert, J. J., Vollmar, A. M., and Dirsch, V. M. (2003). Application of 4,5-diaminofluorescein to reliably measure nitric oxide released from endothelial cells in vitro. *Biol Proced Online* **5**, 136-142.

- Ravi, K., Brennan, L. A., Levic, S., Ross, P. A., and Black, S. M. (2004). S-nitrosylation of endothelial nitric oxide synthase is associated with monomerization and decreased enzyme activity. *Proc Natl Acad Sci U S A* **101**, 2619-2624.
- Rezniczek, G. A., de Pereda, J. M., Reipert, S., and Wiche, G. (1998). Linking integrin alpha6beta4-based cell adhesion to the intermediate filament cytoskeleton: direct interaction between the beta4 subunit and plectin at multiple molecular sites. *J Cell Biol* **141**, 209-225.
- Rezniczek, G. A., Janda, L., and Wiche, G. (2004). Plectin. *Methods Cell Biol* **78**, 721-755.
- Rogers, K. R., Herrmann, H., and Franke, W. W. (1996). Characterization of disulfide crosslink formation of human vimentin at the dimer, tetramer, and intermediate filament levels. *J Struct Biol* **117**, 55-69.
- Rogers, K. R., Morris, C. J., and Blake, D. R. (1989). Cytoskeletal rearrangement by oxidative stress. *Int J Tissue React* **11**, 309-314.
- Rogers, K. R., Morris, C. J., and Blake, D. R. (1991). Oxidation of thiol in the vimentin cytoskeleton. *Biochem J* **275**, 789-791.
- Roper, K., Gregory, S. L., and Brown, N. H. (2002). The 'spectraplakins': cytoskeletal giants with characteristics of both spectrin and plakin families. *J Cell Sci* **115**, 4215-4225.
- Rosevear, E. R., McReynolds, M., and Goldman, R. D. (1990). Dynamic properties of intermediate filaments: disassembly and reassembly during mitosis in baby hamster kidney cells. *Cell Motil Cytoskeleton* **17**, 150-166.
- Ruhrberg, C., Hajibagheri, M. A., Parry, D. A., and Watt, F. M. (1997). Periplakin, a novel component of cornified envelopes and desmosomes that belongs to the plakin family and forms complexes with envoplakin. *J Cell Biol* **139**, 1835-1849.
- Ruhrberg, C., Hajibagheri, M. A., Simon, M., Dooley, T. P., and Watt, F. M. (1996). Envoplakin, a novel precursor of the cornified envelope that has homology to desmoplakin. *J Cell Biol* **134**, 715-729.

- Ruhrberg, C., and Watt, F. M. (1997). The plakin family: versatile organizers of cytoskeletal architecture. *Curr Opin Genet Dev* **7**, 392-397.
- Sakoda, T., Hirata, K., Kuroda, R., Miki, N., Suematsu, M., Kawashima, S., and Yokoyama, M. (1995). Myristoylation of endothelial cell nitric oxide synthase is important for extracellular release of nitric oxide. *Mol Cell Biochem* **152**, 143-148.
- Sedgwick, S. G., and Smerdon, S. J. (1999). The ankyrin repeat: a diversity of interactions on a common structural framework. *Trends Biochem Sci* **24**, 311-316.
- Seifert, G. J., Lawson, D., and Wiche, G. (1992). Immunolocalization of the intermediate filament-associated protein plectin at focal contacts and actin stress fibers. *Eur J Cell Biol* **59**, 138-147.
- Sessa, W. C., Garcia-Cardena, G., Liu, J., Keh, A., Pollock, J. S., Bradley, J., Thiru, S., Braverman, I. M., and Desai, K. M. (1995). The Golgi association of endothelial nitric oxide synthase is necessary for the efficient synthesis of nitric oxide. *J Biol Chem* **270**, 17641-17644.
- Shaul, P. W., Smart, E. J., Robinson, L. J., German, Z., Yuhanna, I. S., Ying, Y., Anderson, R. G., and Michel, T. (1996). Acylation targets endothelial nitric-oxide synthase to plasmalemmal caveolae. *J Biol Chem* **271**, 6518-6522.
- Shen, B. Q., Lee, D. Y., Cortopassi, K. M., Damico, L. A., and Zioncheck, T. F. (2001). Vascular endothelial growth factor KDR receptor signaling potentiates tumor necrosis factor-induced tissue factor expression in endothelial cells. *J Biol Chem* **276**, 5281-5286.
- Shinmura, K., Bennett, R. A., Tarapore, P., and Fukasawa, K. (2007). Direct evidence for the role of centrosomally localized p53 in the regulation of centrosome duplication. *Oncogene* **26**, 2939-2944.
- Schröder, R., Kunz, W. S., Rouan, F., Pfendner, E., Tolksdorf, K., Kappes-Horn, K., Al-tenschmidt-Mehring, M., Knoblich, R., van der Ven, P. F., Reimann, J., Furst, D. O., Blumcke, I., Vielhaber, S., Zillikens, D., Eming, S., Klockgether, T., Uitto, J., Wiche, G., and Rolfs, A. (2002). Disorganization of the desmin cytoskeleton and mitochondrial dysfunction in plectin-related epidermolysis bullosa simplex with muscular dystrophy. *J Neuropathol Exp Neurol* **61**, 520-530.

- Schultz, J., Milpetz, F., Bork, P., and Ponting, C. P. (1998). SMART, a simple modular architecture research tool: identification of signaling domains. *Proc Natl Acad Sci U S A* **95**, 5857-5864.
- Simon, M., and Green, H. (1984). Participation of membrane-associated proteins in the formation of the cross-linked envelope of the keratinocyte. *Cell* **36**, 827-834.
- Skalli, O., Chou, Y. H., and Goldman, R. D. (1992). Cell cycle-dependent changes in the organization of an intermediate filament-associated protein: correlation with phosphorylation by p34cdc2. *Proc Natl Acad Sci U S A* **89**, 11959-11963.
- Smith, F. J., Eady, R. A., Leigh, I. M., McMillan, J. R., Rugg, E. L., Kelsell, D. P., Bryant, S. P., Spurr, N. K., Geddes, J. F., Kirtschig, G., Milana, G., de Bono, A. G., Owaribe, K., Wiche, G., Pulkkinen, L., Uitto, J., McLean, W. H., and Lane, E. B. (1996). Plectin deficiency results in muscular dystrophy with epidermolysis bullosa. *Nat Genet* **13**, 450-457.
- Soini, E., and Kojola, H. (1983). Time-resolved fluorometer for lanthanide chelates—a new generation of nonisotopic immunoassays. *Clin Chem* **29**, 65-68.
- Sonnhammer, E. L., Eddy, S. R., and Durbin, R. (1997). Pfam: a comprehensive database of protein domain families based on seed alignments. *Proteins* **28**, 405-420.
- Sowa, G., Pypaert, M., and Sessa, W. C. (2001). Distinction between signaling mechanisms in lipid rafts vs. caveolae. *Proc Natl Acad Sci U S A* **98**, 14072-14077.
- Spazierer, D., Fuchs, P., Pröll, V., Janda, L., Oehler, S., Fischer, I., Hauptmann, R., and Wiche, G. (2003). Epiplakin gene analysis in mouse reveals a single exon encoding a 725-kDa protein with expression restricted to epithelial tissues. *J Biol Chem* **278**, 31657-31666.
- Spurny, R., Abdoulrahman, K., Janda, L., Rünzler, D., Köhler, G., Castañón, M. J., and Wiche, G. (2007). Oxidation and nitrosylation of cysteines proximal to the IF-binding site of plectin: effects on structure, vimentin-binding, and involvement in IF collapse. *J Biol Chem*.
- Stamatakis, K., Sanchez-Gomez, F. J., and Perez-Sala, D. (2006). Identification of novel protein targets for modification by 15-deoxy-Delta12,14-prostaglandin J2 in mesangial cells reveals multiple interactions with the cytoskeleton. *J Am Soc Nephrol* **17**, 89-98.

- Stamler, J. S., and Meissner, G. (2001). Physiology of nitric oxide in skeletal muscle. *Physiol Rev* **81**, 209-237.
- Stamler, J. S., Toone, E. J., Lipton, S. A., and Sucher, N. J. (1997). (S)NO signals: translocation, regulation, and a consensus motif. *Neuron* **18**, 691-696.
- Stappenbeck, T. S., Bornslaeger, E. A., Corcoran, C. M., Luu, H. H., Virata, M. L., and Green, K. J. (1993). Functional analysis of desmoplakin domains: specification of the interaction with keratin versus vimentin intermediate filament networks. *J Cell Biol* **123**, 691-705.
- Steinböck, F. A., Nikolic, B., Coulombe, P. A., Fuchs, E., Traub, P., and Wiche, G. (2000). Dose-dependent linkage, assembly inhibition and disassembly of vimentin and cytokeratin 5/14 filaments through plectin's intermediate filament-binding domain. *J Cell Sci* **113**, 483-491.
- Steinböck, F. A., and Wiche, G. (1999). Plectin: a cytolinker by design. *Biol Chem* **380**, 151-158.
- Steinert, P. M. (1993). Structure, function, and dynamics of keratin intermediate filaments. *J Invest Dermatol* **100**, 729-734.
- Steinert, P. M., Chou, Y. H., Prahlad, V., Parry, D. A., Marekov, L. N., Wu, K. C., Jang, S. I., and Goldman, R. D. (1999). A high molecular weight intermediate filament-associated protein in BHK-21 cells is nestin, a type VI intermediate filament protein. Limited co-assembly in vitro to form heteropolymers with type III vimentin and type IV alpha-internexin. *J Biol Chem* **274**, 9881-9890.
- Strelkov, S. V., Herrmann, H., and Aebi, U. (2003). Molecular architecture of intermediate filaments. *Bioessays* **25**, 243-251.
- Stuehr, D. J., Santolini, J., Wang, Z. Q., Wei, C. C., and Adak, S. (2004). Update on mechanism and catalytic regulation in the NO synthases. *J Biol Chem* **279**, 36167-36170.
- Svitkina, T. M., Verkhovsky, A. B., and Borisy, G. G. (1996). Plectin sidearms mediate interaction of intermediate filaments with microtubules and other components of the cytoskeleton. *J Cell Biol* **135**, 991-1007.

- Tang, H. Y., Chaffotte, A. F., and Thacher, S. M. (1996). Structural analysis of the predicted coiled-coil rod domain of the cytoplasmic bullous pemphigoid antigen (BPAG1). Empirical localization of the N-terminal globular domain-rod boundary. *J Biol Chem* **271**, 9716-9722.
- Tarapore, P., and Fukasawa, K. (2002). Loss of p53 and centrosome hyperamplification. *Oncogene* **21**, 6234-6240.
- Toyoshima, I., Yamamoto, A., Masamune, O., and Satake, M. (1989). Phosphorylation of neurofilament proteins and localization of axonal swellings in motor neuron disease. *J Neurol Sci* **89**, 269-277.
- Traub, P., Kuhn, S., and Grub, S. (1993). Separation and characterization of homo and hetero-oligomers of the intermediate filament proteins desmin and vimentin. *J Mol Biol* **230**, 837-856.
- Tsujimura, K., Ogawara, M., Takeuchi, Y., Imajoh-Ohmi, S., Ha, M. H., and Inagaki, M. (1994). Visualization and function of vimentin phosphorylation by cdc2 kinase during mitosis. *J Biol Chem* **269**, 31097-31106.
- Uversky, V. N. (2002). Natively unfolded proteins: a point where biology waits for physics. *Protein Sci* **11**, 739-756.
- Vermeulen, K., Strnad, M., Krystof, V., Havlicek, L., Van der Aa, A., Lenjou, M., Nijs, G., Rodriguez, I., Stockman, B., van Onckelen, H., Van Bockstaele, D. R., and Berneman, Z. N. (2002). Antiproliferative effect of plant cytokinin analogues with an inhibitory activity on cyclin-dependent kinases. *Leukemia* **16**, 299-305.
- Vikstrom, K. L., Borisy, G. G., and Goldman, R. D. (1989). Dynamic aspects of intermediate filament networks in BHK-21 cells. *Proc Natl Acad Sci U S A* **86**, 549-553.
- Vikstrom, K. L., Lim, S. S., Goldman, R. D., and Borisy, G. G. (1992). Steady state dynamics of intermediate filament networks. *J Cell Biol* **118**, 121-129.
- Virata, M. L., Wagner, R. M., Parry, D. A., and Green, K. J. (1992). Molecular structure of the human desmoplakin I and II amino terminus. *Proc Natl Acad Sci U S A* **89**, 544-548.

- Weitzer, G., and Wiche, G. (1987). Plectin from bovine lenses. Chemical properties, structural analysis and initial identification of interaction partners. *Eur J Biochem* **169**, 41-52.
- Werner, E. R., Gorren, A. C., Heller, R., Werner-Felmayer, G., and Mayer, B. (2003). Tetrahydrobiopterin and nitric oxide: mechanistic and pharmacological aspects. *Exp Biol Med (Maywood)* **228**, 1291-1302.
- West, M. B., Hill, B. G., Xuan, Y. T., and Bhatnagar, A. (2006). Protein glutathiolation by nitric oxide: an intracellular mechanism regulating redox protein modification. *Faseb J* **20**, 1715-1717.
- Wiche, G. (1989). Plectin: general overview and appraisal of its potential role as a subunit protein of the cytomatrix. *Crit Rev Biochem Mol Biol* **24**, 41-67.
- Wiche, G. (1998). Role of plectin in cytoskeleton organization and dynamics. *J Cell Sci* **111**, 2477-2486.
- Wiche, G., Becker, B., Luber, K., Weitzer, G., Castañón, M. J., Hauptmann, R., Stratowa, C., and Stewart, M. (1991). Cloning and sequencing of rat plectin indicates a 466-kD polypeptide chain with a three-domain structure based on a central alpha-helical coiled coil. *J Cell Biol* **114**, 83-99.
- Wiche, G., Gromov, D., Donovan, A., Castañón, M. J., and Fuchs, E. (1993). Expression of plectin mutant cDNA in cultured cells indicates a role of COOH-terminal domain in intermediate filament association. *J Cell Biol* **121**, 607-619.
- Wiche, G., Herrmann, H., Leichtfried, F., and Pytela, R. (1982). Plectin: a high-molecular-weight cytoskeletal polypeptide component that copurifies with intermediate filaments of the vimentin type. *Cold Spring Harb Symp Quant Biol* **46**, 475-482.
- Wiche, G., Krepler, R., Artlieb, U., Pytela, R., and Denk, H. (1983). Occurrence and immunolocalization of plectin in tissues. *J Cell Biol* **97**, 887-901.
- Wildner, H., Muller, T., Cho, S. H., Brohl, D., Cepko, C. L., Guillemot, F., and Birchmeier, C. (2006). dILA neurons in the dorsal spinal cord are the product of terminal and non-termi-

nal asymmetric progenitor cell divisions, and require Mash1 for their development. *Development* **133**, 2105-2113.

Williams, R. L., Courtneidge, S. A., and Wagner, E. F. (1988). Embryonic lethality and endothelial tumors in chimeric mice expressing polyoma virus middle T oncogene. *Cell* **52**, 121-131.

Windoffer, R., and Leube, R. E. (1999a). Detection of cytokeratin dynamics by time-lapse fluorescence microscopy in living cells. *J Cell Sci* **112 (Pt 24)**, 4521-4534.

Windoffer, R., and Leube, R. E. (1999b). Detection of cytokeratin dynamics by time-lapse fluorescence microscopy in living cells. *J Cell Sci* **112**, 4521-4534.

Winter, L., Abrahamsberg, C., and Wiche, G. (2008). Plectin isoform 1b mediates mitochondrion-intermediate filament network linkage and controls organelle shape. *J Cell Biol* **181**, 903-911.

Wu, K. K. (2002). Regulation of endothelial nitric oxide synthase activity and gene expression. *Ann N Y Acad Sci* **962**, 122-130.

Xian, M., Wang, K., Chen, X., Hou, Y., McGill, A., Zhou, B., Zhang, Z. Y., Cheng, J. P., and Wang, P. G. (2000). Inhibition of protein tyrosine phosphatases by low-molecular-weight S-nitrosothiols and S-nitrosylated human serum albumin. *Biochem Biophys Res Commun* **268**, 310-314.

Xu, Z., Cork, L. C., Griffin, J. W., and Cleveland, D. W. (1993). Involvement of neurofilaments in motor neuron disease. *J Cell Sci Suppl* **17**, 101-108.

Yabe, J. T., Pimenta, A., and Shea, T. B. (1999a). Kinesin-mediated transport of neurofilament protein oligomers in growing axons. *J Cell Sci* **112**, 3799-3814.

Yabe, J. T., Pimenta, A., and Shea, T. B. (1999b). Kinesin-mediated transport of neurofilament protein oligomers in growing axons. *J Cell Sci* **112 (Pt 21)**, 3799-3814.

Yamaguchi, T., Goto, H., Yokoyama, T., Sillje, H., Hanisch, A., Uldschmid, A., Takai, Y.,

- Oguri, T., Nigg, E. A., and Inagaki, M. (2005). Phosphorylation by Cdk1 induces Plk1-mediated vimentin phosphorylation during mitosis. *J Cell Biol* **171**, 431-436.
- Yang, Y., Dowling, J., Yu, Q. C., Kouklis, P., Cleveland, D. W., and Fuchs, E. (1996). An essential cytoskeletal linker protein connecting actin microfilaments to intermediate filaments. *Cell* **86**, 655-665.
- Yang, Y., and Loscalzo, J. (2005). S-nitrosoprotein formation and localization in endothelial cells. *Proc Natl Acad Sci U S A* **102**, 117-122.
- Yaoita, E., Wiche, G., Yamamoto, T., Kawasaki, K., and Kihara, I. (1996). Perinuclear distribution of plectin characterizes visceral epithelial cells of rat glomeruli. *Am J Pathol* **149**, 319-327.
- Yoon, M., Moir, R. D., Prahlad, V., and Goldman, R. D. (1998). Motile properties of vimentin intermediate filament networks in living cells. *J Cell Biol* **143**, 147-157.
- Zackroff, R. V., and Goldman, R. D. (1979). In vitro assembly of intermediate filaments from baby hamster kidney (BHK-21) cells. *Proc Natl Acad Sci U S A* **76**, 6226-6230.
- Zieve, G. W., Heidemann, S. R., and McIntosh, J. R. (1980). Isolation and partial characterization of a cage of filaments that surrounds the mammalian mitotic spindle. *J Cell Biol* **87**, 160-169.

CURRICULUM VITAE

Name: Radovan Spurny

Born: October 12, 1977 in Trencin, Slovakia

Address: Department of Molecular Cell Biology
Max F. Perutz Laboratories, University of Vienna
Campus Vienna Biocenter
Dr. Bohrgasse 9, A-1030 Vienna, Austria
e-mail: spurny@gmail.com

Education

- 1996 – 2001 Faculty of Natural Sciences, Comenius University, Bratislava, Slovakia
Graduated in chemistry, specialization biochemistry
Master's thesis: "Study of properties of glucan synthase isoforms in *Saccharomyces cerevisiae*"
- 2001 – 2008 Ph.D. study, Department of Molecular Cell Biology, Max F. Perutz
Laboratories, University of Vienna, Austria
Ph.D. thesis: "Nitrosylation and phosphorylation of plectin affect vimentin network dynamics"

Conferences, Workshops and Poster Presentations

Spurny R., Janda L., Abdourahman K., and Wiche G. (2002) Single plectin repeats form multimerical globular structure (poster), Joint Annual Meeting of the ÖGBM, ÖGGGT, ÖGBT and ANGT, Paris Lodron University, Salzburg, Austria, September 2002

Proceeding of the 5th International Conference on Molecular Structural Biology, Vienna, Austria, September 2003

Crystallization Course: The Principles of Crystallography, Nove Hradky, Czech Republic, October 2003

Research Skills

DNA methods; Protein Expression, Purification on ÄKTA-FPLC, and Crystallization; CD spectroscopy, Western Blotting, Cell Culture, Transfections and Immunofluorescence Microscopy, Live-cell Imaging, Electron Microscopy

IT Skills

MS Office, Adobe Photoshop, Adobe Illustrator, Corel Draw, Image Quant, Zeiss LSM Software, PyMol, Yasara, Pdb-Viewer

List of publications

Spurny, R., Abdoulrahman, K., Janda, L., Runzler, D., Kohler, G., Castanon, M.J., and Wiche, G. (2007). Oxidation and nitrosylation of cysteines proximal to the IF-binding site of plectin: effects on structure, vimentin-binding, and involvement in IF collapse. *The Journal of Biological Chemistry* 282, 8175-8187.

Spurny, R., Gregor, M., Castanon, M.J., and Wiche, G. (2008) Plectin deficiency affects precursor formation and dynamics of vimentin networks. *Experimental Cell Research*, accepted